



## Area Specific Stripping of lower energy windows for AGS and CGS Nal systems

Korsbech, Uffe C C; Aage, Helle Karina; Byström, Sören; Wedmark, Mats; Thorshaug, Svein; Bargholz, Kim

*Publication date:*  
2006

*Document Version*  
Publisher's PDF, also known as Version of record

[Link back to DTU Orbit](#)

*Citation (APA):*  
Korsbech, U. C. C., Aage, H. K., Byström, S., Wedmark, M., Thorshaug, S., & Bargholz, K. (2006). *Area Specific Stripping of lower energy windows for AGS and CGS Nal systems*. Nordic Nuclear Safety Research. NKS-B No. 109

---

### General rights

Copyright and moral rights for the publications made accessible in the public portal are retained by the authors and/or other copyright owners and it is a condition of accessing publications that users recognise and abide by the legal requirements associated with these rights.

- Users may download and print one copy of any publication from the public portal for the purpose of private study or research.
- You may not further distribute the material or use it for any profit-making activity or commercial gain
- You may freely distribute the URL identifying the publication in the public portal

If you believe that this document breaches copyright please contact us providing details, and we will remove access to the work immediately and investigate your claim.



Nordisk kernesikkerhedsforskning  
Norrænar kjarnöryggisrannsóknir  
Pohjoismainen ydinturvallisuustutkimus  
Nordisk kjernesikkerhetsforskning  
Nordisk kärnsäkerhetsforskning  
Nordic nuclear safety research

NKS-109

ISBN 87-7893-168-1

---

## Area Specific Stripping of lower energy windows for AGS and CGS NaI systems

Uffe Korsbech and Helle Karina Aage  
Technical University of Denmark

Sören Byström and Mats Wedmark  
Geological Survey of Sweden

Svein Thorshaug  
Norwegian Radiation Protection Agency

Kim Bargholz  
Danish Emergency Management Agency

May 2005

## Abstract

The report describes the results from a NKS (Nordic Nuclear Safety Research) project aiming at examining the possibilities for extracting stripping factors for Airborne Gamma-ray Spectrometry (AGS) data and Carborne Gamma-ray Spectrometry (CGS) data directly from the recorded set of data, i.e. without having to calibrate the detector systems on beforehand.

The project – NKS project ASSb - has been carried out between 1 August 2004 and 31 March 2005 by a research group composed of persons from Technical University of Denmark (DTU), Danish Emergency Management Agency (DEMA), Geological Survey of Sweden (SGU), and Norwegian Radiation Protection Authority (NRPA).

The AGS and CGS data sets used for the project were recorded by SGU, DEMA, NGU (Geological Survey of Norway), and SSI (Swedish Radiation Protection Institute).

Most of the project effort has been directed towards analysing AGS and CGS data with point source signals recorded at the Barents Rescue 2001 LIVEX exercise at Boden in Sweden.

Possibilities and limitations for the method have been identified

## Key words

Stripping, Gamma Spectra, AGS, CGS, Area Specific, Source Search, Radiation Anomaly, Barents Rescue, LIVEX

NKS-109  
ISBN 87-7893-168-1

Electronic report, May 2005

The report can be obtained from  
NKS Secretariat  
NKS-775  
P.O. Box 49  
DK - 4000 Roskilde, Denmark

Phone +45 4677 4045  
Fax +45 4677 4046  
[www.nks.org](http://www.nks.org)  
e-mail [nks@nks.org](mailto:nks@nks.org)

# Area Specific Stripping of lower energy windows for AGS and CGS NaI systems

NKS-B ASSb

by

Uffe Korsbech, DTU  
Helle Karina Aage, DTU  
Sören Byström, SGU  
Mats Wedmark, SGU  
Svein Thorshaug, NRPA  
Kim Bargholz, DEMA

April 2005



## **Abstract**

This report describes the results from a NKS (Nordic Nuclear Safety Research) project aiming at examining the possibilities for extracting stripping factors for Airborne Gamma-ray Spectrometry (AGS) data and Carborne Gamma-ray Spectrometry (CGS) data directly from the recorded set of data, i.e. without having to calibrate the detector systems on beforehand.

The project – NKS project ASSb - has been carried out between 1 August 2004 to 31 March 2005 by a research group with persons from Technical University of Denmark (DTU), Danish Emergency Management Agency (DEMA), Geological Survey of Sweden (SGU), and Norwegian Radiation Protection Authority (NRPA).

The AGS and CGS data sets used for the project were recorded by SGU, DEMA, NGU (Geological Survey of Norway), and SSI (Swedish Radiation Protection Institute). Most of the project effort has been directed towards analysing AGS and CGS data with point source signals recorded at the Barents Rescue 2001 LIVEX exercise at Boden in Sweden.

The project ASSb and its predecessor have been supported economically by the Nordic Nuclear Safety Research (NKS-B).

## **Key words**

Stripping, Gamma Spectra, AGS, CGS, Area Specific, Source Search, Radiation Anomaly, Barents Rescue, LIVEX

# Contents

List of symbols	ii
Summary	iii
0. Introduction	1
1. Theory for the Area Specific Stripping	3
2. Previous Danish results obtained by the ASS method	4
2.0 Method testing	4
2.1 AGS experiences with Danish data	4
2.2 CGS experiences with Danish data	6
2.3 City CGS measurements	7
3. Results for Norwegian CGS data	9
3.0 Data and energy calibration	9
3.1 Energy calibration Barents Rescue LIVEX	9
3.2 Area specific stripping factors	9
3.3 Results from Barents Rescue LIVEX	12
4. Results for Swedish CGS data	22
4.0 Data	22
4.1 Energy calibration	22
4.2 Area Specific Stripping factors	23
4.3 Results from Barents Rescue LIVEX	24
5. Results for Swedish AGS data	27
5.0 General information and selection of standard windows	27
5.1 Area 1 with background subtraction	28
5.2 Area 1 without background subtraction	29
5.3 Area 2 without background subtraction	31
5.4 Stripping factor height dependency for Area 1	31
5.5 Synthetic spectra for Area 2	34
5.6 Search for weak source signals in Area 2	37
5.7 Single channel stripping factors for SGU system	39
5.8 Intensity maps for Area 1	41
References	43
Appendix A. Theory for Area Specific Stripping	44
Appendix B. Energy calibrations	46
Appendix C. Maps of sources at Barents Rescue LIVEX	49
Appendix D. Fluence rates and detection limits for Area 2 sources	51
Appendix E. Th and U gamma lines	59
Appendix F. SGU AGS background	62
Appendix G. Cross plots for SGU AGS data	63
Appendix H. The influence of neglecting background radiation	66
Appendix I. Stripped window count rates and altitudes	69
Appendix J. Understanding the Area Specific Stripping factors	71
Appendix K. Area Specific Stripping factors	72
Appendix L. Single channel stripping factors for CGS	78
Appendix M. Window count rates	83
Appendix N. Data file processing	97
Appendix O. Definitions and units	99

## List of symbols and abbreviations

$a''$	Single channel stripping factor. Thorium to low energy window
$b''$	Single channel stripping factor. Uranium to low energy window
$c''$	Single channel stripping factor. Potassium to low energy window
$\delta$ , delta	Window stripping factor, background subtracted. Th to low energy window
$\varepsilon$ , epsilon	Window stripping factor, background subtracted. U to low energy window
$\zeta$ , zeta	Window stripping factor, background subtracted. K to low energy window
$\delta'$	Window stripping factor, background included. Th to low energy window
$\varepsilon'$	Window stripping factor, background included. U to low energy window
$\zeta'$	Window stripping factor, background included. K to low energy window
$\delta''$	Window stripping factor, net Th to low energy, net counts background corrected
$\varepsilon''$	Window stripping factor, net U to low energy, net counts background corrected
$\zeta''$	Window stripping factor, net K to low energy, net counts background corrected

*In earlier reports (and in some of the figures in the present report) the window stripping factors are termed a, b, and c. In NucSpec the factors are termed A, B, and C*

Low energy photons are photons with energies below the lower limit of the K window

High energy photons are photons with energies above the lower limit of the K window

$a$	Stripping ratio U to Th (unit counts/counts), std. windows method
$b$	Stripping ratio K to Th (unit counts/counts), std. windows method
$g$	Stripping ratio K to U (unit counts/counts), std. windows method
$\alpha$	Stripping ratio Th to U (unit counts/counts), std. windows method
$\beta$	Stripping ratio Th to K (unit counts/counts), std. windows method
$\gamma$	Stripping ratio U to K (unit counts/counts), std. windows method

$\theta$ , theta Angle between an incoming photon and a Compton scattered photon

$E_p$  Energy of a primary (original) gamma photon i.e. before an interaction

$E_s$  Energy of a (Compton) scattered photon

$\varphi$  (phi) Fluence rate (earlier also flux) (unit photons per  $m^2$  and s or just  $m^{-2}s^{-1}$ )

$\mu$  (mu) Linear attenuation coefficient (unit  $m^{-1}$  or  $cm^{-1}$ )

$\mu/\rho$  ( $\mu$  over  $\rho$ ) Mass attenuation coefficient (unit  $m^2/kg$  or  $cm^2/g$ )

$N$  Number of photons

$Q$  Source activity (unit Bq, kBq, MBq or similar)

$r$  Count rate (unit cps = counts per second)

$s_x$  Spectral component (spectrum shape) resulting from a NASVD processing (Ref. 15)

NucSpec: An advanced set of co-ordinated computer programs for post-processing sets of gamma spectra from scintillator detectors for example mobile measurements with airborne or carborne detectors – or spectra from stationary detectors continuously controlling the radiation level and composition (Ref. 14).

LIVEX Source search part of the Barents Rescue exercise at Boden in Sweden in 2001

NASVD Noise Adjusted Singular Value Decomposition. Used for extracting basic spectrum information from a set of NaI spectra

AGS Airborne Gamma-ray Spectrometry

ASS Area Specific Stripping

CGS Carborne Gamma-ray spectrometry

DEMA Danish Emergency Management Agency

DTU Technical University of Denmark

NGU Geological Survey of Norway

NKS Nordic Nuclear Safety Research

NRPA Norwegian Radiation Protection Authority

SGU Geological Survey of Sweden

SSI Swedish Radiation Protection Institute

## Summary

By the Area Specific Stripping (ASS) method for NaI gamma detectors it is possible in a simple way obtain the parameters (stripping factors) that are needed for being able to discern between natural radioactivity signals and signals from manmade radioactivity and radiation anomalies in general. The method has earlier been tested only for a few sets of Danish AGS and CGS data (Refs. 2, 8, 10 and 13).

1. One of the goals of the project has been to investigate to which extent it is possible to use the ASS method for a number of different sets of gamma spectra recorded by different teams with different types of equipment in different environments.
2. Another goal of the project has been to investigate why (earlier) one sometimes got oddly-looking ASS parameters that worked correctly when seen from a mathematical point of view but seemingly had no physical meaning.
3. It was also a goal that the successful parts of the ASS technique should be developed to a point where other Nordic teams could use it for practical purposes.
4. Besides that, new possibilities or problems that came up during the project should be evaluated whenever possible.

During the project the ASS technique was mainly tested with AGS data recorded by SGU at the LIVEX exercise in 2001 (Ref. 2) and with CGS data from SSI and NGU/NRPA also from the LIVEX exercise. Danish data that have been examined earlier are also included to some extent.

The ASS parameters in principle depend both on detector type and size, on the selected energy windows, and on the environmental geometry, and - for AGS - also on the altitude. One of the conclusions of the project is that for AGS data recorded within a limited height interval – for example 35m to 85m - it is (in general) possible to neglect the influence of the altitude on the stripping factors. The results hereby become erroneous but the errors are small when compared to other errors and uncertainties.

The origin of the oddly looking stripping parameter values observed at earlier examinations of the method (Ref. 13) has been identified. For AGS (and perhaps also for CGS) one may sometimes have to record data in areas where the window count rates are only slightly higher than the background rates (due to cosmic radiation and radioactivity in the detector system). Fluctuations due to the counting statistics hereby sometimes generate negative (or zero) net window counts i.e. measured counts minus background counts. The mathematics of the ASS method can only handle a positive number of counts. The solution to the problem is to perform the calculations on gross window counts.

The use of gross window counts instead of net (background corrected) window counts in principle generates erroneous stripping factors. However, experiences tell that the errors for the calculated stripping factors are negligible for the majority of the data sets examined. (Even at significantly varying live time acceptable stripping parameters are calculated.) The reason is assumed to be that the general shape of a background spectrum is quite similar to the shape of environmental spectra of natural radioactivity. This means that the background spectrum – "hidden" in the measured spectra – ensures an almost correct stripping of itself. The effect of the simplification - using gross window count instead of net counts - has been evaluated

thoroughly; and the conclusion is that errors introduced in this way can be neglected compared to other errors and uncertainties.

The investigations of the ASS method with the AGS data from SGU have generated a number of stripping factors that have been tested with the files. Tests with use of stripping factors from one set of data together with spectra from another set of data have also been carried out. The examinations tell that it is possible to have one set of stripping parameters that fits for stripping of spectra recorded in areas with the same "structure" i.e. topology, geology and vegetation.

A new feature – channel stripping factors – has been developed. The statistics of the channels counts does not allow for a determination of stripping factors for a window including only a single channel. But based on stripping factors for a large number of windows it is possible to assign stripping factors to each channel. If stripping factors for an unusual window are needed one just add together the single channel stripping factors for the appropriate channels. Hereby one gets the ordinary window stripping factors.

Most tests of the method on AGS data concern data from the LIVEX exercise (Ref. 2) where a number of gamma sources were distributed at unknown and "hidden" positions within seven different areas – Area 1 to Area 7. Unfortunately the signals from the sources were either very strong – and the sources could be detected with almost any radiation detector – or so weak that the sources only were detectable by chance.

A search for weak signals was, however, carried out for DEMA and SGU AGS data recorded within Area 2 of the LIVEX exercise. When care with data processing and presentation was exerted the ASS method unveiled a single, weak radiation anomaly that fits to the radiation from a collimated  $^{60}\text{Co}$  source beaming at  $30^\circ$  into the air. It should, however, be stressed that without knowing the existence of a source at the locality, the anomaly could have been taken as a rare, strong but natural "outlier". Hereby an indication of a detection level for ASS is obtained. (The source was not detected by any method during the LIVEX exercise.)

In order to obtain more tests than was possible with the actually measured spectra tests with addition of a synthetic source signal to some of the measured spectra were carried out. A strong  $^{99}\text{Mo}$  signal (spectrum) was extracted from one of the AGS files. This spectrum was reduced in intensity and added to some randomly selected measured AGS spectra. The stripping was carried out for a few windows. It was observed – as expected – that a specific source signal could sometimes be detected more easily than in other cases. In cases where the source signal was added to a low measured window count rate – randomly low due to counting statistics – it was more difficult to observe the signal than in cases where it was added to a measured high count rate.

The stripping factors for the three AGS examined areas (by SGU) at the LIVEX exercise (Ref. 2) resembled each other, and a common set (Area 1 and 2) of window stripping factors could be determined. Those ASS parameters may also be usable for other types of areas. It has, however, only partly been possible to test this. The fourth data set examined originates from a survey at Gävle North of Stockholm in 1996-97. At Gävle there is a medium level  $^{137}\text{Cs}$ -contamination from the Chernobyl accident in 1986 (Ref. 4). The  $^{137}\text{Cs}$  signal "distorts" most of the spectra recorded at Gävle. Therefore reliable stripping factors can hardly be extracted from the file. The

stripping can be carried out with the stripping factors determined from the LIVEX spectra. It is, however, difficult (or impossible) to check the quality of the stripping.

The use of the ASS method described in this report is – except for the Danish CGS measurements during the LIVEX exercise – carried out as post processing. When reliable ASS parameters have been obtained for a detector system one may, however, also use them while measuring, as did the Danish CGS team at the exercise.

In a search for point sources or other radiation anomalies the highest sensitivity is obtained by plotting the stripped window counts as a function of measurement number and then investigating the distribution of "surplus" counts. This especially is important in cases where a source emits photons only within a narrow solid angle. In this case the signal may be detectable only in a single spectrum, and mapping – including some spatial smoothing – may bring the signal below the level of detection.

When searching for a source signal assumed to be at the limit of detection one may also investigate the average value for two consecutive spectra. Source signals may be detected in both spectra whereas a high number due to statistical variations very seldom has a "neighbouring" spectrum also with a high number of counts.

Based on simple models the expected count rates for AGS systems have been calculated for some of the sources that were not detected – neither during the exercise nor during this project. Based on the source information one has in two cases to expect that the sources would generate signals that could be detected by some AGS systems. But by some reason the sources were not detected by any team.

In cases where the "LIVEX stripping factors" are used with data from an area with a different structure one may have a zero level shift – and this zero shift may be different for areas with different density of vegetation and different types of topology.

For the LIVEX CGS measurements this zero shift can sometimes be seen more than once during a survey, although stripping factors have been calculated for that very same area. This is a consequence of the quite different field of view for the AGS and the CGS detector systems. The CGS detector is placed at a very low position, sometimes inside the car (NGU/ NRPA and SSI) and sometimes on top of the car (DTU/DEMA). But in any case the signal recorded is much more susceptible to local changes in the environment. For example, the change from one road type to another, e.g. new asphalt on a standard country road to narrow, muddy roads in the forest will produce very different signals for the CGS system whereas the AGS system will be only slightly affected. AGS can see both roads and the surrounding terrain at the same time with slow changes as a consequence, but CGS can only see the nearest surroundings. This zero shift was observed more than once for team NOK (Norwegian car) for measurements recorded within the same area on the same day. Should the ASS technique be used for other purposes than searching for point sources it is therefore of great importance to have some geographic knowledge on the area to be surveyed. (It should be stressed that any method for stripping gamma spectra will meet the same problem.)

The height above ground for the CGS detectors also has some importance at a point source search. At the LIVEX exercise a point source was detected by a CGS detector placed above the car (2.2 m above ground) whereas another (and larger) CGS detector placed inside the car at app. 1 m above ground did not detect the source.

Another interesting observation for the CGS measurements was that sometimes the uranium stripping factor is larger than the thorium stripping factor, and sometimes the opposite was the case – probably dependent on minor variations of the spectrum shape and statistical noise.

For team NOK the ASS method was not able to find more sources than had already been reported (Ref.2). All sources reported was also found by the ASS method, but the well-camouflaged sources, found by almost no teams, the stripping procedure could not find either. In this quest it was noticed that in the vicinity to one of those sources team NOK had driven along the same path as team DKK. Team DKK had found the source, but team NOK had not, although the source had been passed twice. This was investigated further and led to the conclusion that the detector size might be of less importance than the detector position. Team DKK used a 4L NaI detector and team NOK used a 16L detector – but the NOK detector was inside the vehicle whereas the DKK was placed above the car roof. The heights above ground were app. 1 m and 2.2 m respectively.

DTU and NRPA in common also put an effort in tracking down two  $^{226}\text{Ra}$  sources not previously reported by anyone. Sadly, but perhaps not so surprising since  $^{226}\text{Ra}$  is part of the natural uranium decay chain, there was no trace of those.

The analysis of the Swedish (SSI) and Norwegian (NRPA/NGU) data proved that ASS was able to find every source previously reported. To be able to conclude this the track lines for both vehicles were plotted together with the information on source positions. The source type could not always be identified. For sources for which only scattered radiation had been registered it was possibly only to say something about the minimum gamma energy. (During the LIVEX exercise those sources were typically identified by investigations on foot in places where the car could not be brought.) Other sources of very high source strengths introduced problems, too, regarding the identification.

Sometimes the vehicles and measurement systems came so close to the sources that a huge spectrum drift was introduced in the systems with the displacement of counts towards higher channels as a consequence hereof. This meant that the counts in the Th-, U-, and K-windows were unreliable due to drift and pile-up. Naturally, this lead to an erroneous stripping, sometimes with a large negative error as a consequence before and after parking next to a source. Large negative count (rate) errors may therefore also be of interest when the ASS method is used.

In theory, a  $^{60}\text{Co}$  source should give counts in the  $^{60}\text{Co}$ -window as well as in the  $^{137}\text{Cs}$  window and thereby one may identify the source as  $^{60}\text{Co}$ . However, in a few cases it was seen that due to pile up a very strong caesium source could lead to a surplus of counts (after stripping) in the cobalt-window as well. Therefore the use of ASS is a valuable tool, but it should be used with caution without the knowledge of a skilled data analyst. When provided with a set of appropriate stripping factors an unskilled operator would be able to see if there is a low-medium intensity source present by looking solely at results presented as numbers in the form of stripped

counts or count rates (no spectrum analysis). But for determination of correct source type and source strength a spectrometry expert still is needed.

In general, the ASS method – like any other stripping method – does not work correctly in case of strong spectrum drift as observed in the Norwegian and Swedish data. The Swedish data apparently was recorded with a non-gain-stabilised system and shows a continuous spectrum drift. This type of spectrum drift is by far the worst (compared to the spectrum sliding upwards but resuming its old position after a high count rate with pile-up) and it is difficult to calculate an appropriate stripping factor for a window that is in reality changing position all the time. In order to lessen this problem, the data sets were broken down into smaller data sets. For the data provided by SSI, it is therefore an open question whether weaker sources, had they been passed, could have been found by the ASS method.

For CGS data recorded in a rapidly changing geometry the ASS method will - as any other stripping method - generate zero level shifts. This is acceptable during a source search, but when using CGS measurements for a contamination mapping one should be aware of the zero shifts. For AGS data this problem is of less importance.

Processing of spectra recorded in a city area may cause a special problem for CGS. Here one may observe a fast varying geometry that causes a significantly varying spectrum shape for natural radioactivity. When using the ASS technique - or any other stripping technique - the zero level for the stripped count rates also exhibits major variations. Therefore one has to use more advanced methods than ASS for searching low level signals from sources.

The calculation of the area specific stripping factors for this project has been quite tedious and time consuming. With the inclusion of the ASS technique in the NucSpec program package (Ref. 14) the stripping factor calculations probably can be carried out in couple of minutes – some ten times faster than obtainable until now.

The energy windows to be used for the ASS technique could be the standard windows for Th, U, and K together with one or several "low energy" windows covering photon energies of interest. In a search for  $^{60}\text{Co}$  signals one may have to raise the lower limit of the K-window a little in order to avoid cobalt counts in the K-window.

The statistical noise of the Th, U, and K window counts is transferred to the low energy window(s) by the stripping. By using NASVD and reconstructed spectra one may reduce this statistical noise. However, one should ensure that the NASVD and reconstruction cover only the natural radiation. If signals from artificial radioactivity are included in NASVD and reconstruction, then the count rates of the Th, U and K window may be erroneously increased - and a too strong stripping occurs. (Calculation of the stripping factors should be based on the raw data, and then the raw data for the low energy window(s) are stripped using reconstructed Th, U and K window counts.)



## 0. Introduction

The technique described in this report - termed Area Specific Stripping (ASS) – has earlier been used with success on Danish Carborne Gamma-ray Spectrometry (CGS) measurements (Ref. 2 and 10). The technique also has been used with some success on Danish Airborne Gamma-ray Spectrometry (AGS) measurements (Ref. 13). Although acceptable results were obtained here the processing (for AGS) resulted in some interim parameter values that could not be understood from a physical point of view. The NKS project therefore also has investigated this phenomenon and found an explanation and a solution.

The ASS technique examines a set of gamma spectra and looks for a simple (linear) relation between the count rates for the standard energy windows used for measuring natural radioactivity – represented by  $^{208}\text{Tl}$  (Th),  $^{214}\text{Bi}$  (U) and  $^{40}\text{K}$  (K) – and the count rate in any low energy window. (In this report a low energy window is any energy window placed below the lower limit of the K-window.) The "best relation" is determined by a least squares fitting including all gamma spectra, and the result is three stripping factors –  $\delta'$ ,  $\epsilon'$ , and  $\zeta'$  – that relate the count rates of the three "high energy" windows for natural radioactivity to the natural radioactivity signal in a low energy window. (Appendix A, Ref. 10 and 13).)

The gamma spectrum for natural radioactivity as for example  $^{40}\text{K}$  does not always have the same shape i.e. the relation between the count rate of the "high energy" window (1461 keV) and the count rate of a "low energy" window is not a constant. For AGS there is a height variation, which – when for example going from 60 m altitude to 70 m - will change the  $^{40}\text{K}$  spectrum to have relatively (slightly) more counts in the low energy windows than in the high energy window. A dense cover of vegetation will have a similar effect. Therefore, one in principle should determine the stripping parameters for different altitudes. In practice this could be done if the data set includes a sufficient large number of spectra for each height interval.

For other sets of data this may not be the case. Therefore one has to carry out the calculations without taking altitude variations into account.

When reliable stripping factors for a specific type of environment have been determined one may use them both while measuring and at post processing of data. They may be used for source search and for mapping "surplus counts" in low energy windows (Ref. 8). In order to calculate contamination levels one also need to know the detector sensitivities. In case of a mixed-nuclides contamination one probably have to present a "common concentration" for the mixture – but with a possible check by comparing the count rates of different low energy windows. This question has not been discussed and tested in this report that only investigates a new method for stripping of scintillator spectra.

Using aircrafts or cars for mobile measurement of environmental gamma-spectra is an established technique (Ref. 1, 2, and 6). It is used for mapping natural radioactivity i.e. uranium, thorium and potassium (Ref. 1), and manmade radioactivity (Ref. 3, 4, 5, 7, 17, and 18) and for search of lost sources and other radiation anomalies (Ref. 2, 6, 9, 10, 11, 12, and 15). The detector systems usually include large NaI(Tl) crystals; typically 12-32 L for airborne measurements and 1-16 L for carborne measurements.

In order to get useful results from the measurements one has to know a number of parameters – e.g. the stripping factors and the sensitivities – that are used when the

measured data are interpreted quantitatively. With the stripping factors one separates the spectrum information into different net parts of different origin, and the sensitivities then are used for converting the net parts (counts) into concentrations or source activity.

For many tasks the knowledge on sensitivities is not needed, and sensitivities are not directly included in the new ASS technique described in this paper. This technique can be used for extracting the signals due to non-natural radioactivity from the measured spectra; but the technique cannot itself be used for separating the signals from U, Th, and K from each other. The major application of the ASS technique therefore is in the search of lost or illegal sources and other radiation anomalies – and for mapping of contamination levels.

A major benefit of the ASS method is that the parameters needed for a separation of natural and non-natural signals often can be extracted from the actual set of measured spectra. It is also a benefit that the ASS parameters are adapted to the actual detector, vehicle and environmental geometry including topology and vegetation (Ref. 9). The "old" standard method for determining stripping parameters in general generates parameters that are adapted to a specific situation and a specific detector set-up that may differ from that actually experienced during a survey - especially for the lowermost energy range.

The ASS method was developed by DTU and was originally tested successfully with Danish CGS data (Ref. 8 and 10). Then during a pilot project supported by NKS the method was tested with Danish AGS data (Ref. 13). The method also worked well for Danish AGS data with respect to final results, but some interim parameters obtained non-physical values.

The goal of the project described in the present report can shortly be described as including the following parts:

- a. Investigate further the basic properties of the ASS method aiming at understanding the possibilities and the limitation of the method when used for different tasks.
- b. Examine sets of data from different detector systems used by different AGS or CGS teams.
- c. Develop methods and programs that enable all project participants to use the ASS technique for future sets of own data.

## 1. Theory for the Area Specific Stripping

Gamma photons from natural radioactivity in or on the ground may enter the air and here possibly be detected by a NaI detector crystal. The photons are emitted from the radioactive nuclei with very specific energies. Potassium-40 for example emits photons of 1461 keV energy. The decay chains following thorium and uranium emit photons of several different energies a few of which, however, are the most important. (In Appendix E are shown high resolution spectra with a number of gamma lines corresponding to different energies.)

A photon may, however, lose part of its energy by impacts on electrons of atoms in the ground and/or in the air. The Compton formula describes the loss of energy for each scatter of a photon. Due to the scatters, a detector in the air above the ground will detect both photons of primary energy – e.g. 1461 keV for  $^{40}\text{K}$  – and photons of lower energies. The number of low energy photons relative to the amount of primary photons hereby increases (slightly) with the altitude of the detector (Ref. 1 and 9).

Stripping of a gamma spectrum means that one – based on knowledge on the ratio between scattered and primary photons – is able to eliminate the contribution of e.g.  $^{40}\text{K}$  radiation to the low energy windows (Ref. 7 and 16). This ratio is the simple stripping factor, which therefore depends on the altitude of the detector – or more correctly on the amount/number of electrons (or mass of matter) between the gamma emitter and the detector. A dense cover of vegetation acts in the same way as a mass of air; it increases the stripping factor. The value of the stripping factor of course also depends on the energy windows used for the calculations. Finally the geometry of the environment around the detector – including the carrying vehicle and the topology – slightly influences the stripping factor.

For Th and U the situation is a little more complicated. A number of low energy photons are emitted together with the "high" energy photons by the radioactive nuclei of the Th and U decay chains. The low energy photons may be detected in the low energy windows of the detector together with high-energy photons that have lost part of their energy by Compton scatters. Primary low energy photons are attenuated faster than high-energy photons. This counteracts the increase of the stripping factors for Th and U with the altitude for AGS.

The standard method for determining (ordinary) stripping factors is to record a number of spectra for different mixtures of Th, U, and K with different amounts of material between the "source" and the detector. The source may in principle be the natural ground (Ref. 1 and 19), but usually the calibration measurements are performed in the laboratory with different types of "synthetic" ground – the composition of which is known. The problem with this laboratory type of calibration is that it is difficult to get sufficient large calibration set-ups and, therefore, a deficit of low energy (multi-scattered) photons usually is experienced. The calibration task with different types of soil – and different "altitudes" for AGS measurements – may be very extensive and troublesome. For CGS calibration it may be impossible to simulate the measuring geometry in the laboratory (Ref. 17).

[The determination of the stripping factors between the high-energy windows can reliably be determined in a laboratory set-up, because multi-scattered photons have (almost) no influence here.]

## 2. Previous Danish results obtained by the ASS method

### 2.0. Method testing

The Technical University of Denmark first used the method of area specific stripping for CGS measurements while participating in the Barents Rescue exercise (Ref. 2 and 8) on behalf of DEMA. The method was a great help in locating sources during CGS measurements from the presence of scattered photons only.

The method was further investigated and exercised on Danish AGS data for the first time in the predecessor for this report "Area Specific Stripping factors for AGS" (Ref. 13). The standard procedure for processing AGS data is the three-window method following the IAEA guidelines (Ref. 1). The window count rates are background corrected and stripped using stripping factors calibrated according to survey height. It was thought that the use of area specific stripping, i.e. the use of a set of stripping factors calculated directly on the data set in itself would – when investigating a limited height interval - incorporate the height dependency associated with the data. For a given survey height the amount of "down scattered" K photons registered in a low energy window is proportional to the amount of K photons registered in the standard "high" energy windows for K. Similarly for Th and U.

### 2.1. AGS experiences with Danish data

The ASS method was used for two different areas: the Danish Island Bornholm (Ref. 18) and Boden, Sweden (Ref. 2).

The Bornholm measurements were sorted in 5m-flight height intervals and each interval was treated separately. This was done in order to find a possible height dependency. Also, a set of mean stripping factors was calculated. (Mean survey height 84 m.) The stripping factor,  $\zeta$ , from the potassium window to a low energy window was found to be only slightly dependent on survey height, but very dependent on the examined window energy intervals. The stripping factor  $\zeta$  was found to increase almost inversely proportional to the gamma energy. It was noticed that the uranium stripping factors,  $\varepsilon$ , (Figure 2.1.2), seemed to mirror the thorium stripping factors,  $\delta$ , (Figure 2.1.1), i.e. when  $\delta$  went up,  $\varepsilon$  typically went down.

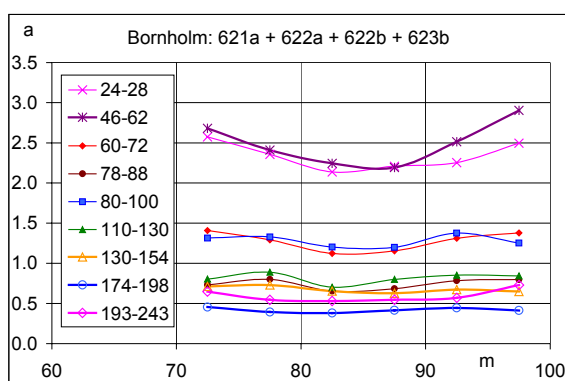


Figure 2.1.1. Average Th stripping factors versus survey height for a number of low energy windows, Bornholm.

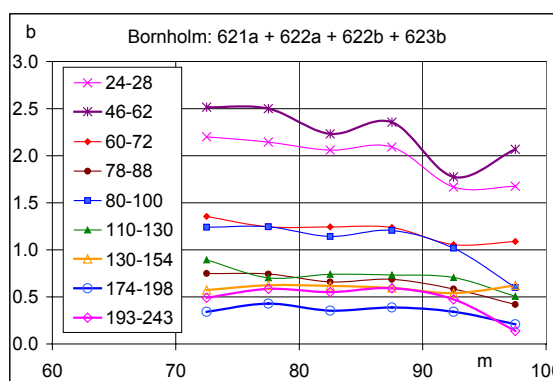


Figure 2.1.2. Average U stripping factors versus survey height for a number of low energy windows, Bornholm.

The measurements from Bornholm contained no sources. The only non-natural signals came from traces of Chernobyl fall-out without importance for the calculation of the stripping factors.

The examined Danish AGS data covered two of the areas included at the LIVEX exercise, A1 and A2 (Ref. 2). (Survey heights 30-70 m.)

Initially a set of stripping factors for area A1 was calculated for the survey height 55-60 m (strong source signals were removed). For the uranium stripping factors the curves looked very oddly and this was thought to be partly due to variations of radon daughters in the air or natural anomalies; but certainly it called for a closer examination of other data.

Plots of stripped counts made it possible to identify the four sources present in area A1. It was noticed that the  $^{131}\text{I}$  source (1:2) also created a large error in the  $^{137}\text{Cs}$  window. (637 keV gamma line, 7%, versus 82% for the 364 keV line for  $^{131}\text{I}$ ).

The set of stripping factors calculated from Area A1 (55-60m) was also used on Area A2 (30-80m) and XY co-ordinate plots showing the ten largest errors for nine low energy windows were made. For all windows below 870 keV a small cluster of errors was found (the  $^{99}\text{Mo}$  source (2:4)). The  $^{60}\text{Co}$  source (2:2) was indicated by two errors close to the source position, but only from errors in the cobalt-window. In general, the cobalt-errors were of more doubtful significance.

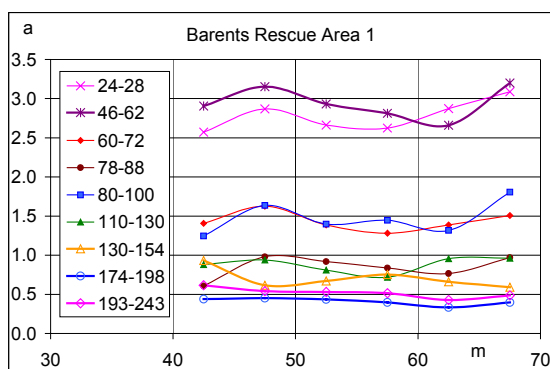


Figure 2.1.3. Average Th stripping factors versus survey height, Boden, A1 (Ref. 13).

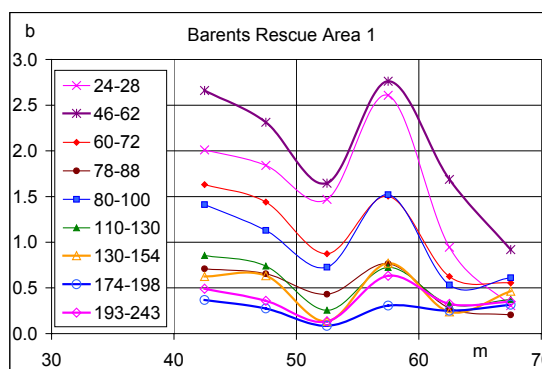


Figure 2.1.4. Average U stripping factors versus survey height, Boden, A1 (Ref. 13).

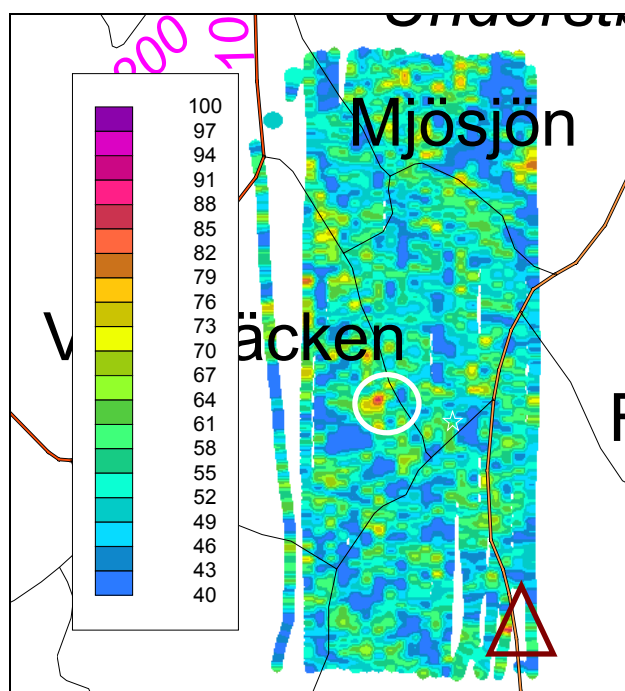


Figure 2.1.6. Normalised error colour plot for Area A2. Plot interval 40-100% (Ref. 13).

Next, a set of stripping factors for Area A2 data (30-80m) was calculated. (Measurements from source 2:4 were not included.) This time the cobalt window showed far larger errors than when stripping factors for a narrow height interval were used for the stripping. The errors in each window were normalised (max. 100%) and added together and a plot of the total errors was made. In this plot the position of the  $^{60}\text{Co}$  source (in reality two cobalt sources, see also Appendix C) was clearly identified. The white circle of Figure 2.1.6 shows this. (The triangle shows the  $^{99}\text{Mo}$  source, 2:4)

## 2.2. CGS experiences with Danish data

Area specific stripping was first used with CGS surveys during the Barents Rescue exercise mentioned above. The stripping procedure was used both in real time and as a post-processing tool.

During the measurements it was sometimes observed that a shift in zero level occurred, especially when changing from one road type to another. For processing tools that can manage to display negative count rates this is, however, not a problem in a survey situation.

The stripping procedure was used with success, e.g. in identifying a source from which apparently only scattered radiation was registered. The source was in reality two  $^{60}\text{Co}$  sources, namely 4:4 and 4:5 in search area C4. Figure 2.2.1 shows the source type identification performed by comparing the stripped counts in a low energy window (chns. 10-13, 47.1 keV to 65.3 keV) and the stripped counts in a window of "medium energy" (chns. 180-220, 1094.7 keV to 1346.0 keV). The latter curve is plotted on the secondary ordinate axis. One notices that the background level is on the average some 60 counts on the positive side of zero. This was caused partly by spectra "infected" by spectrum drift after a long time survey period close to the source(s) (team DKK left the car to perform manual measurements and found two sources) and partly by having a varying environmental geometry included in the calculation of the stripping factors.

Post processing of the data with area specific stripping also made it possible to find a  $^{60}\text{Co}$  source in area C7 that NASVD processing – in general a powerful technique for detecting radiation anomalies - with NUCSpec (Ref.14) was not able to find. This was source 7:3 or 7:4 passed at a medium car speed (55 km/h). The two sources were collimated towards each other. Figure 2.2.2 shows the track line and the source positions. The stripped counts can be found in Ref. 2 and 10.

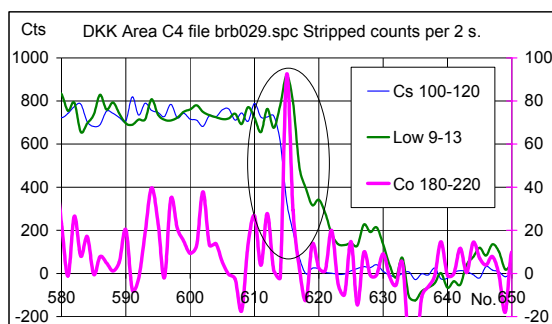


Figure 2.2.1. Stripped counts for different sources energy windows, Area C4 (Ref. 2).

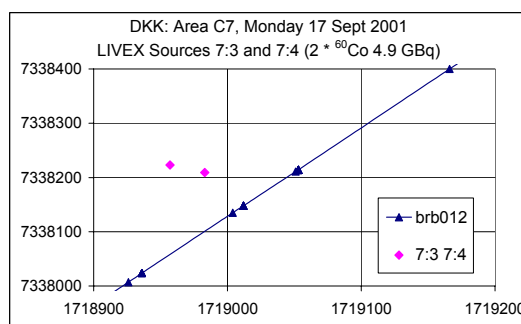


Figure 2.2.2. Track lines and two sources in Area C7.

### 2.3. City CGS measurements

The ASS method was also used in the search for anomalous gamma-radiation in the city of Copenhagen, Denmark. Spectra recorded in open terrain differ from spectra recorded in city areas. One would expect to have for the city spectra a smaller fraction of low energy photons than one would observe in the country (multiple scattering) and when a city spectrum for e.g. a narrow street is stripped one might expect a deficit of photons at the lowermost energies.

The same route, Christiansborg (parliament), Ridebanen, Bredgade, was surveyed twice to see whether the results obtained from the first area specific stripping were consistent: i.e. could one create a set of city stripping factors to be used for another city survey at another time?

One of the first things that were noticed was the very fast variations in count rates and that the level of the stripped windows count curves did not quite follow each other. Consider e.g. Figure 2.3.1 that shows the stripped counts in three low energy windows. Window 1 covers the chns. 20-45, window 2 covers the chns. 48-65, and window 3 covers the channels 67-84. [E (keV) =  $0.00077 \cdot \text{chns}^2 + 5.868 \cdot \text{chns} + 20.47$  keV; Th chns. 387-450; U chns. 267-311; K chns. 217-260.] The stripped counts of window 2 and window 3 have been scaled to fit with the number of counts (approx.) in window 1 around channel 100.

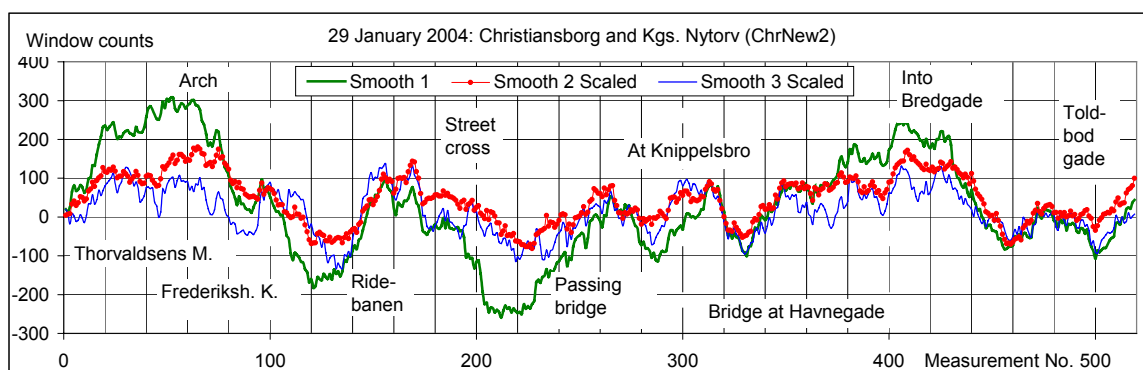


Figure 2.3.1. Smoothed, stripped windows counts for three low energy windows. Scaled counts for the windows 2 and 3.

From measurement No. 10 to 60 the curve for window 1 is much above the other curves meaning that there is a relatively large fraction of very low energy scattered photons here; the same is the case around measurement No 420. The opposite is the case around measurement Nos. 110 (center of low count spectrum block) and 220 (center of low count spectrum block).

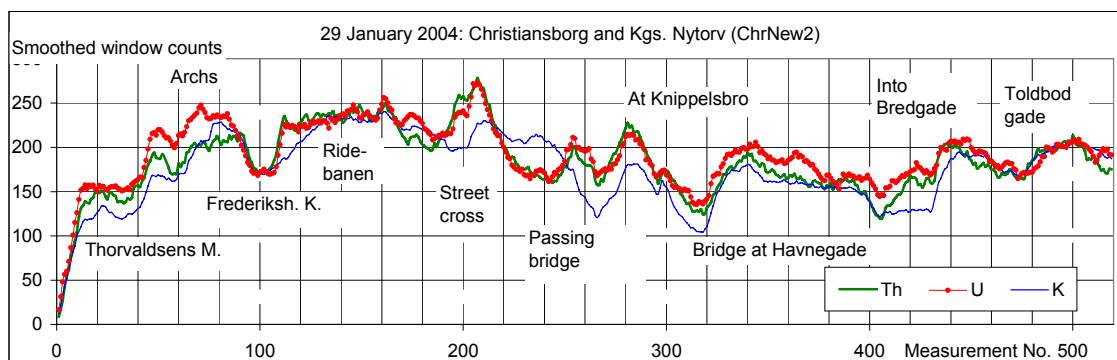


Figure 2.3.2. Smoothed Th, U, and K window counts.

Figure 2.3.2 shows the corresponding counts in the natural radionuclide windows. The number of counts for Th and U has been scaled to fit with potassium (approx.) around channel 100. Most often Th and U follow one another, but K shows independent variations in some places.

For spectra recorded within a city it was found that the remaining counts were very dependent on the geometry surrounding the car. In Ref. 20 a detailed discussion of the results step by step (with increasing spectrum number) is given. The results are compared to road types, positions of monuments and the composition of those (e.g. granite, marble) and the surrounding buildings (e.g. sandstone, bricks). The majority of the differences were explained, yet some remains unsolved. Also the traffic, the position and number of larger vehicles such as buses introduced difficulties, which was seen by comparing the area specific stripping factors calculated for two different surveys following (almost) the same path made in October 2003 and January 2004, respectively.

The same background (measured with CGS car on a wooden ferry) was subtracted for both sets of calculations. The area specific stripping factors are shown in Table 2.3.1. Apparently the greatest variation is found for window 1 but when one recalculates as ratios the result is seen to be different. The ratios are shown in Table 2.3.2 and it is noticed that the ratios for all three windows behave more or less in the same manner. From October to January the stripping factor for Th apparently decreases and the stripping factor for potassium increases, whereas the uranium stripping factor ratios are almost constant. One might believe that this could be caused by seasonal variations, however, what cannot be seen from the results is the fact that the October measurements were made with a slightly malfunctioning detector system with inferior resolution as a consequence hereof. The thorium full energy peak of  $^{208}\text{Tl}$  was very wide. Taking this into consideration it is likely to be responsible for the  $\delta$ -ratio being different. It was therefore concluded that it should be possible to determine a set of area specific stripping factors and reuse them during another survey.

Table 2.3.1. Area specific stripping factors for measurements in Copenhagen.

Window	$\delta$		$\varepsilon$		$\zeta$	
	October	January	October	January	October	January
1	10.606	8.724	14.593	14.797	4.554	5.785
2	2.675	2.208	3.291	3.266	1.247	1.434
3	1.552	1.373	1.632	1.620	0.731	0.801

Table 2.3.2. Area specific stripping factors for measurements in Copenhagen.

Window	$\delta$ Oct/Jan-ratio	$\varepsilon$ Oct/Jan-ratio	$\zeta$ Oct/Jan-ratio
1	1.216	0.986	0.787
2	1.212	1.008	0.870
3	1.130	1.007	0.913

Figure 2.3.3 shows the smoothed stripped counts in low energy window 1 and smoothed, gross counts in the potassium window. The curves at many, short distances follow each other, but pay attention to the non-correlated variations. Varying measuring geometry is the major cause for this.



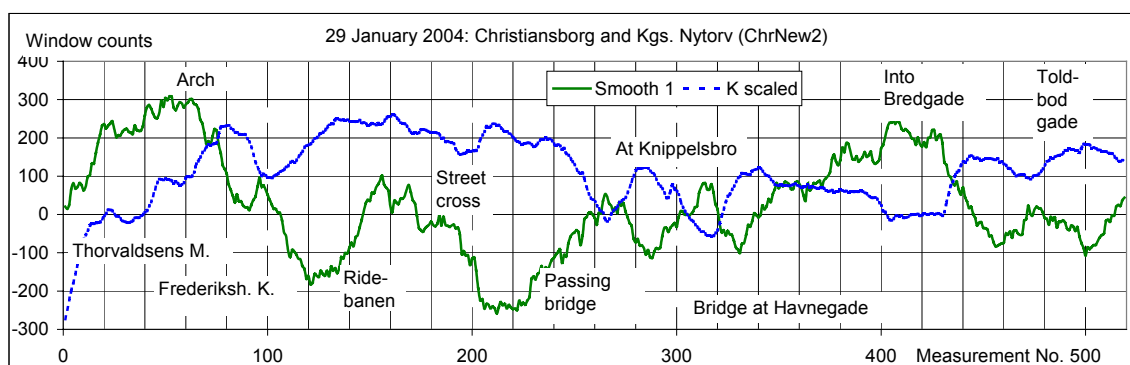


Figure 2.3.3. Smoothed, stripped counts in window 1 and smoothed, gross counts in potassium window.

### 3. Results for Norwegian CGS data

#### 3.0. Data and energy calibration

NRPA delivered 2 data sets consisting of 1-s 256-channels CGS measurements made with a 16L NaI detector. The detector was placed inside the vehicle. The data originates from the LIVEX exercise (team NOK), September 2001 (Ref. 2). The data contain very strong point source signals.

Area specific stripping factors have been calculated for both data files; however, each file has been split into a series of minor files in order to obtain a higher degree of environmental homogeneity for smaller areas (shorter distances).

#### 3.1. Energy calibration Barents Rescue LIVEX

The data are of a very good quality concerning spectrum drift. Only when a very strong source is encountered (profound) spectrum drift is observed. The same energy calibration was therefore used on all the data. NRPA (NGU) uses standard IAEA windows (Ref. 1) and NGU supplied information of the corresponding channels (no information below 662 keV). The windows are shown in Table 3.1.1 and the first channel is channel 1. An additional energy calibration (DTU) were made using information of channels for lower energies (extracted from a NASVD processing of the data). Both calibrations are of the type polynomial of second order, please confer Appendix B.

Table 3.1.1. NRPA (NGU) natural radionuclide windows.

Window	LL (chn.)	UL (chn.)	LL (keV.)	UL (keV.)
K	109	125	1370	1570
U	132	148	1660	1860
Th	189	220	2410	2810

#### 3.2. Area Specific stripping factors

For each of seven smaller files two sets of area specific stripping factors were calculated and each set contains stripping factors for nine windows. Tables with results for the NGU energy calibration are shown in Appendix K. The DTU energy calibration gave quite similar results that are not presented in this report. Prior to the calculations of the stripping parameters all data containing strong source signals were removed based on determination from rainbow plot using NUCSpec (Ref. 14).

Next all files - including source signals - were stripped. The results, stripped window count rates are shown as plots in Appendix M. Additionally, plots of the gross window count rates for the natural radionuclides and the nine windows are shown.

No background data information was available for the NRPA (NGU) system and due to having live times variations ranging from 0.1 s to 1.200 s caution should be exercised in the interpretation of the results.

Table 3.2.1 shows the nine low-energy windows for which area specific stripping factors were calculated. The numbers shown relate to the energy calibration based on energies above 662 keV.

Table 3.2.1. ASS windows, NRPA, Barents Rescue. NGU information.

Window	LL (chn.)	UL (chn.)	LL (keV)	UL (keV)
1	14	18	189.9	238.4
2	19	25	250.5	323.3
3	26	31	335.5	396.4
4	32	40	408.6	506.5
5	49	58	617.0	728.1
6	59	88	740.5	1101.9
7	89	110	1114.5	1379.6
8	32	38	408.6	482.0
9	39	48	494.2	604.7

Table 3.2.2 shows two examples of stripping factors. It is noticed that for file170901a (Nos. 0-8000) the stripping factors for thorium are larger than for uranium and vice versa for 170901d (Nos. 25001-32251).

Table 3.2.2. Area specific stripping factors  $\delta'$ (Th),  $\varepsilon'$ (U), and  $\zeta'$ (K). NGU information.

Window	170901a (C7)			170901d (C4)		
	$\delta'$	$\varepsilon'$	$\zeta'$	$\delta'$	$\varepsilon'$	$\zeta'$
1	4.65637	3.81138	1.97537	3.73475	4.74149	1.91612
2	3.75232	3.27126	1.80198	3.72960	4.22682	1.64459
3	1.55503	1.36437	0.75541	2.01274	2.42320	0.81395
4	1.67240	1.49151	0.87128	1.75307	2.18807	0.77078
5	0.93587	0.95274	0.60968	1.11847	1.32346	0.54006
6	1.63387	1.53415	1.08069	1.94917	2.08125	0.95495
7	0.54779	0.56483	0.51761	0.52033	0.80993	0.47673
8	1.36129	1.20625	0.70042	1.41324	1.76932	0.62158
9	1.37096	1.28131	0.77609	1.59603	1.91415	0.65554

In order to use the method on windows of other energy levels, the single channel stripping factors have been calculated, too, and plotted versus the centre channel of the window. Two plots are shown here; more plots can be found in Appendix L.

It is interesting to note the difference between the two plots. Figure 3.2.1 that uses no calibration data lower than 662 keV shows flat curves. In Figure 3.2.2 (< 662 keV energies included in the calibration) a characteristic "bump" is seen on both the uranium (b") and the thorium (a") curve. Pay attention to the fact that the centre channels are different. The Swedish CGS and AGS data followed the same tendency as the latter figure (Chapter 4 and 5).

The bump is the result of the stripping for window 4 and window 5. Those windows differ by slight displacements only in the following way (Left and Right refer to the page position of the two figures):

Left 4	channel 32-40	Right 4	channel 35-43
Left 5	channel 49-58 ( $^{137}\text{Cs}$ )	Right 5	channel 51-60 ( $^{137}\text{Cs}$ )

The selection of proper window limits for calculation of single channel stripping factors therefore is important, if details should be unveiled.

Window 5 (617 keV to 728 keV) includes part of the full-energy peak of the 609 keV  $^{214}\text{Bi}$  gamma line and is also affected by the low-level area sources of  $^{137}\text{Cs}$  (depositions) found in the surveyed areas.

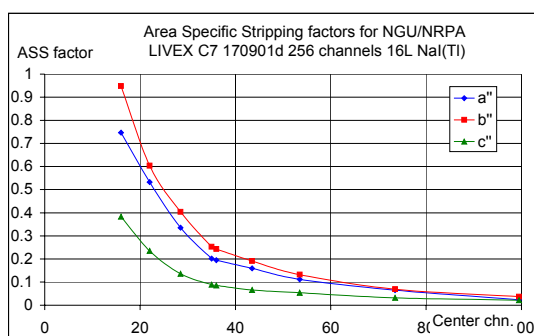


Figure 3.2.1. 170901d. NGU calibration.  $a''$ ,  $b''$ , and  $c''$ . (Single channel.)

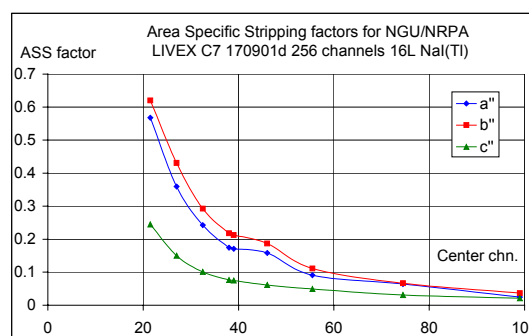


Figure 3.2.2. 170901d. DTU calibration:  $a''$ ,  $b''$ , and  $c''$ . (Single channel.)

When all data are combined and a total mean calculated, one obtains a plot like that of Figure 3.2.3 (18 data points). The "bump" is still visible. It is seen that there is not much difference between the single channel stripping factors for uranium and thorium with those for uranium being slightly higher. (For file 170901 the mean values for uranium are the highest for all data points, but for the file 180901 the mean values for thorium are the highest for all data points in two out of the three smaller files, Appendix L)

The mean values of the area specific stripping factors are shown in Appendix L. Data for the entire window is shown in Table L.1, and single channel stripping factors are shown in Table L.2.

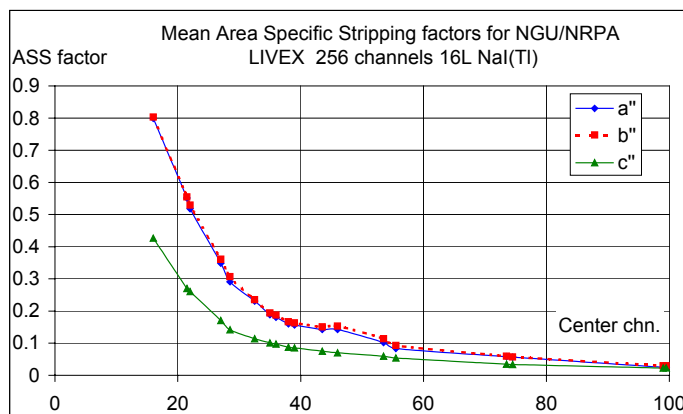


Figure 3.2.3. Norwegian single channel area specific stripping factors. Mean of all calculated values.

### 3.3. Results from LIVEX

The first part of the file from Area C7 (170901a) showed peculiar results around the measurements nos. 4600 to 6400 (Figure 3.3.1 and 3.3.3). In every window including window 7 that covers  $^{60}\text{Co}$  there is a large surplus of stripped counts. One might therefore assume that there is a source present. However, consider the rest of the curve for this area. The curves for the smoothed, stripped count rates are quite wavy with high fluctuations; seemingly this is not justified by the changes in count rates for the natural radionuclides only, although the potassium curve does show a slight decrease here, Figure 3.3.2.

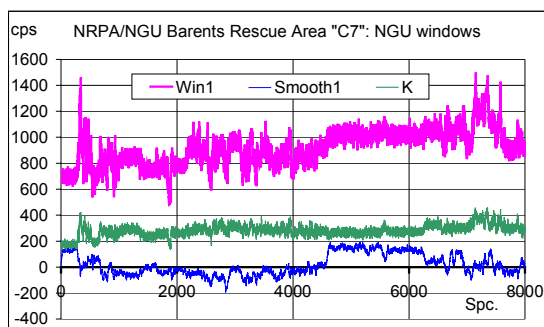


Figure 3.3.1. Gross cps in window1, and K window and smoothed, stripped cps in window 1, file 170901a.

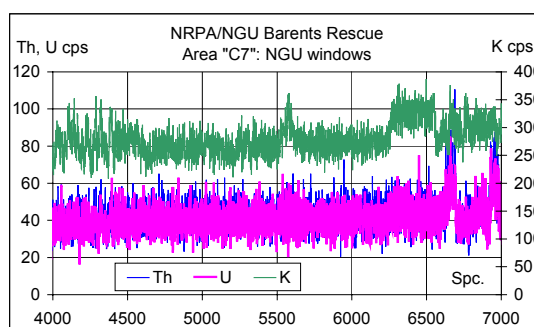


Figure 3.3.2. Gross cps for Th, U, and K, file 170901a.

The rainbow presentation of the file did not show distinct point sources, and area specific stripping factors were calculated based on the entire file. (Between measurement no. 4500 and 6200 (Figure 3.3.1) the car moved only 300 m and, therefore, this interval with a significant amount of unusual radiation influenced the stripping parameter calculations rather much whereby negative stripped counts are obtained for distances without this unusual radiation)

The reason for the unusual radiation has not been identified. Presumably the reason is a rather special environmental geometry.

The Danish team DKK also noticed unusual radiation in this area around Älvsbyn (NASVD analysis) but it was not reported.

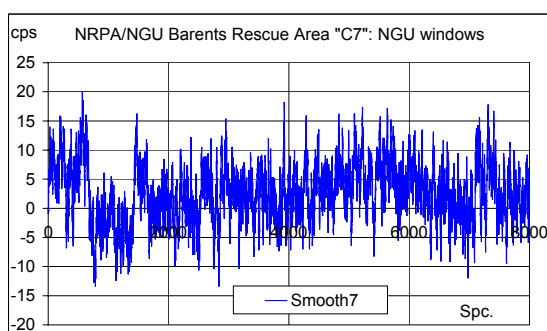


Figure 3.3.3. Smoothed, stripped cps in window 7 ( $^{60}\text{Co}$ ), file 170901a.

The curve for the smoothed, stripped cps in window 1 presented in Figure 3.3.1 is not representative for the general results of the area specific stripping procedure. In Figure 3.3.4 the gross cps and the smoothed, stripped cps resulting from file 170901b (Nos. 8001-14000) are shown for the same window.

The curve for the stripped cps, Figure 3.3.5 (take-out from Figure 3.3.4), fluctuates nicely around 0 with an average excess of 8.7 counts, except for two strange negative peaks (<-100) around measurements nos. 4449-4451 (4428-4510) and 4893 (4855-4911). Those peaks are found to exist for the windows 1-4. The reason is assumed to be a local geometry peculiarity e.g. road type, buildings and/or topography.

From the information presented after the LIVEX exercise it was made known that in this area there was a  $^{226}\text{Ra}$  source (piece of rock from Kvarnån). The position of this source (7:8) is indicated on Figure 3.3.6 together with the track lines for team NOK. The triangles represent the start and end of the negative peaks and the round dots are the minimum values (most negative).

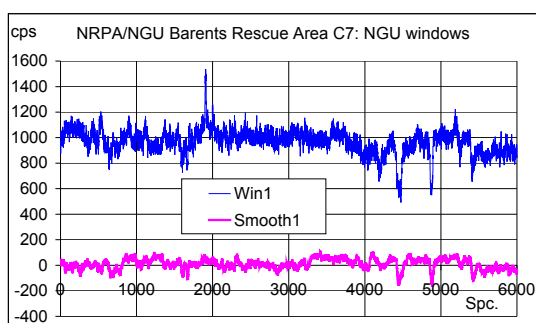


Figure 3.3.4. Gross cps and stripped, smoothed cps in window1, file 170901b.

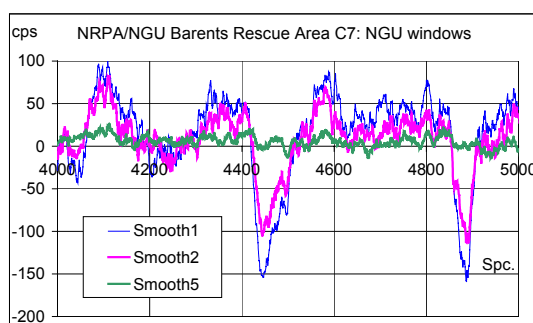


Figure 3.3.5. Smoothed, stripped cps in three low-energy windows. (Win5:  $^{137}\text{Cs}$ ).

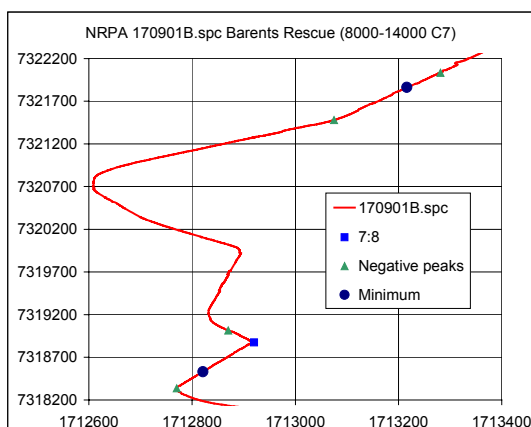


Figure 3.3.6. Track lines, negative peaks and  $^{226}\text{Ra}$  source.

The distances corresponding to those measurements seem far too long to be related to the source. The lowest triangles (first negative peak) and the lowest dot are possibly close enough to the source to be related to it, however, the upper triangles (second negative peak) surely are not. Yet, for some reason, a large "over-stripping" has occurred on those distances. Figure 3.3.7 shows the gross cps for the natural radionuclides (measurement nos. 4000-5000 in file 170901b). Due to large variations in the measurement time the counts have been normalised with the live time. The corresponding live time plot is shown as Figure 3.3.8. The count rates for all three radionuclides decrease for those two distances and it is not live time related.

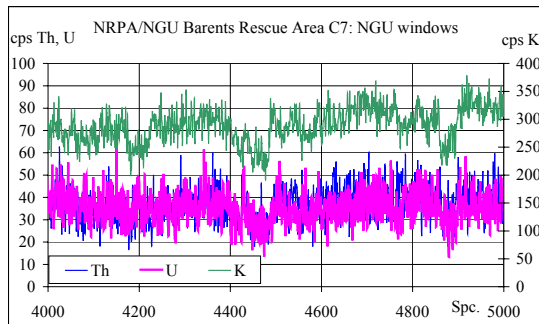


Figure 3.3.7. Gross count rates for the natural radionuclides, file 170901b.

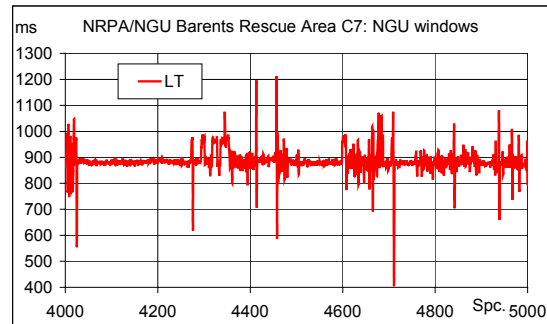


Figure 3.3.8. Live times in milliseconds, file 170901b.

The apparent independent variation of K to that of Th/U is believed to be the main reason that this source was not found during the LIVEX exercise (NOK did find this source during post processing of data). "Anomalies" of potassium was a frequent occurrence on the monitor screens (small rocks) and this is very likely to make an operator display less suspicion in case of other "natural anomalies" such as a rock  $^{226}\text{Ra}$  source.

Many of the exercise sources were of very high source strengths. The area specific stripping method meets no problems in finding those sources; the recorded signals for team NOK are so strong that the sources can be found without any other data processing than extraction of count rates from the data set. Figure 3.3.9 shows the gross window count rates for the natural radionuclides in file 170901c (all measurements). It is evident that there is something not natural around measurement nos. 9500-10000. The count rates of all three radionuclides increase, even Th. The live time drops to very close to zero, spectrum drift occurs and as a consequence the source is registered in the "natural" windows, too. Figure 3.3.10 shows a rainbow presentation of the measurements around spectrum number 9500. Without any doubt this is a  $^{60}\text{Co}$  source.

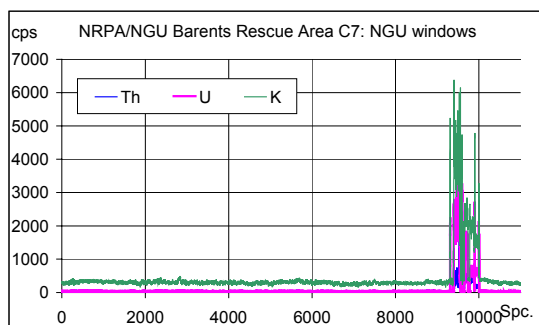


Figure 3.3.9. Gross window count rates, for natural radionuclides, file 170901c.

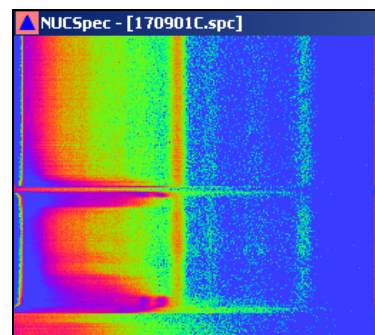


Figure 3.3.10. NUCSpec plot around measurement no. 9500, file 170901c.

Figure 3.3.11 shows another group of spectra with a significant surplus of stripped counts for the spectra nos. 400 to 950. Figure 3.3.9 - and Figure 3.3.12 - show that the natural radiation level is not unusual here. There is a high excess of counts in both the caesium (5), the cobalt (7) and the lower energy windows (e.g. 2) signifying a source of high to medium energy and the source is believed to be  $^{60}\text{Co}$ , but it cannot be shown for sure due to the poor energy stabilisation at the high count rate.

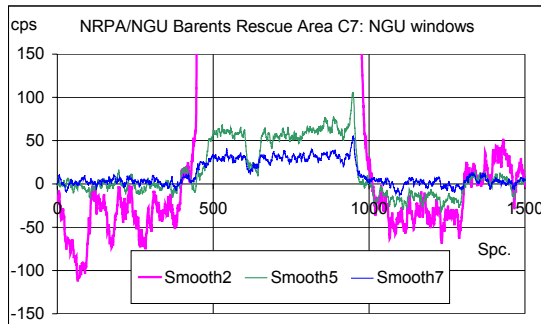


Figure 3.3.11. Smoothed, stripped count rates for three low energy windows (C7:5).

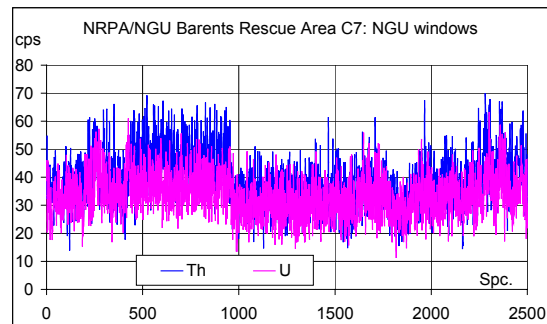


Figure 3.3.12. Gross window count rates, for U and Th, file 170901c.

Analysis with NUCSpec shows no full-energy peak signals. [Ref. 2 informs that it is a  $^{60}\text{Co}$  source, C7:5. ] One also notices the "over-stripping" just before and after the occurrence of the source.

Over-stripping when close to a source is even more significant in Figure 3.3.13. Occurrence of negative counts (or count rates) do not necessarily signify that the applied stripping factors are incorrect. The figure shows the stripped, smoothed count rates for two low energy windows together with gross potassium count rates (last measurements in the file 170901c only). This is undoubtedly due to a  $^{60}\text{Co}$  source – or possibly more than one, Figure 3.3.12.

The source increases the number of counts in the potassium window and the stripping is not performed correctly. One should therefore pay attention to negative outliers as well as positive outliers when using the ASS method.

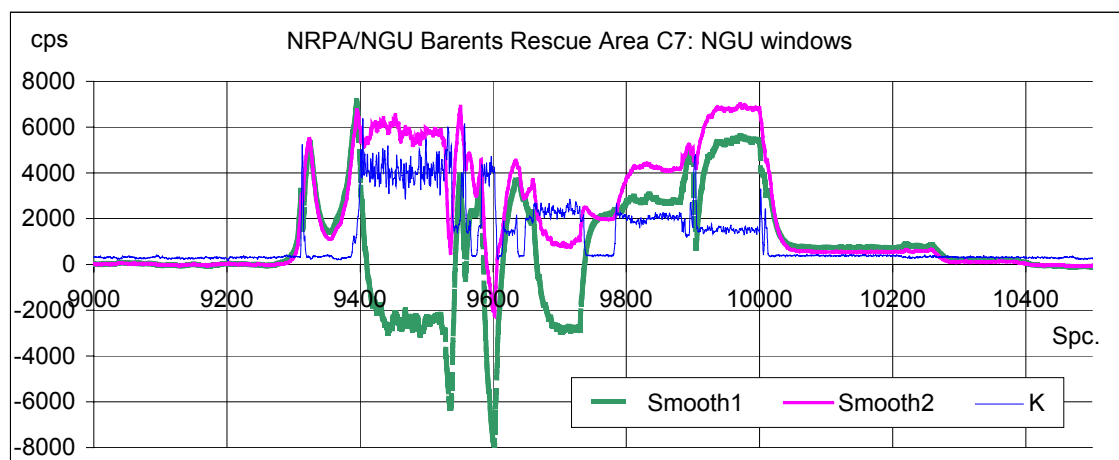


Figure 3.3.13. Smoothed count rates for two low energy windows (chns. 14-18 and chns. 19-25) and gross potassium count rates for file 170901c.

The information on the sources used in the exercise also lists a  $^{226}\text{Ra}$  source (rock from Kvarnån) located in the same area. This source was not detected by the ASS method; neither before nor after co-ordinate plots of track lines were made (Figure 3.3.14) to estimate the spectrum numbers for a source signal. It was expected to find this source (7:7) around measurement No. 9055 but it was not observed. NASVD was not able to spot this source either. (No figures shown.)

The file 170901d contains the last 7251 measurements from the area C7. NGU made identification in real-time of two  $^{60}\text{Co}$  sources, 7:1 and 7:2, in this area. A  $^{226}\text{Ra}$  source, 7:6, was hidden in the vicinity of the  $^{60}\text{Co}$  source 7:2. This source was not identified by NGU either in real-time or during post processing of the data sets.



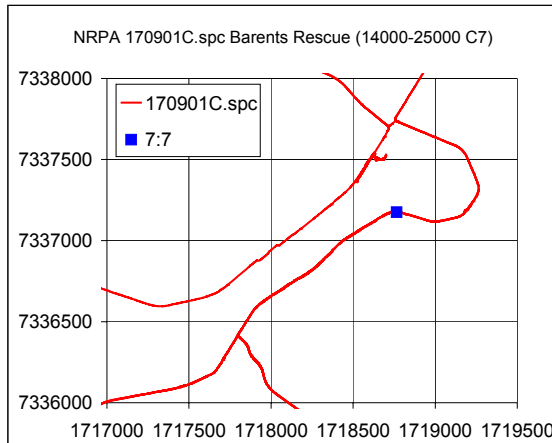


Figure 3.3.14. Location of source 7:7.

The file 170901d contains the last 7251 measurements from the area C7. NGU made positive identification in real-time of two  $^{60}\text{Co}$  sources, 7:1 and 7:2, in this area. A  $^{226}\text{Ra}$  source, 7:6, was hidden in the vicinity of the  $^{60}\text{Co}$  source 7:2. This source was not identified by NGU either in real-time or during post processing of the data sets.

The exact location of the  $^{226}\text{Ra}$  source was revealed after the LIVEX exercise and has been plotted on the map in Fig. 3.3.15 together with the  $^{60}\text{Co}$  source 7:2 and track lines for the NGU team. The measurement closest to the hidden source is measurement No. 1049.

The measurements for the area with the  $^{226}\text{Ra}$  source were first investigated using NucSpec. The visual inspection using NucSpec, Figure 3.3.16, revealed no information about the hidden  $^{226}\text{Ra}$  source and determination of the source location based on rainbow plots and spectral information in NucSpec is not possible.

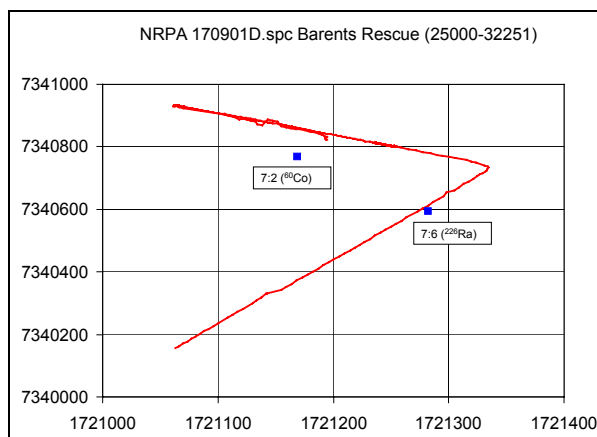


Figure 3.3.15. Track lines and location of  $^{60}\text{Co}$  source 7:2 and  $^{226}\text{Ra}$  source 7:6.

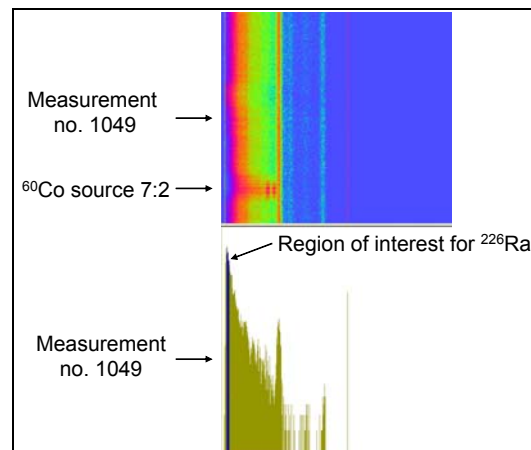


Figure 3.3.16. NUCSpec image: Searching for a hidden  $^{226}\text{Ra}$  source (186 keV).

The data were further investigated by plotting the stripped and smoothed count rates as a function of measurement number. This was done for all the windows (1-9) for the measurements no. 950-1150 which cover the location where the  $^{226}\text{Ra}$  source was placed.

The results from the investigation of the stripped and smoothed count rates in the windows No. 1-3 are shown in Figure 3.3.17 (stripped) and 3.3.18 (stripped and smoothed).



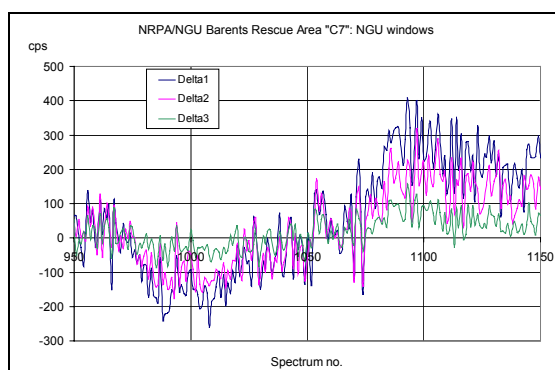


Figure 3.3.17. Stripped cps win 1-3, spectrum Nos. 950-1150, file 170901d.

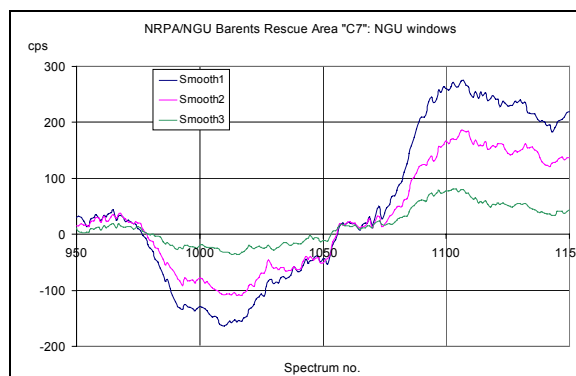


Figure 3.3.18. Stripped smoothed cps win 1-3, spectrum Nos. 950-1150, file 170901d.

A  $^{226}\text{Ra}$  source may - dependent on the distance - be identified by the at 186 keV gamma line. If detectable, the source would result in a surplus of stripped (and smoothed) count rates in window No. 1 which has a lower and an upper limit of 189.9 keV and 238.4 keV respectively. This is not optimal for a  $^{226}\text{Ra}$  source with its 186 keV energy peak, but sufficiently close for a signal to be detected. However,  $^{226}\text{Ra}$  is part of the uranium decay chain so it is also possible that a  $^{226}\text{Ra}$  source could result in a surplus of stripped count rates in one of the other windows due to gamma radiation from  $^{214}\text{Bi}$  in the uranium/radium decay chain.

The presumed location of the  $^{226}\text{Ra}$  source is close to where measurement No. 1049 was carried out. The measurement nos. 0-1000 exhibit variations in stripped count rate ranging from 100 to -100 cps. There were no sources present in the area where these measurements were carried out so count rate variations within this range is representative for measurements of natural activity and a varying geometry.

The stripped and smoothed count rates for the measurements located in the vicinity of the  $^{226}\text{Ra}$  source (measurement nos. 1040-1060) fluctuate around zero with a slight negative shift for all the windows 1-3. The measurements to the left (measurement nos. < 1040) seem to be slightly "over-stripped". The measurements to the right (measurement nos. > 1060) seem to be influenced by the radiation from the  $^{60}\text{Co}$  source 7:2. The curves in Figure 3.3.17 and 3.3.18 do not exhibit a pattern of surplus stripped or smoothed count rates around measurement no. 1049 which would clearly indicate the presence of a  $^{226}\text{Ra}$  source.

More plots showing the results from stripping of measurement data in the other windows (4-9) are found in Appendix M. Similar to the figures 3.3.17 and 3.3.18, some of the plots in Appendix M show signs of being slightly "over-stripped" in the region to the immediate left of where the  $^{226}\text{Ra}$  was located. However, this is almost within the range of the natural variations. There is no clear indication of the hidden  $^{226}\text{Ra}$  source in any of the figures.

It is not possible from the stripped and smoothed count rates and with the applied window settings to determine the position of the hidden  $^{226}\text{Ra}$  source (7:2) for the measurements in the file 170901d. Recalculating the stripping factors for a window optimised for  $^{226}\text{Ra}$  might result in a different conclusion. A  $^{226}\text{Ra}$  source may - dependent on the distance - expose the detector to a spectrum with a surplus (low distance) or deficit (long distance) of low energy photons relative to the amount of high energy photons (1765 keV). Therefore - in principle - a  $^{226}\text{Ra}$  source may generate a surplus or a deficit of low energy window (stripped) count rates.

Narrow windows centred around the low energy gamma lines from  $^{214}\text{Bi}$  and  $^{214}\text{Pb}$  in theory will have the highest sensitivity. This has not been examined during the project.

The files 180901a and 180901b both cover area C3 of the Barents Rescue exercise. The count rates in the natural radionuclide windows show normal fluctuations; occasionally the ratio of potassium to thorium (or uranium) increases but this only introduces minor errors in the low energy windows. The only existing source is very easily found in both files. In file 180901a, Figure 3.3.19, the source was passed for the first time and is evident that team NOK performed a further investigation here.

Figure 3.3.19 that shows the stripped count rates in the cobalt-60 window clearly indicates that this is a  $^{60}\text{Co}$  source. The same is the case for Figure 3.3.20 (second encounter with the source) that also shows the stripped count rates in the cobalt-60 window (almost flat curve) along with the stripped count rates in a low energy window and gross potassium count rates (upper curve). This time (180901b) the source was not investigated, yet there are enough measurements (5) giving errors large enough to identify the source as  $^{60}\text{Co}$ . Figure 3.3.21 and 3.3.22 show the track lines for the Norwegian car.

For some reason the GPS results are bad here, which could have given a bad estimate of the source position, had the source not been investigated on foot (Ref. 2).

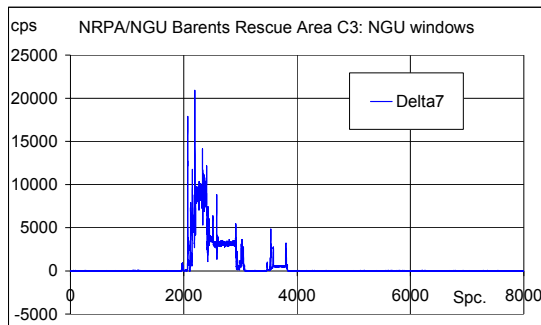


Figure 3.3.19. Stripped count rates in cobalt window, file 180901a.

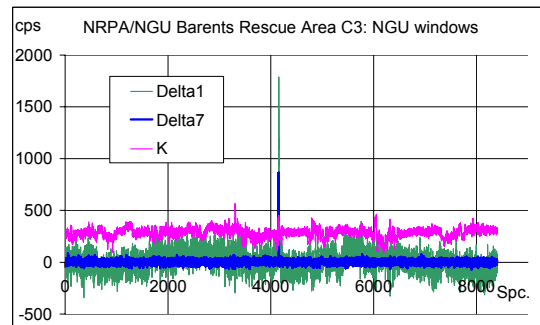


Figure 3.3.20. Stripped count rates in cobalt window and low energy window 1 together with gross count rates for K, file 180901b.

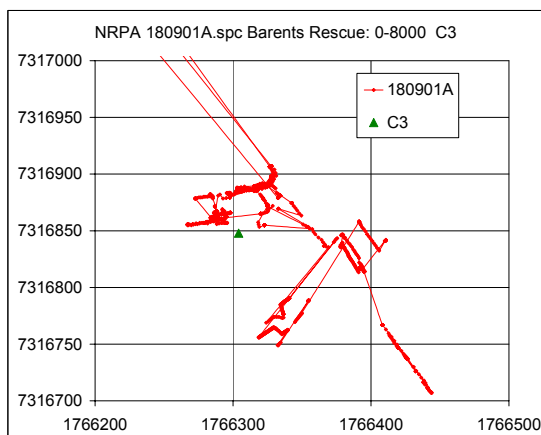


Figure 3.3.21. Track lines 180901a.

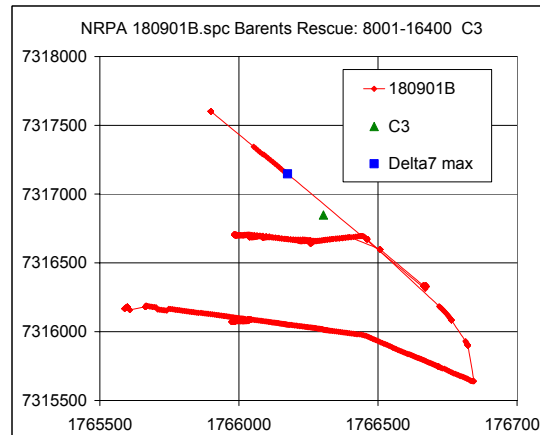


Figure 3.3.22. Track lines 180901b.

There is no doubt that the file 180901c contains sources and – judging from the track lines – there are more than one source of the same source type. Figure 3.3.23 shows the smoothed count rates (and potassium gross count rates) for the caesium

window (5) and the cobalt window (7). Around measurement Nos. 608-1180 there is a high number of surplus counts in the caesium and cobalt window both. Since a high stripped count rate in the cobalt window usually signifies a cobalt source one might come to this conclusion by looking solely at the cobalt window.

Consider Figure 3.3.24; this figure shows the full ordinate scale and it is noticed that the stripped count rates in the caesium window are of a much higher order of magnitude. This could, of course, mean that the source in question was a thoroughly shielded cobalt source. For a cobalt source to produce an error this large in the caesium window that cobalt source must be very strong indeed and is likely to interfere with the potassium window also. This is not observed (Figure 3.3.23). In all likelihood the source is  $^{137}\text{Cs}$  source.

Around measurement nos. 3356-3774 another source is observed (track lines prove that this is another source). This time the error count rates in the cobalt window are far greater than in the caesium window. This is undoubtedly a  $^{60}\text{Co}$  source.

However, Figure 3.3.25 and Figure 3.3.26 pose some questions.

The source around measurement Nos. 9355-10841 is actually the same source as in the previous figures around measurement nos. 3356-3776 but this time the caesium errors are far greater than the cobalt errors and one might easily come to the conclusion that this is a  $^{137}\text{Cs}$  source. The small peak around measurement no. 9370 should make the interpreter suspicious of this conclusion, however, (that same peak is found in Figure 3.3.23 around measurement no. 3100); this very distinct peak could mean  $^{60}\text{Co}$  instead of  $^{137}\text{Cs}$ . For comparison consider again Figure 3.3.23 around the measurement nos. 608-1180. Although there are counts in the cobalt window too, not supposed to be there, there is not one single remarkable peak, but a wobbly curve consisting of several minor spikes.

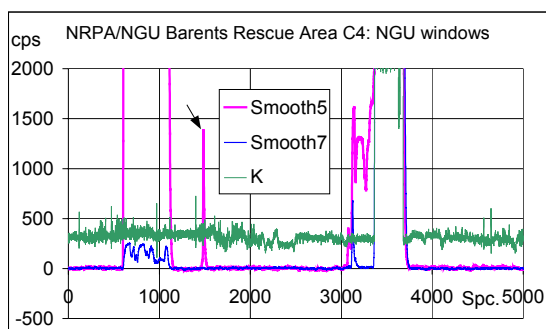


Figure 3.3.23.  $^{137}\text{Cs}$  source and  $^{60}\text{Co}$  source, file 180901c.

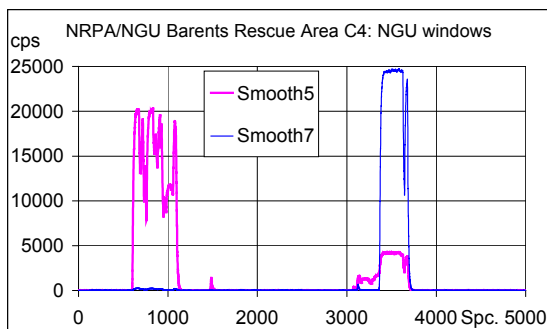


Figure 3.3.24. Same as 3.3.21 with changed ordinate axis, file 180901c.

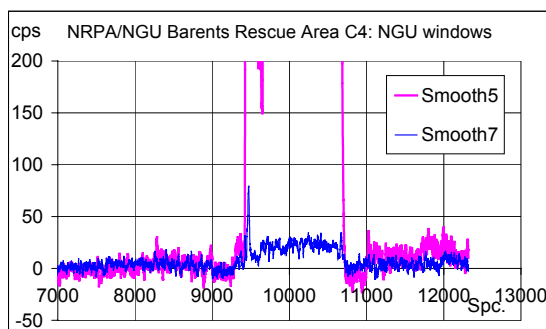


Figure 3.3.25. Same  $^{60}\text{Co}$  source as in Figure 3.3.23. Different field of view.

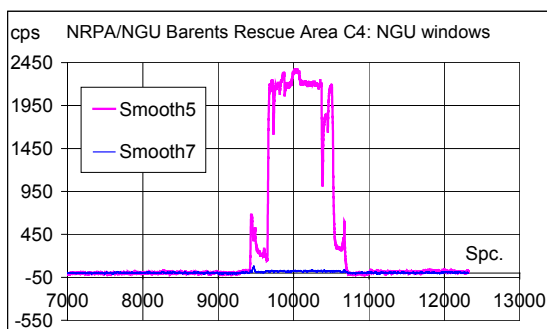


Figure 3.3.26. Same as 3.3.25 with changed ordinate axis.

When the data are treated using a program providing a visual colour representation of the data, there is no doubt that the first source of Figure 3.3.23 is a  $^{137}\text{Cs}$  source. The 662 keV full energy peak is visible and there is no doubt that the second source of Figure 3.3.23 is a  $^{60}\text{Co}$  source because the full energy peaks are visible, too. In the case of Figure 3.3.25 and the doubtful source type the ASS method cannot be used without the knowledge of a skilled data operator. No full energy peaks are seen at all but the pattern of the scattered radiation will tell a skilled spectrum interpreter that this is indeed a  $^{60}\text{Co}$  source and not a  $^{137}\text{Cs}$  source.

Concluding from the results from Figure 3.3.23 and Figure 3.3.25 the area specific stripping method should not be used on its own. It will definitely help the user to spot sources where no full energy peaks are available but the source cannot always be correctly identified by type. Nothing can replace skilled personal on this topic, but even a person with no specific training would be able to detect that there definitely is something not related to natural radiation.

During the LIVEX exercise the Danish carborne team DKK found another source in this area. The source was found by investigations on foot due to an increase in the amount of scattered radiation in low energy windows (ASS was used during the survey). Figure 3.3.27 shows the track lines for team DKK and the position of the source ( $^{137}\text{Cs}$  1.3 GBq) and Figure 3.3.28 shows the track lines for team NOK who did not find this source that was passed in both directions with a distance of approximately 120 m.

In order to examine in greater detail the possibility of finding this source by the ASS method some “cheating” was done. From the plot of the track lines the source signals, if any, were expected to be found around measurements nos. 2535-2565, 2903-2922, and 9235-9267. Around measurement no.9256 one can observe a single measurement with an increase in count rate but this seems to be natural and is very likely related to passing a road crossing where there were no vegetation to shield natural radioactivity in the ground. (The source was down a side row out very poor quality.)

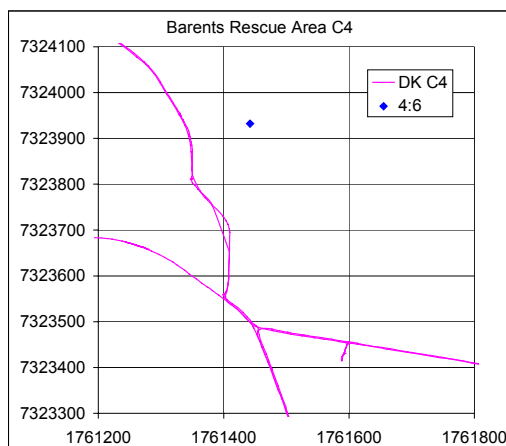


Figure 3.3.27.  $^{137}\text{Cs}$  source location and path for the DKK car.

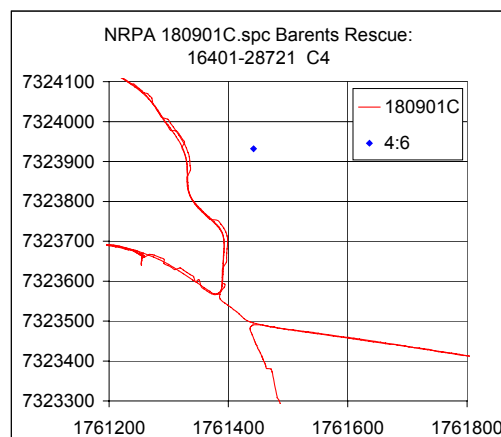


Figure 3.3.28.  $^{137}\text{Cs}$  source location and path for the NOK car.

The stripped window count rates, however, do not show any signs of this source – not even when one knows where to look. The DKK team used a 2-s sampling time and team NOK used a sampling time of 1-s and although the NOK detector was 4 times as large as the DKK detector there is simply no trace of this source in the NOK data set. It is assumed that even with the very large detector the position of the

detector inside the car renders the ASS method partly unusable for location of “weak” (strongly shielded) sources emitting only photons of very low energy. The detector height above the ground may be the most important factor. (The DKK detector was placed outside on the roof of the car at a height of 2.2m.)

## 4. Results for Swedish CGS data

### 4.0. Data

This report describes the result for 3 data sets delivered by SSI. The sets consist of 5-s 256-channels CGS measurements made with a 3"×3" NaI detector. The detector was placed inside the vehicle. The data sets all include point source signals and originate from the LIVEX exercise (Ref. 2).

### 4.1. Energy calibration

The data supplied by SSI are characteristic of what one would obtain for a detector with no gain stabilisation. Spectrum drift is observed; the spectra slides continuously up or down the energy axis as time progresses and the presence of strong point sources further provokes the spectrum drift.

The data files show different positions of the natural nuclide full energy peaks the position of which forms the basic for the energy calibration of the system. Therefore an energy calibration for each measurement file has been determined. One might argue that it is not necessary to perform an energy calibration in order to calculate stripping factors for a low-energy window as long as the upper and lower channel number of the window is known. However, since data material from several contributors: NGU/NRPA, SGU, and SSI are treated in this report (together with previous investigations of the Danish systems), it was considered reasonable for comparative reasons to choose windows covering approximately the same energy intervals for all systems.

The energy windows normally used by SSI are quite wide and the potassium and the uranium windows have channels in common. In this report the standard windows recommended by IAEA have been used.

The spectrum drift is shown in Figure 4.1.1. Here the mean spectra for the three Barents Rescue files are shown in the same plot. It can be observed that there exists a difference of approximate seven channels between the series C3\_1 and C4\_2 (C3 Area, C4 Area). For a system using 256 channels this corresponds roughly to 85 keV displacement.

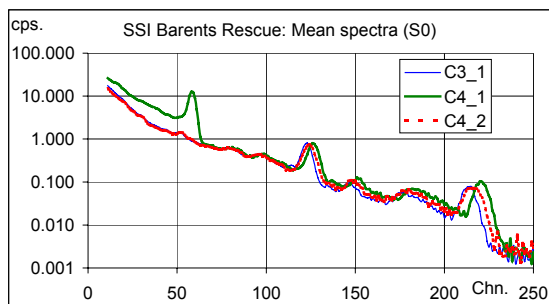


Figure 4.1.1. Mean spectra. SSI, Barents Rescue.

Each file was energy calibrated using outcome from a NASVD processing of the data. The full energy peak positions were found from the mean spectrum,  $s_0$ , and the next two spectral components  $s_1$ , and  $s_2$ . Spectral components of higher number included strong spectrum drift and could not be used for this purpose. The upper and lower channel for nine low-energy windows were defined from the energy calibration so as to cover the same energy intervals determined for the data from SGU.

It has been assumed that SSI denotes the first channel as channel 1. DEMA/DTU has the habit of denoting the first channel as channel 0. All energy calibrations were performed using a polynomial of order 2 and plots are shown in Appendix B. The trend line equations refer to first channel being channel 1. (The offset if counting from channel 0 instead is also stated.)

In the calculation of the area specific stripping factors those nine windows were used together with the three standard windows for Th, U, and K. For each file the calculations were performed with channel levels found from the energy calibration to correspond to the energy intervals suggested by IAEA (Ref. 1).

## 4.2. Area Specific stripping factors

For each of the files supplied by SSI area specific stripping factors were calculated for nine windows. Tables with the results are shown in Appendix K. The results given as stripped window counts are shown as plots in Appendix M. Additionally, plots of the gross window counts for the natural radionuclides and the nine windows are shown. The BASIC program cgslaes.bas was used for the data processing. No background spectrum data information was available for the SSI systems.

It was necessary to exclude parts of data containing very strong source signals before the area specific stripping factors could be calculated. The entire data sets including source signals were stripped using the respective stripping factors. No measurements were excluded due to spectrum drift.

The following is an example of the results for one data set, Barents Rescue, Area C4\_1. Table 4.2.1 shows the channel intervals for the low-energy windows for which area specific stripping factors were calculated and the set of corresponding stripping factors are shown in Table 4.2.2.

Table 4.2.1. ASS windows. SSI, Barents Rescue, Area C4\_1.

Window	LL (chn.)	UL (chn.)	LL (keV)	UL (keV)
1	17	21	191.5	236.4
2	23	29	259.0	326.7
3	30	35	338.0	394.7
4	36	45	406.0	508.5
5	54	64	611.6	726.7
6	65	96	738.2	1099.7
7	97	120	1111.4	1384.0
8	36	42	406.0	474.3
9	43	53	485.7	600.1

Table 4.2.2. Area specific stripping factors  $\delta'$ (Th),  $\varepsilon'$ (U), and  $\zeta'$ (K).

Window	$\delta'$	$\varepsilon'$	$\zeta'$
1	4.57778	3.19525	3.71330
2	3.37372	2.50633	2.85551
3	1.81626	1.25900	1.50467
4	2.20108	1.35448	1.64051
5	1.01337	0.75712	0.96437
6	1.88686	1.360085	1.80091
7	0.52523	0.52358	0.72522
8	1.53814	0.97300	1.18620
9	1.82713	1.28190	1.52803

The stripping factors for thorium and potassium are almost the same for all three files whereas the uranium stripping factor varies. For two of the three files, the thorium stripping factors are higher than the uranium stripping factors.

Additional plots of single "channel" stripping factors can be seen in Appendix L. (Due to different energy calibrations in the SSI files, the stripping factors were calculated as a function of energy in keV.)

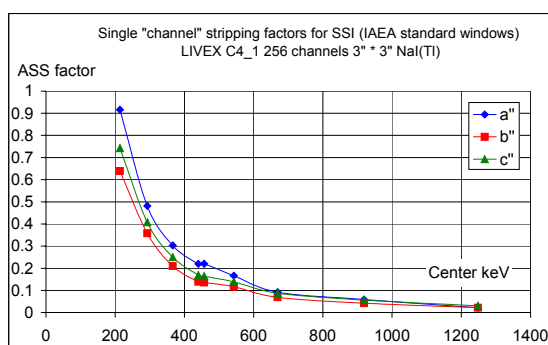


Figure 4.2.1. Single "channel" stripping factors for SSI, LIVEX, Area C4\_1

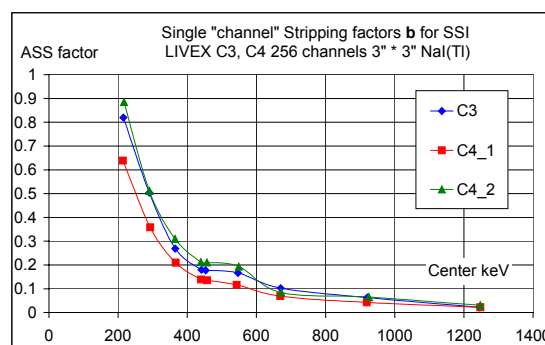


Figure 4.2.2. Uranium single "channel" stripping factors for SSI, LIVEX.

### 4.3. Results from Barents Rescue LIVEX

The data from the Barents Rescue exercise included signals from strong sources and signals from weak sources. In Appendix C are listed the source types and activities for the survey areas. Track lines for the CGS measurements are shown there, too, with source positions indicated.

The stripping of the file C3 from Area 3 leads to no surprising results. The area only included one source and this source is easy to find with or without applying the stripping procedure. The source is found due to the dramatically increased number of (stripped or non-stripped) counts in all the low-energy windows. Figure 4.3.1 shows an example.

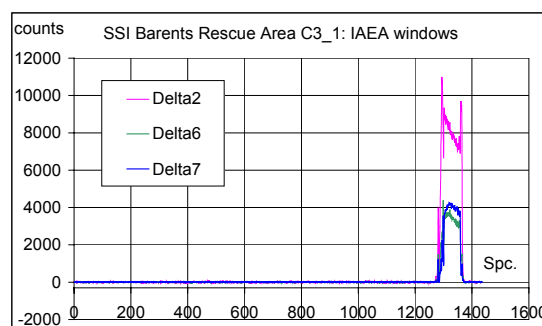


Figure 4.3.1. Surplus (stripped) counts in low-energy windows after stripping.



Delta5 refers to a stripped  $^{137}\text{Cs}$  window and Delta7 refers to a stripped  $^{60}\text{Co}$  window. That the source is a  $^{60}\text{Co}$  source is seen from the pile up: a very high number of counts is found in all three natural radionuclide windows, Figure 4.3.2. and Figure 4.3.3. (both gross counts), especially in the potassium window that partly overlaps with the cobalt window (window 7).

It is worth to notice the influence from the spectrum drift on the number of measured counts: the number of counts in the potassium window increases when the number of counts in the cobalt window decreases. For data influenced by strong spectrum drift, the method cannot be used directly for estimation of source strengths.

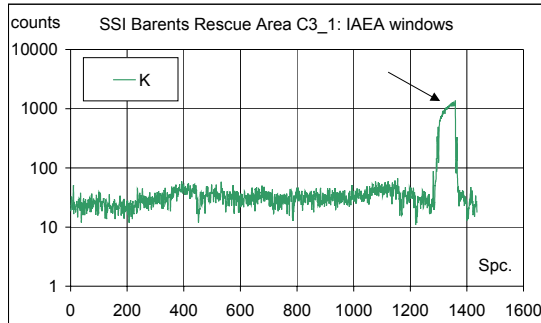


Figure 4.3.2. Increased K counts and spectrum drift.

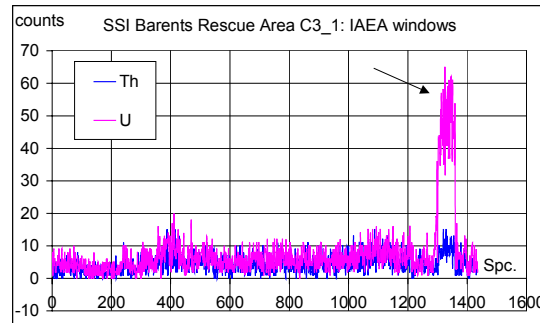


Figure 4.3.3. Pile up in U-window and Th-window.

In the file C4\_1 one source was found. Figure 4.3.4 (and 4.3.5) shows the stripped counts for the  $^{137}\text{Cs}$  window (Delta5), the  $^{60}\text{Co}$  window (Delta7) and a lower energy window. The source is not  $^{60}\text{Co}$ , there is no increase in the cobalt window, so the source must have a gamma energy lower than that of  $^{60}\text{Co}$ . The source is identified as  $^{137}\text{Cs}$  and judging from the track lines there is only one source. (This is source 4:1,  $^{137}\text{Cs}$ , 0.4 GBq.) No other changes in the stripped counts level that fluctuates around zero, indicate that special anomalies or other sources should be present.

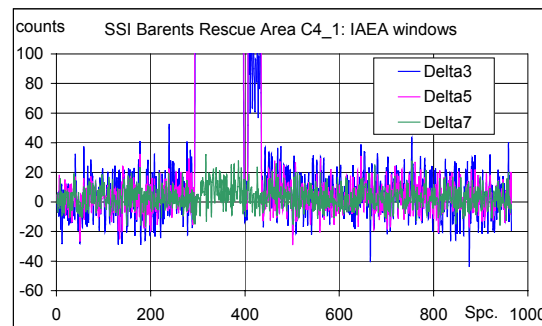
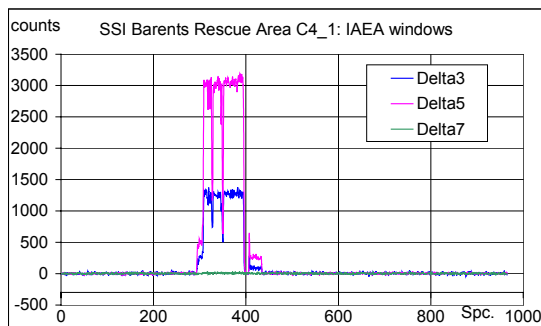


Figure 4.3.4. Stripped window counts, C4\_1. Figure 4.3.5. Different scaling of Figure 4.3.4.

Area C4\_2 was very homogeneous with respect to the ratios between Th, U, and K, Figure 4.3.6. Around measurement Nos. 91-166 the stripped count rates in the lower windows presented a small bump that was very dominant in window 5 representing  $^{137}\text{Cs}$ . Also around measurements Nos. 562-572 a small peak was found. Those signals were not present in windows above window 5, Figure 4.3.9. Track line analysis made it likely to assume that the two groups of spectra were related to the same source, expected to be  $^{137}\text{Cs}$ . Signals with very high spikes were found around measurements Nos. 32-53. Arrows in Figure 4.3.7 indicate the mentioned groups of spectra.

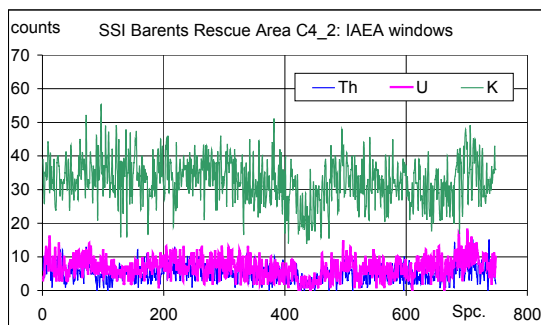


Figure 4.3.6. Area C4\_2. Th, U, and K gross counts.

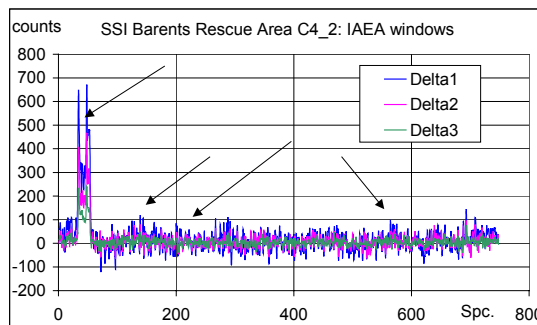


Figure 4.3.7. Stripped counts in three low-energy windows, Area C4\_2.

In the Barents Rescue LIVEX exercise report (Ref. 2) it is mentioned that there is a  $^{192}\text{Ir}$  source close by. The 605 keV full energy peak from this nuclide will also be found in window 5 ( $^{137}\text{Cs}$ -window) and the 315 keV full energy peak partly in window 2 and partly in window 3.

The latter two windows will also contain scattered radiation from caesium. The  $^{192}\text{Ir}$  source was found but could not be identified by the area specific stripping procedure.

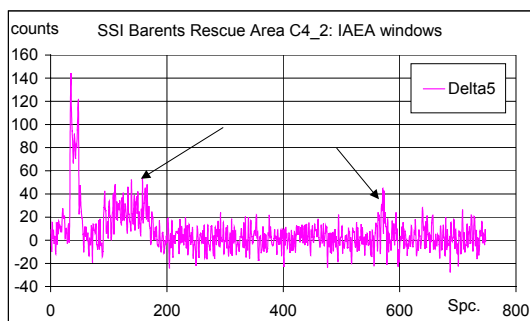


Figure 4.3.8. Source 4:2 passed twice. Stripped counts in  $^{137}\text{Cs}$  window.

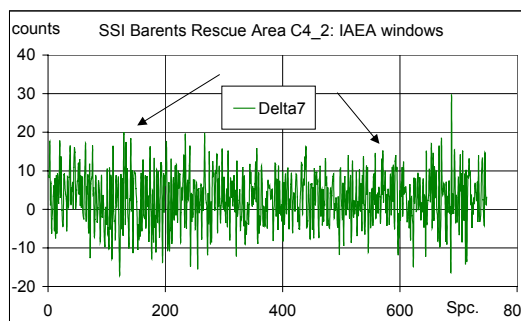


Figure 4.3.9. Stripped counts in  $^{60}\text{Co}$  window.

The spike signals found around measurements Nos. 32-52 also were seen in window 6 (not shown, please confer Appendix M) and the two high peaks and one smaller peak found in e.g. window 2 and window 5, Figure 4.3.10 could be an indication of more than one source present. The source(s) must have an energy at least as high as  $^{137}\text{Cs}$  with pile-up or the source(s) is likely to be  $^{60}\text{Co}$ .

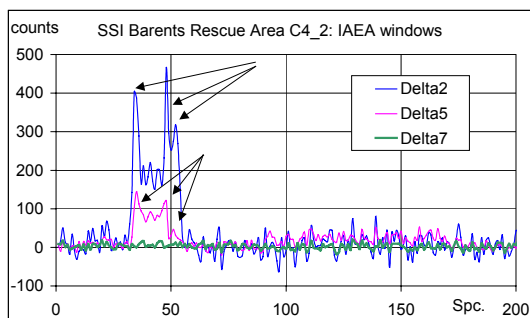


Figure 4.3.10. Stripped counts in  $^{137}\text{Cs}$  window (5),  $^{60}\text{Co}$  window (7) and low energy window.

The curve of the stripped counts in window 7, Figure 4.3.11, shows a flat, positive plateau with two flat spikes consisting of more than one measurement, i.e. more than normal fluctuations. This indicates, that the source(s) in fact is  $^{60}\text{Co}$ .

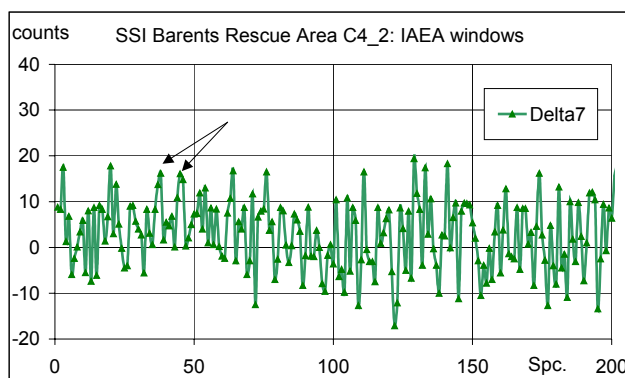


Figure 4.3.11. Stripped counts in  $^{60}\text{Co}$  window.

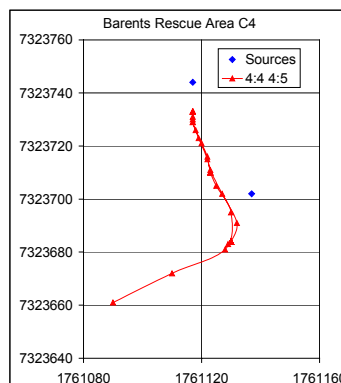


Figure 4.3.12. Sources 4:4 and 4:5.

By using the information on source position presented in the Barents Rescue report (Ref. 2), the track lines, Figure 4.3.12, indicate that first source 4:4 was passed, and then source 4:5 and that source 4:4 was revisited upon return to the main road.

Two other sources that, according to the track lines, could have produced signals were not found. Those sources (4:6 1.3 GBq  $^{137}\text{Cs}$  and 4:7 1.9 GBq  $^{137}\text{Cs}$ ) were expected to show up around measurement Nos. 225-235 (arrow, Figure 4.3.7) if the signals were strong enough, but were not found by the method used.

## 5. Results for Swedish AGS data

The experiences with Danish AGS data – including data from the exercise LIVEX at Boden (Ref. 2) - are discussed in Chapter 2. SGU also joined this exercise and in the following the analyses of the Swedish AGS data are discussed; primarily Area1 and Area2 data but Area3 data are also touched upon. During the examinations only a part of a file was sometimes included in the analysis for example only spectra recorded within a specific height interval.

### 5.0. General information and selection of standard windows

A major part of the investigations concerned Area1 and Area2 data. For both areas the Area Specific Stripping factors ( $\delta$ ,  $\epsilon$ , and  $\zeta$  as well as  $\delta'$ ,  $\epsilon'$ , and  $\zeta'$ ) with and without inclusion of spectra with significant point source signals were generated for a number of different windows. The stripping factors have been tested with different files and average stripping factors – Area1 and Area2 - are calculated.

The windows used for the calculations are shown below together with the SGU background count rates. The background spectrum was, however, only included in a few of the calculations.

The energy calibration for the SGU AGS system is quite constant and one can use the relation:  $E \text{ (keV)} = 12.5 \times \text{Channel No.} + 3.5 \text{ keV}$ . On beforehand specific energy windows were not defined, and during the project the following window limits were used as standards, Table 5.0.1.

The energy intervals correspond to the *centre* of the channels. Taking the channel width into account the Th-window for example covers the energies from 2435 keV to 2785 keV. Windows with other energy limits could be defined. The lower limit of window 7 could be channel 87 to include a larger part of the full energy peak of 1173 keV photons from  $^{60}\text{Co}$ .

Table 5.0.1. Windows – channel and energy limits.

Win	Name	LL (chn.)	UL (chn.)	LL (keV)	UL (keV)	Background cps
1	Ultra low	15	19	191	241	18.72
2	Low scatter	20	26	253.5	328.5	29.97
3	I-131	27	31	341	391	15.59
4	Ir-191	32	48	403.5	603.5	31.91
5	Cs-137	49	58	616	728.5	14.78
6	Mixed	59	88	741.5	1103.5	18.93
7	Co-60	89	110	1116	1378.5	9.12
8	Low1	32	38	403.5	478.5	13.40
9	Low2	39	48	491	603.5	18.51
	Th	195	222	2441	2778.5	2.27
	U	132	147	1653.5	1841	4.09
	K	110	123	1378.5	1541	7.44

### 5.1. Area 1 with background subtraction

The theory for the Area Specific Stripping technique is based on background corrected window count rates, and the first tests with SGU data used background subtraction i.e. the values of  $\delta$ ,  $\epsilon$ , and  $\zeta$  were determined (see Appendix A). The background subtraction, however, resulted in the oddly looking parameter values shown in Table 5.1.1. Here all spectra from 40m to 70m were included i.e. also spectra with strong sources. Stripping factors calculated without inclusion of the source signals only deviate a little from those of Table 5.1.1.

Table 5.1.1. Stripping factors for Area1 (40m to 70m) with source signals.  
Background subtracted before processing.

Win	$\delta$	$\epsilon$	$\zeta$
1	2.76790	0.99845	1.47741
2	1.70739	4.37644	1.33924
3	2.65461	0.48540	0.45981
4	0.12352	0.70982	1.62942
5	1.90273	-0.75659	0.66387
6	0.50615	2.08420	1.26082
7	0.26201	-1.99247	0.51946
8	0.42422	0.75329	0.99269
9	1.69020	1.34826	0.81826

It is noticed that negative  $\epsilon$ -values (for uranium window stripping) are found for window 5 and window 7. From a physical point of view negative stripping factors should normally not come up. However, the mathematics behind the program (Appendix A and Ref. 10) just "demands" the best (least squares) fitting. In most cases the stripping worked well with those "odd" stripping factors; the mathematics in general ensured that the total stripping was acceptable when the stripping was performed for just that file, which was used for generating the parameters.

The data for Area1 were sorted into the altitude intervals 40-50m, 50-60m, 60-70m. For each altitude interval the ASS parameters were calculated - both when all spectra were included and when spectra with evident source signals were excluded. The Area1 file includes a large number of strong  $^{60}\text{Co}$ -signals and significant signals

from  $^{131}\text{I}$ . It was observed that even the inclusion of very strong  $^{60}\text{Co}$  signals did not influence the values of the calculated stripping factors very much. A first conclusion therefore is that during a search for weak and medium level sources or other local anomalies there is no need for doing some sorting during a post processing of data.

The values of the potassium window stripping (parameter  $\zeta$ ) varied with the altitude almost as expected, but a "peculiar" behaviour of the stripping parameters  $\delta$  and  $\varepsilon$  with altitude was observed similarly to the observations for Danish AGS data from Bornholm (Chapter 2 and Ref. 13) although they were not as "peculiar" as for the SGU data.

As for the Danish AGS data radon daughters in the air were at first thought to be (part of) the explanation. If the concentration of radon daughters goes up strongly with increasing amplitude - or if the aircraft accumulates radon daughters e.g. in air filters - then negative stripping could be needed. However, it was soon recognised that the background subtraction was the reason. The AGS files from SGU included spectra that were close to being background spectra and, therefore, due to counting statistical variations one sometimes obtained (slightly) negative net window counts. (Background spectra usually are determined when flying over the sea at least 600-1000 m from the shore, but when flying over a lake or a bog one almost obtains background levels.) The theory behind the Area Specific Stripping method assumes only positive window counts.

The reason for having not recognised this as the problem earlier is that the ASS technique previously has been used mostly for CGS spectra where survey spectra seldom reach levels comparable to the background. In the few cases (Ref. 13) where AGS spectra earlier have been processed by the ASS method all spectra recorded when flying over or near the sea were removed before data processing.

Earlier experiences with CGS data have shown that the ASS technique works very well even without including background correction. Therefore it was decided to carry out calculation without including background correction. In Appendix H is discussed the reason for success for ASS without background correction.

## **5.2. Area 1 without background subtraction**

When it was recognised that subtraction of the background prior to the data processing could give negative net window counts it was decided to carry out the calculations without paying attention to the background. All spectra for Area1 between 40m and 70 m were included and all recognised point source spectra were excluded from the calculations.

The results are shown in Table 5.2.1 that also include the average stripping factor per channel for the examined windows (termed single channel stripping factors).

The window 4 covers the same channels as window 8 and window 9 together. Therefore one should have the sum of the stripping factors for window 8 and window 9 (almost) equivalent to the stripping factors for window 4. This is almost the case. The stripping factors  $\delta'$  and  $\varepsilon'$  for window 4 is a little larger than the sum. For the stripping factor  $\zeta'$  the opposite is the case.

Table 5.2.1. Stripping factors  $\delta'$ ,  $\epsilon'$ , and  $\zeta'$  for standard windows and for single channels. No background subtraction. Single channel stripping factors  $a''$ ,  $b''$ , and  $c''$  are given *in italics*.

Stripping factors	$\delta'$ and $a''$	$\epsilon'$ and $b''$	$\zeta'$ and $c''$	Centre channel
WIN1	2.620042	3.00469	1.160425	
<i>5 channels</i>	<i>0.524</i>	<i>0.601</i>	<i>0.232</i>	17
WIN2	2.806673	3.557577	1.405994	
<i>7 channels</i>	<i>0.401</i>	<i>0.508</i>	<i>0.201</i>	23
WIN3	1.361974	1.742331	0.6912824	
<i>5 channels</i>	<i>0.272</i>	<i>0.348</i>	<i>0.138</i>	29
WIN4	3.170154	3.778964	1.569226	
<i>17 channels</i>	<i>0.186</i>	<i>0.222</i>	<i>0.0923</i>	40
WIN5	1.049802	1.470747	0.6083982	
<i>10 channels</i>	<i>0.105</i>	<i>0.147</i>	<i>0.0608</i>	53.5
WIN6	1.492632	2.012584	1.229633	
<i>30 channels</i>	<i>0.0234</i>	<i>0.0671</i>	<i>0.0410</i>	73.5
WIN7	0.4506544	0.6007786	0.6285968	
<i>22 channels</i>	<i>0.0205</i>	<i>0.0273</i>	<i>0.0286</i>	99.5
WIN8	1.388671	1.661051	0.7586038	
<i>7 channels</i>	<i>0.198</i>	<i>0.237</i>	<i>0.108</i>	35
WIN9	1.723198	1.969403	0.8182603	
<i>10 channels</i>	<i>0.172</i>	<i>0.197</i>	<i>0.0818</i>	43.5
SUM8-9	3.111869	3.630454	1.5768641	

Now one observes that all stripping factors have reasonable values when seen from a "physical point of view".

The stripping factors per channel  $a''$ ,  $b''$ , and  $c''$  are plotted in Figure 5.2.1. One notices that there is a smooth variation with energy (channel No.) for both  $a''$ ,  $b''$ , and  $c''$ . The single channel stripping factors are discussed in Section 5.7.

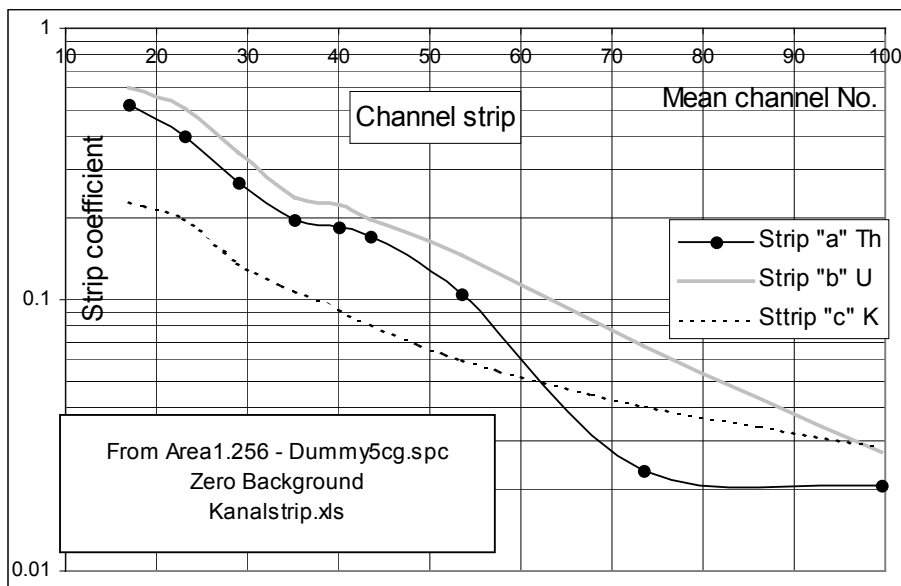


Figure 5.2.1. Energy dependency of the single channel stripping factors  $a''$ ,  $b''$ , and  $c''$  calculated for height 40-70 m at Area1.

### 5.3. Area 2 without background subtraction

For Area 2 all spectra for altitudes from 30 m to 80 m were processed without background subtraction – and spectra with point source signals were included. The results are shown in Table 5.3.1 (bold text) together with the stripping parameters for Area1 (40-70 m) excluding all point source spectra (background not subtracted).

Table 5.3.1. Area 1 and Area 2 window stripping factors  $\delta'$ ,  $\epsilon'$ , and  $\zeta'$ .

	$\delta'$	$\epsilon'$	$\zeta'$
WIN1	<b>2.26924</b> 2.620042	<b>2.965668</b> 3.00469	<b>1.193651</b> 1.160425
WIN2	<b>2.658012</b> 2.806673	<b>3.410452</b> 3.557577	<b>1.432764</b> 1.405994
WIN3	<b>1.285186</b> 1.361974	<b>1.388477</b> 1.742331	<b>0.7494193</b> 0.6912824
WIN4	<b>3.054212</b> 3.170154	<b>3.541717</b> 3.778964	<b>1.597261</b> 1.569226
WIN5	<b>1.054223</b> 1.049802	<b>1.330374</b> 1.470747	<b>0.6205875</b> 0.6083982
WIN6	<b>1.688199</b> 1.492632	<b>1.50616</b> 2.012584	<b>1.289763</b> 1.229633
WIN7	<b>0.5726671</b> 0.4506544	<b>0.5534713</b> 0.6007786	<b>0.6142001</b> 0.6285968
WIN8	<b>1.322404</b> 1.388671	<b>1.439828</b> 1.661051	<b>0.7876298</b> 0.7586038
WIN9	<b>1.673942</b> 1.723198	<b>1.900389</b> 1.969403	<b>0.8262111</b> 0.8182603

The table 5.3.1 tells that there are only minor differences between the stripping factors for Area1 and Area2 – yet with  $\delta'$  and  $\epsilon'$  generally slightly lower for Area2 (**bold**) than for Area1 while the opposite is the case for the parameter  $\zeta'$ .

### 5.4. Stripping factor height dependency for Area 1

The table 5.4.1 shows the stripping factors for Area1 calculated for the SGU AGS system. Spectra with visible signals from point sources have been eliminated during the calculations of the stripping factors. Background has not been subtracted. The table shows results for height intervals 40-50m, 50-60m, and 60-70m. The numbers can be compared to those of Table 5.2.1 with the stripping factors when data for the whole altitude interval (40-70m) are processed together.

The height dependence of the stripping factors is shown in the figures 5.4.1 to 5.4.3. Figure 5.4.1 with the stripping factor  $\delta'$  (Th) tells that  $\delta'$  in general decrease with the altitude. Three of nine  $\delta'$ -values exhibit a minor increase when going from 50-60m to 60-70m. An overview of Figure 5.4.2 with the height dependency of the  $\epsilon'$ -strip (U) indicates no definite height dependency. As a first approximation one may claim that the  $\epsilon'$ -values are not dependent on the height from 40m to 70m.

Figure 5.4.3 with the  $\zeta'$ -values tells that the value generally increases with the altitude. This is basically what one should expect from theory. The intensity (fluence rate) of primary photons from  $^{40}\text{K}$  decreases faster than the intensity of scattered

(original  $^{40}\text{K}$ ) photons because new scattered photons are generated everywhere in the air – due to Compton scatter of the primary photons. (Furthermore the absorption of low energy photons is stronger in the ground than in the air i.e. a deficit of low energy photons exists for the flux of photons passing the ground-air interface.)

Table 5.4.1. Area1 stripping factors for different height intervals.

		$\delta'$	$\epsilon'$	$\zeta'$
WIN1	40-50m	3.435417	3.004185	1.048144
	50-60m	2.411164	2.940802	1.207252
	60-70m	2.219303	2.965355	1.220179
<b>40-70m together</b>		<b>2.620042</b>	<b>3.00469</b>	<b>1.160425</b>
WIN2	40-50m	3.75341	3.568221	1.264541
	50-60m	2.659376	3.483445	1.441968
	60-70m	2.003547	3.417308	1.564101
<b>40-70m together</b>		<b>2.806673</b>	<b>3.557577</b>	<b>1.405994</b>
WIN3	40-50m	1.769692	1.845612	0.6100467
	50-60m	1.229777	1.752406	0.7134378
	60-70m	1.161594	1.490073	0.7683394
<b>40-70m together</b>		<b>1.361974</b>	<b>1.742331</b>	<b>0.6912824</b>
WIN4	40-50m	4.234257	3.617434	1.438057
	50-60m	2.831645	3.72467	1.624974
	60-70m	2.89399	3.885751	1.620514
<b>40-70m together</b>		<b>3.170154</b>	<b>3.778964</b>	<b>1.569226</b>
WIN5	40-50m	1.271014	1.53023	0.5617299
	50-60m	0.9373851	1.516816	0.6206518
	60-70m	1.004222	1.202154	0.6649317
<b>40-70m together</b>		<b>1.049802</b>	<b>1.470747</b>	<b>0.6083982</b>
WIN6	40-50m	2.159099	2.146891	1.112166
	50-60m	1.333205	1.798599	1.286838
	60-70m	1.19898	2.340012	1.23696
<b>40-70m together</b>		<b>1.492632</b>	<b>2.012584</b>	<b>1.229633</b>
WIN7	40-50m	0.5292329	0.6859993	0.605342
	50-60m	0.4247104	0.5256246	0.6417432
	60-70m	0.439828	0.7055946	0.6246385
<b>40-70m together</b>		<b>0.4506544</b>	<b>0.6007786</b>	<b>0.6285968</b>
WIN8	40-50m	1.920833	1.598516	0.6939981
	50-60m	1.278023	1.637679	0.7769391
	60-70m	1.110812	1.68025	0.8065845
<b>40-70m together</b>		<b>1.388671</b>	<b>1.661051</b>	<b>0.7586038</b>
WIN9	40-50m	2.281653	1.91532	0.7456027
	50-60m	1.518178	1.975578	0.8464115
	60-70m	1.597044	1.910606	0.860272
<b>40-70m together</b>		<b>1.723198</b>	<b>1.969403</b>	<b>0.8182603</b>

Whereas the height dependency of the stripping factor  $\zeta'$  can easily be explained by physical arguments it is not as easy to explain the height dependency of the other parameters  $\delta'$  and  $\epsilon'$ . The stripping based on the thorium window (with 2615 keV photons from  $^{208}\text{Tl}$ ) generally decreases with the altitude. The Th decay chain emits gamma photons of many different energies. (In Appendix H are shown high-resolution (Ge-detector) gamma spectra for Th and U. Here one notices a lot of separate gamma lines. Most of those cannot be resolved with a



NaI AGS detector. Therefore they generate an almost continuous spectrum signal for the AGS detector.) Photons of those energies are (full energy) recorded in the windows 1 to 9 together with scattered "high" energy radiation (in the air) and incomplete energy transfer in the detector crystal.

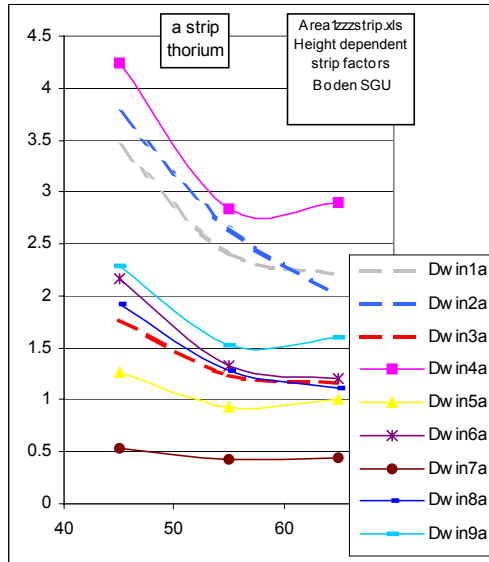


Figure 5.4.1. Height dependency of stripping factor  $\delta'$  (termed a in the figure)

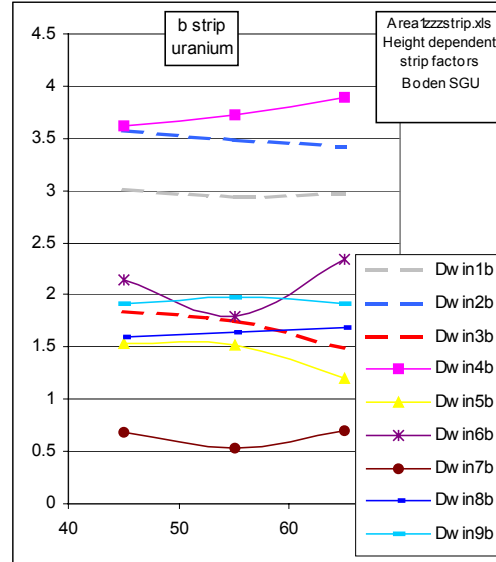


Figure 5.4.2. Height dependency of stripping factor  $\epsilon'$  (termed b in the figure).

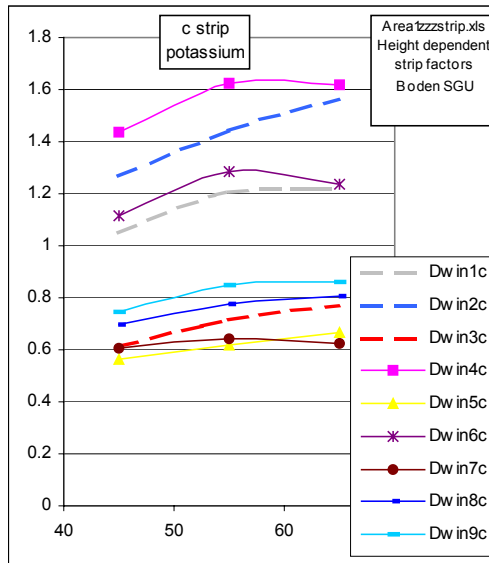


Figure 5.4.3. Height dependency of stripping factor  $\zeta'$  (termed c in the figure).

Consider for example the 583 keV photons emitted by  $^{208}\text{Tl}$  of the Th decay chain (yield 28% including branching ratio). At 583 keV the mass attenuation coefficient of air is about  $0.008 \text{ m}^2/\text{kg}$ , whereas it is about  $0.004 \text{ m}^2/\text{kg}$  for 2615 keV photons. This means that 583 keV photons entering the air from the ground are attenuated much stronger with height than are 2615 keV photons. At ground level the 583 keV photons contribute strongly to the counts of window 4. With increasing height those photons disappear faster than the 2615 keV photons, and this effect will cause a stripping factor  $\delta'$  to decrease with increasing height. On the other hand there is a "build-up" of scattered (primary 2615 keV) photons with height – as is the case for the 1462 keV photons from  $^{40}\text{K}$ .

Those two effects, therefore, counteract each other, and seemingly the reduction of the intensity of low energy photons in the air dominates the result i.e. the stripping parameter  $\delta'$  decreases with the height. At much higher altitudes – than 40-70m – one will reach a quasi equilibrium with a constant stripping factor  $\delta'$ . Somewhere between 200m and 300m one will meet (almost) only photons that originally were emitted as 2615 keV photons – except at the lowermost energies where multi-scattered photons from any primary energy still exist.

For uranium the situation becomes even more complicated. The same effects as are active for K and Th are of course active for U. In addition one has to take into account that from the uranium decay chain are emitted (low intensity) photons of energies higher than 1765 keV (the dominating uranium line). One also should notice that scattering of 2615 keV photons (dominating Th line) generates photons with energies included in the uranium window. This also is the case for the potassium window, but usually the count rate of the potassium window is quite dominated by 1461 keV photons from  $^{40}\text{K}$ . The same is not the case for the uranium window. Here almost half of the counts are due to thorium (Ref. 7).

The final complication that may come up for uranium is the radon (daughter) problem. Radium-226 that is part of the uranium decay chain decays to  $^{222}\text{Rn}$ , which is a noble gas. When generated in the ground  $^{222}\text{Rn}$  may diffuse and eventually reach the air above the ground. Here air movements may carry  $^{222}\text{Rn}$  up in the atmosphere and far away from its origin. Radon-222 has a half-life of 3.8 days and it decays to a short chain of radon daughters including  $^{214}\text{Bi}$  and  $^{214}\text{Pb}$  that are the dominating gamma emitters of the uranium decay chain. Therefore "uranium radiation" may originate from the air itself in amounts that may depend on the weather and on the altitude. Therefore, the stripping parameter  $\epsilon'$  may exhibit a height dependency that cannot be explained simply – and it may vary slightly from hour to hour.

## 5.5. Synthetic spectra for Area 2

SGU AGS data from Area2 of the Barents Rescue exercise were used for testing both the single channel stripping factors and the addition of "synthetic" gamma spectra to the recorded spectra.

Within Area2 only one source (Source 2:4;  $^{99}\text{Mo}$ ) was detected at the exercise. During the SGU AGS measurements the activity was 4 GBq. Molybdenum-99 emits 739.5 keV photons (12.2%) and 777.9 keV (4.3%) and decays to  $^{99\text{m}}\text{Tc}$  that emits 140.5 keV photons (89%). However, the lower limit cut-off energy is app. 200 keV; therefore the spectra contain no  $^{99\text{m}}\text{Tc}$  signal.

In order to get an idea of the detection limit for the ASS technique a synthetic  $^{99}\text{Mo}$  spectrum was produced. The spectrum with the strongest source signal was extracted and a neighbouring spectrum was subtracted. The channel counts of the difference spectrum was divided with two and smoothed a little. The result – Figure 5.5.1 – was the synthetic spectrum to be used for tests.

Next the synthetic spectrum was added to the following measured spectra from Area2 (only added once per spectrum), see Table 5.5.1. Also indicated here is the number of surplus counts in the selected window after ASS processing. Spectrum numbers are counted from No. 1.

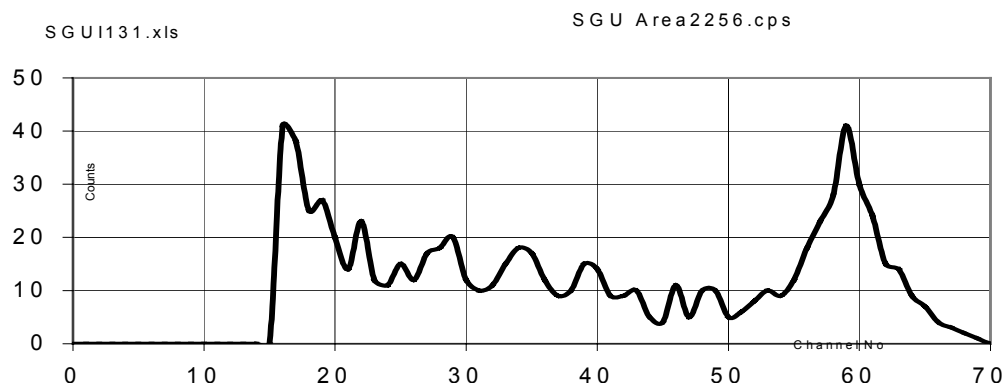


Figure 5.5.1. Synthetic spectrum based on a  $^{99}\text{Mo}$  point source in Area2. X-axis: channels

Table 5.5.1. Positions of measured spectra to which are added a synthetic spectrum.

	X	Y		
#225	1764705	7309854	<b>A</b>	The environmental background is rather high
#226	1764711	7309783		Result easily seen. Surplus counts 254-256
#820	1765116	7309180	<b>B</b>	Transition from high to low background. The signal is observed without problems. Surplus counts 219
#1081	1764246	7307815		Very low background. Very easily seen. Surplus counts 249.
#1292	1765368	7309399	<b>D</b>	Medium level environmental background
#1293	1765364	7309331		Very easily noticed
#1294	1765363	7309262		Surplus counts 209-235-272
#1343	1765395	7305521		<b>Or.</b> Original signal. Medium level environmental background. Is very easily detected. Surplus counts 38-579-82. Source noticed for three consecutive spectra.

The full energy peak(s) of a  $^{99}\text{Mo}$  source covers the channels 53 to 66. This window does not correspond to any of the "standard" windows. Therefore stripping factors were determined for this new window. This was done based on the channel stripping factors of the figures 5.7.1 to 5.7.3. An **average** channel stripping factor for the window was estimated and then multiplied with 14 (= number of channels).

The results are:  $\delta' = 1.05$      $\epsilon' = 1.12$      $\zeta' = 0.763$

The stripping factors and the "low energy window" 53 to 66 were introduced in NucSpec (Ref. 14) together with the standard (SGU/DTU) windows for Th, U, and K. (All other stripping ratios were set to zero and sensitivities to 1.0.) The output from NUCSpec is count rates (Ref. 16).

Figure 5.5.2 shows the results i.e. the ASS stripped low energy window count rates for all the measurements in Area2. The non-stripped window count rates (grey) are also shown. (The NucSpec program version used could not generate negative count rates. Therefore the stripped count rate curve has a "cut-off" at 0 cps.)

The purpose of adding synthetic spectra to the measured spectra was to test whether it was easier to detect a signal in two or three neighbouring spectra than in single spectrum. The additions of the synthetic spectrum were to environmental spectra with an environmental background of varying intensity.

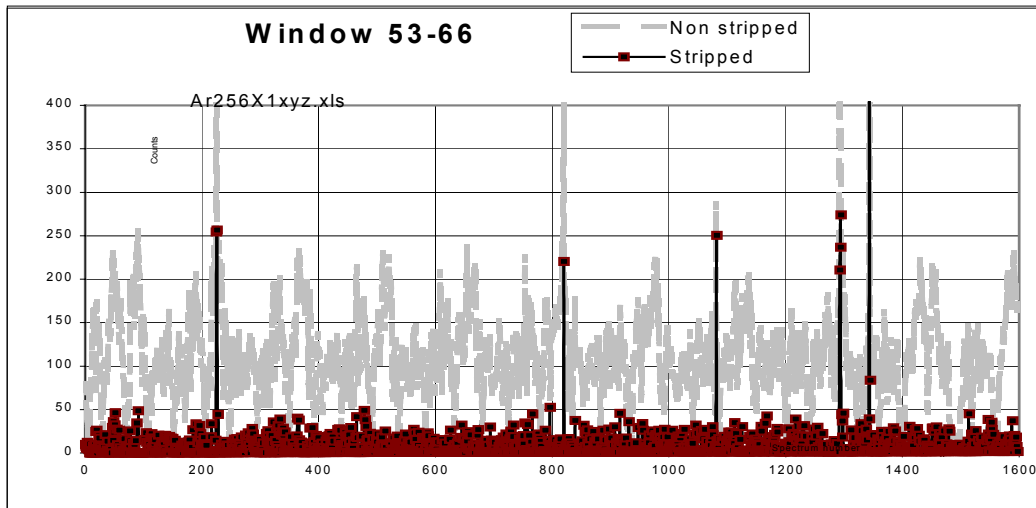


Figure 5.5.2. Stripped and non-stripped window count rates for the channels 53-66.

The neighbouring spectra Nos. 225-226 both got a synthetic spectrum added. The same was the case for the spectra Nos. 1292, 1293, and 1294. None of the neighbours to the spectra 820 and 1081 have got an extra signal. The original source signal is seen in the spectra 1343 and 1344. Also spectrum 1342 has a surplus count rate for the "53-66 window"; but the signal here is within the statistical noise of the stripped count rate.

A simple visual examination of the stripped window count rate easily unveils where the synthetic spectrum has been added. The "noise level" of the stripped count rates is slightly above 50 cps. The synthetic spectrum in all cases generates a surplus of some 250 cps. Even with a reduction of the synthetic signal a factor 4 it would have been observed – when the results are presented as in Figure 5.5.2. This means that a source similar source 2:4 – but of about 8 times lower activity i.e. 0.5 GBq – also should be detected by the ASS technique.

This of course assumes the same source arrangements for this source as for the source used in the exercise. Source 2:4 was not collimated (Ref.2).

Figure 5.5.3 shows a "map" for Area2. The stripped window count rate is plotted in a standard way for all of Area2. The synthetic sources of Table 5.5.1 are seen on the map. The actual source (Or.) is very easily noticed. The same is the case for the triple source D and the single source C. The double source A and the single source B are also detected; but the single synthetic source B only exceeds the "statistical noise" of the map a factor 2. The reason may partly be that the "source" is "placed" at a position with a transition of the environmental background level from rather high to low.

It should be noticed that source C also is a single synthetic source; and it is very easily detected. Furthermore, the surplus count rate of position B and C are not very different – 219 vs. 249. Therefore the different signals of the map may also be due to the method of processing the map results.

Each point of the map is assigned a value calculated as a weighted average of results within a specified distance from the point in question. Several measurements may be found within the averaging area for position B whereas position C only covers measurements #1081 with the synthetic spectrum. This could be the case if more than one flight line has been close to position B. This, however, means that in a

real world measurement a source signal perhaps also had been recorded when flying along the other flight line – and a mapping therefore had generated a somewhat stronger signal.

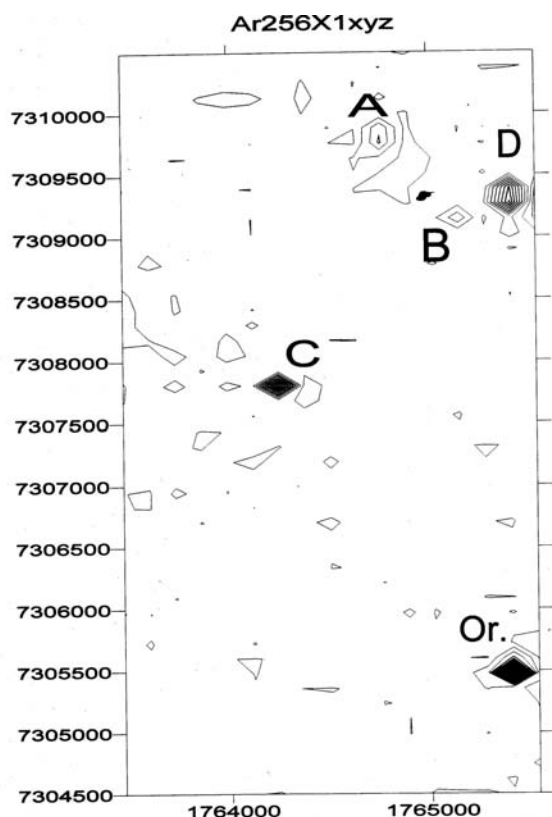


Figure 5.5.3 Map of Area2 with actual source (Or.) and the synthetic sources A to D.

## 5.6. Search for weak source signals in Area 2

Area 2 included six sources in all (see Appendix C), and only source 2:4 ( $^{99}\text{Mo}$ ) was easily detected. Therefore a new way of processing the data was tried. The stripping factors  $\delta'$ ,  $\epsilon'$ , and  $\zeta'$  were calculated for the windows covering the channels 16-105, 59-108, 29-58, and 16-28. Spectra with strong signals from source 2:4 were eliminated before the processing. (Also see Appendix D).

After having calculated the stripped count rates for the four windows the spectra having the highest stripped (surplus) counts were identified and their corresponding co-ordinates were plotted in

the co-ordinate system for Area 2. Figure 5.6.1 shows this plot. The symbol explanation of the points is as follows:

Violet, small square	Actual sources
Green triangle	Surplus counts ( $> 300$ ) in a total low energy window (channels 16-105)
Brown X	Surplus counts ( $> 75$ ) in window 59-108
Small black circle	Surplus counts ( $> 120$ ) in window 29-58
Large, brown, open square	Surplus counts ( $> 150$ ) in window 16-28

The strong  $^{99}\text{Mo}$  (2:4) source is placed in the lower right corner of the figure. Two spectra with signals from this source were eliminated from the file before processing. Therefore no window surplus counts are seen there.

The source at the right centre of the figure is a  $^{99}\text{Mo}$  source (2:3) of activity about 0.7 GBq. No signal is observed here. The source beams vertically into the air within a  $45^\circ$  solid angle (Ref. 2). The source activity is a factor 6 weaker than the activity of source 2:4 that was easily detected. According to the earlier estimates the activity of source 2:3 is above the detection limit – if the source geometry had been as that for source 2:4. The Swedish flight line passed almost directly above the source. The Danish AGS measurements for Area 2 were recorded on the same day as the Swedish data; and the Danish unveiled neither not a source signal near the source 2:3 position. Seemingly the source geometry was not as expected.

Two sources (2:5-1 and 2:5-2),  $3 \times 0.5 \text{ GBq } ^{137}\text{Cs}$  and  $3 \times 0.02 \text{ GBq } ^{60}\text{Co}$  are placed at the leftmost flight line. No significant signal was detected near those sources. In

Appendix D are given theoretical estimates of the expected signals from those sources.

The  $^{60}\text{Co}$  sources 2:1 and 2.2 each of 4.9 GBq activity are placed at app. position 1764000, 7307200. The source 2:1 emits photons in a horizontal beam whereas source 2:2 beams in direction  $30^\circ$  with horizontal. Source 2:1 cannot be detected directly from the air, but in principle scattered photons might be detectable just above the beam (see Appendix D). In the beam from the other source (2:2) primary photons may also be detectable if the detector pass through the beam, and scattered photons may be detectable here, too, when the detector is close to the beam.

Some signals are observed near the position of the two sources (Figure 5.6.1). The total window (chns. 16-105; 204-1316 keV; small black circles) has a significant surplus of counts at one position some 60-70 m south-east of the sources. The same is the case for the "medium" window (chns. 29-58; 366-729 keV; green triangle) whereas the "upper" window (chns. 59-108; 741-1354 keV; primary photons and forward scattered photons; brown X'es) has a significant surplus of counts at three locations near the sources. There is no significant surplus of counts for the "lower" window here (chns. 16-28; 204-354 keV; open brown squares).

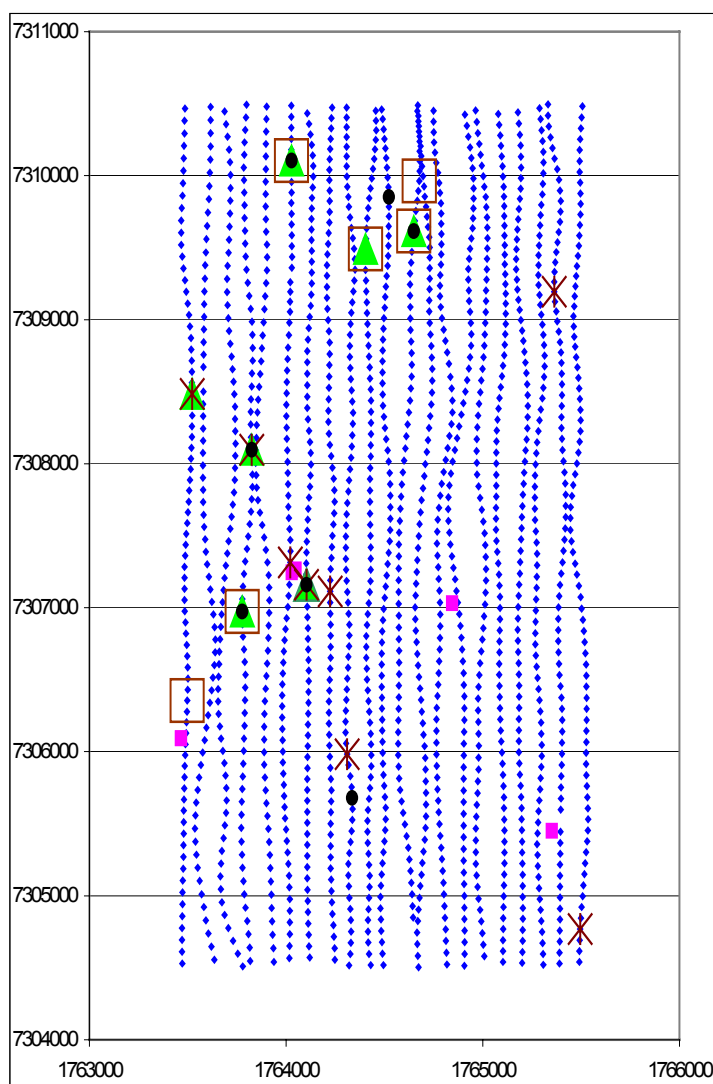


Figure 5.6.1 Area2. Positions of actual sources (small squares) and large "surplus counts" for the special windows. A spectrum near source 2:4 is omitted.

A photo of the (bunker) position of source 2:2 tells that the source beams in a direction between south and south-east (Ref. 2). This fits well with the positions of the surplus counts. For the signal ("upper" window) close to the sources scattered photons have been detected. (The lower limit of the "upper" window corresponds to  $45^\circ$  forward scattered 1250 keV photons. Photons scattered more than  $45^\circ$  would be detected in the other windows.) Therefore, the relative positions of the sources 2:2 and 2:3 in Figure 5.6.1 and the spectra recordings may not be 100% correct.

It should, however, be pointed out that statistical variations and maybe the environmental geometry also can generate significant surplus counts alone with natural radioactivity. For example there is a surplus of counts both for the "total", "upper", and "medium" window at position app. 1763900, 7308100 (RT90). If the positions of the sources were not known one might assume that there could be a weak source here. At other locations – without known sources - there are surplus counts in other windows.

The conclusion therefore is that the (assumed) signal from source 2:2 (and 2:1) is just at the threshold of detection. A similar conclusion is reached in Appendix D where the Area 2 sources are searched for using other energy windows.

## 5.7. Single channel stripping factors for the SGU system

The window stripping factors are – of course – fitted for specific windows. One may, however, envision situations with a need for examining a special, new window. The straightforward method then is to perform a calculation of a new set of stripping factors designed for just this window. This is possible for a post processing of data. It is, however, also possible to determine on beforehand a set of single channel stripping factors i.e. a set of parameters that describe the stripping of each low energy channel counts for the contribution from Th, U, and K.

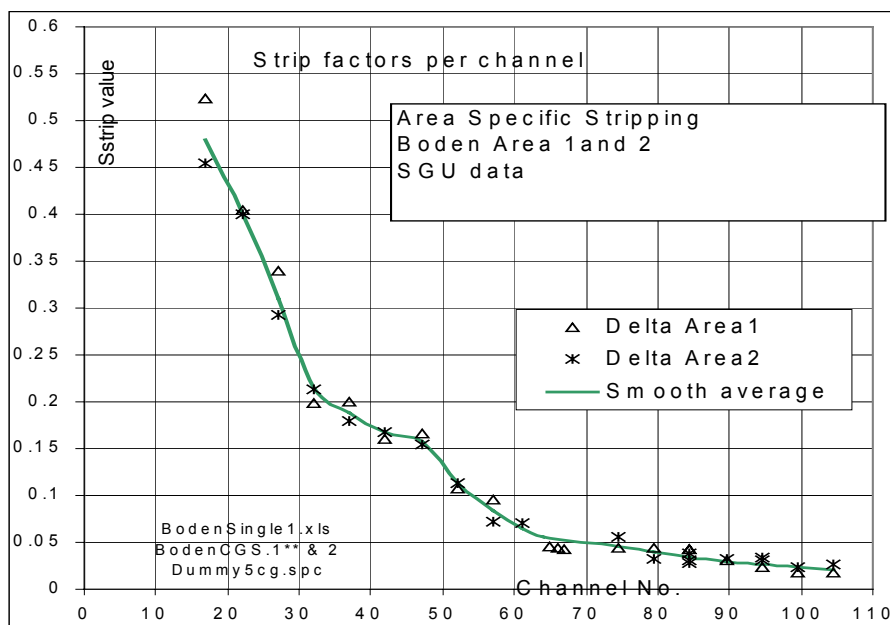


Figure 5.7.1. Single channel stripping factor  $a''$  for Area 1 and 2 of the LIVEX exercise. In the figure the single channel stripping factor is termed delta referring to stripping of the Th-signal. A common smoothed average curve is also shown. Notice the change of the single channel stripping factor at the 583 keV line from  $^{228}\text{Ac}$  (Ch. 47).

The single channel stripping factors of course refer to specific windows for Th, U, and K. One also has to assume that the energy calibration is the same – just as for window stripping factors. Single channel stripping factors have been calculated for Area 1 and Area 2 – partly based on the tables 5.2.1 and 5.3.1.

If one has to use the stripping factors for a special window one just add together the single channel stripping factors for all channels included in the special window.

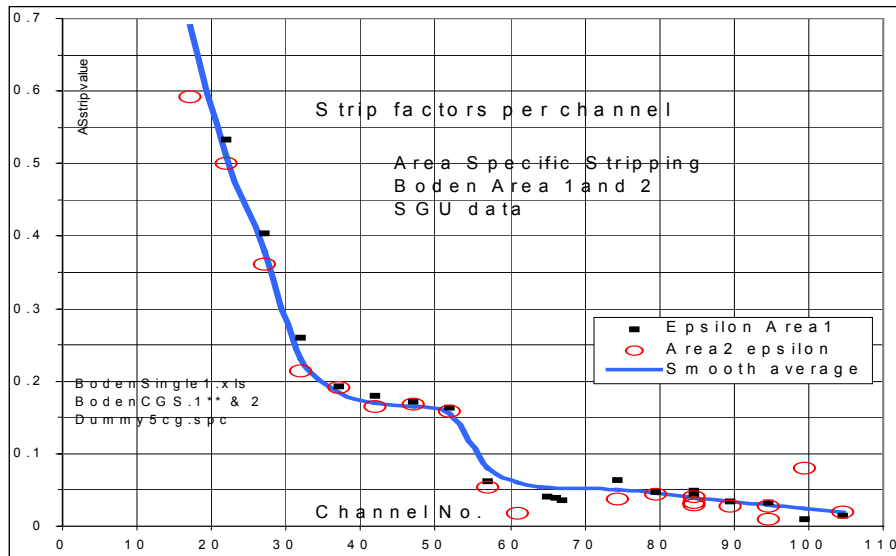


Figure 5.7.2. Single channel stripping factor  $b''$  for Area 1 and 2 of the LIVEX exercise. In the figure the single channel stripping factor is termed epsilon referring to stripping of the U-signal. A common smoothed average curve is also shown. The influence of the 609 keV line from  $^{214}\text{Bi}$  is seen in the figure (Ch. 49).

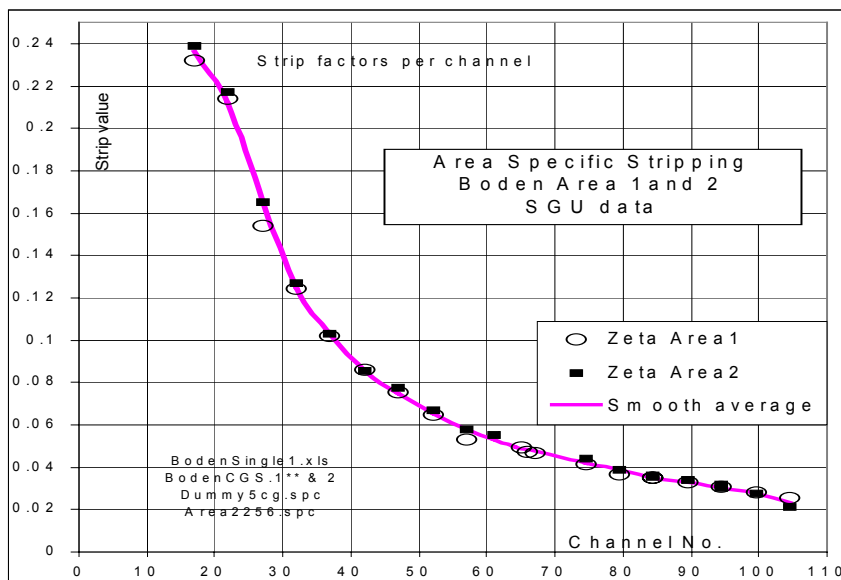


Figure 5.7.3. Single channel stripping factor  $c''$  for Area 1 and 2 of the LIVEX exercise. In the figure the single channel stripping factor is termed zeta referring to stripping of the K-signal. A common smoothed average curve is also shown.



## 5.8. Intensity maps for Area 1

The figures 5.8.1-3 show maps of the stripped window count rate for the three lowermost windows for Area 1. All four sources are easily seen.

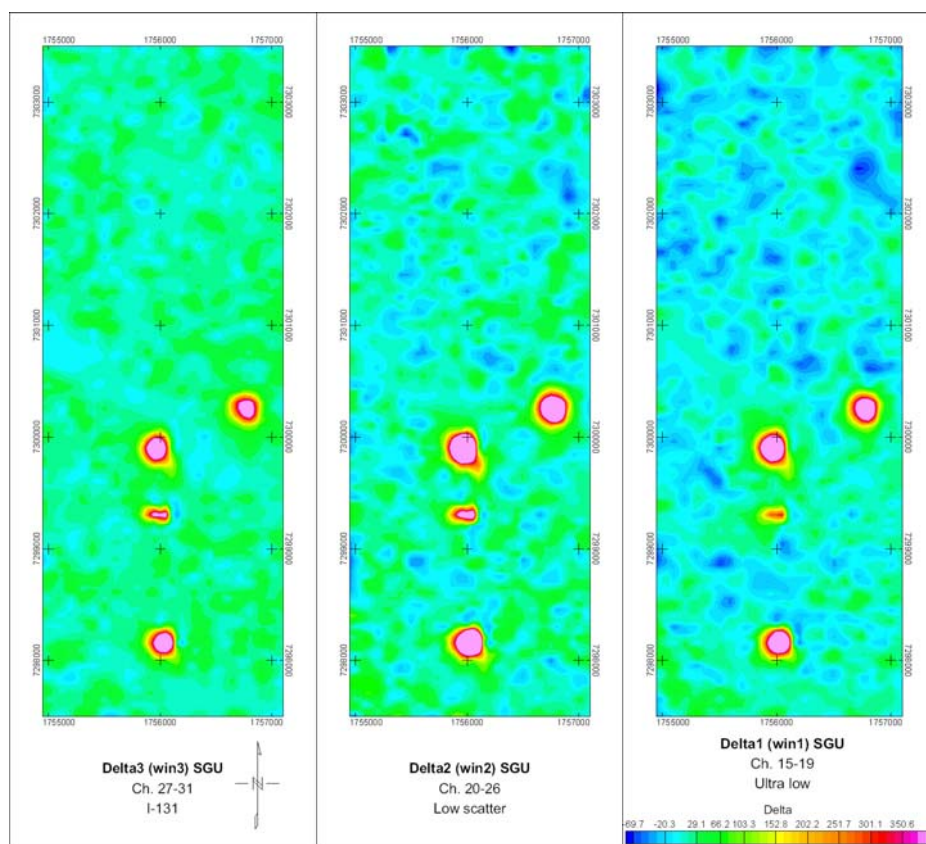
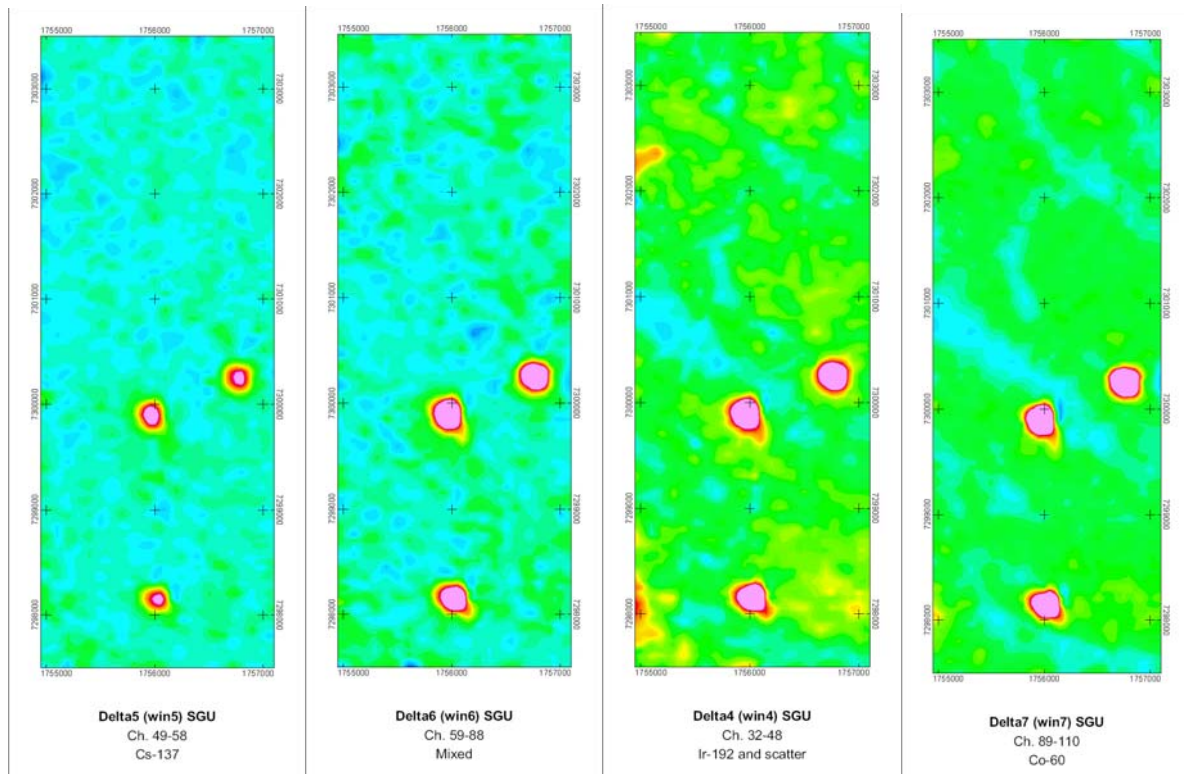


Figure 5.8.1-3. Maps of the stripped count rates for Area1 at the LIVEX exercise. The low energy windows 1, 2, and 3 (Table 5.0.1) are stripped with the stripping factors listed in Table 5.2.1.

The zero level is between the light blue and the light green colour. For the lowermost window (191 keV to 241 keV) one recognises a difference between background level for the southern and the northern part of the map. A minor deficit of photons of the lowermost energy is found at the northern part of the area. This could be caused by having a lower altitude here – or by having a lower density of vegetation. See the discussion in Appendix I.

The figures 5.8.4 to 5.8.6 show the stripped count rates for the windows 4 to 6 for Area 1. Here only the three strong  $^{60}\text{Co}$  sources are seen. The strong  $^{131}\text{I}$  source that is seen the figures 5.8.1 to 5.8.3 has disappeared. The most intense gamma radiation (yield 81%) from  $^{131}\text{I}$  has an energy of 364 keV that is well below the lower limit of window 4 at 403.5 keV. Gamma radiation from  $^{131}\text{I}$  of energy 637 keV (yield 7%) is detected in window 5 (616 keV to 728 keV). However, no source signal is seen at the position of the  $^{131}\text{I}$  source in Figure 5.8.5.

The average background colours of the figures 5.8.4 and 5.8.5 differ. Figure 5.8.4 is green indicating an average stripped count rate above zero, whereas the major part of the background of Figure 5.8.5 is (slightly) below zero. The reason for this difference has not been identified. The yellow-red "spots" at the western part of Figure 5.8.6 probably are artefacts.



Figures 5.8.4-7. Stripped count rates for Area 1. The counts rates for the windows 4 to 7 tell where three  $^{60}\text{Co}$  sources are placed. Figure 5.8.7 refers to window 7 This window covers the energy (1173 keV and 1332 keV) of the primary photons from the strong  $^{60}\text{Co}$  sources.

## References

- 1 IAEA Airborne gamma ray spectrometer surveying. 1991. IAEA Technical Reports Series No. 323, IAEA Vienna.
- 2 Thomas Ulvsand, Robert R. Finck and Bent Lauritzen.:(eds) NKS/SRV Seminar on Barents Rescue 2001 LIVEX Gamma Search Cell, NKS-54, ISBN 87-7893-108-8, April 2003.
- 3 Hans Mellander, Helle Karina Aage, Simon Karlsson, Uffe Korsbech, Bent Lauritzen and Mark Smethurst: Mobile Gamma Spectrometry, Evaluation of The Resume 99 Exercise. NKS-56 ISBN 87-7893-111-8, June 2002.
- 4 Simon Karlsson, Hans Mellander, Jonas Lindgren, Robert Finck and Bent Lauritzen (eds.): RESUME99 Rapid Environmental Surveying Using Mobile Equipment. NKS-15, ISBN 87-7893-065-0, August 2000.
- 5 D. C. W. Sanderson, A. J. Cresswell and J. J. Lang (eds): An international comparison of airborne and ground based gamma ray spectrometry, Results of the ECCOMAGS 2002 Exercise held 24th May to 4th June 2002, Dumfries and Galloway, Scotland, SUERC. University of Glasgow, Glasgow, Scotland, UK, 2003 ISBN 0 85261 783 6.
- 6 RESUME 95, Hovgaard, J. (Ed), Rapid Environmental Surveying Using Mobile Equipment. Nordic Nuclear Safety Research, Copenhagen, ISBN 87-7893-014-6.
- 7 ICRU (1994). Gamma-Ray Spectrometry in the Environment. ICRU Report No. 53. International Commission on Radiation Units and Measurements. December 1994.
- 8 H. K. Aage and U. Korsbech: Search for orphan sources using CGS equipment - a short handbook. Report NT-59, DTU, November 2002. 77 p.
- 9 Helle Karina Aage and Uffe Korsbech: Handbook on Mobile Gamma-ray Spectrometry, Basic physics and mathematics for Airborne and Car-borne Gamma-ray Spectrometry supplemented with practical examples and methods for advanced data processing, Ørsted-DTU, Measurement & Instrumentation Systems, Technical University of Denmark, Report NT-65, December 2003.
- 10 H. K. Aage and U. Korsbech: Search for lost or orphan radioactive sources based on NaI gamma spectrometry. Applied Radiation and Isotopes, Volume 58, Issue 1, pp.103-113, January 2003.
- 11 Hjerpe, T., Finck, R.R., Samuelsson, C.: Statistical data evaluation in mobile gamma spectrometry; an optimization of on-line search strategies in the scenario of lost point sources. 2001 Health Phys. 80 (6) 563-570.
- 12 T. Hjerpe and C. Samuelsson: A comparison between Gross and Net Count Methods when Searching for Orphan Radioactive Sources. Health Physics, Vol. 84 No. 2, pp. 203-211, 2003.
- 13 Helle Karina Aage and Uffe Korsbech: Area Specific Stripping factors for AGS, a method for extracting stripping factors from survey data, Ørsted-DTU, Measurement & Instrumentation Systems, Technical University of Denmark, Report NT-62, July 2003.
- 14 NUCSpec ver. 3.5, Danish Emergency Management Agency, Nuclear Safety Division, 2001.
- 15 Hovgaard, J.: Airborne gamma-ray spectrometry, Statistical Analysis of Airborne Gamma-Ray Spectra, Ph.D. thesis, Technical University of Denmark, October 1997.
- 16 Bargholz, Kim: Dose rate and nuclide mapping from airborne and ground based gamma-ray instrumentation, Ph.D. thesis. Technical University of Denmark, April 2001.
- 17 Aage, H. K., Bargholz, K., Korsbech, U.: CGS and In Situ Measurements in Gävle 1999, RESUME99, Department of Automation, Technical University of Denmark, December 1999.
- 18 Aage, H. K., Bargholz, K., Korsbech, U., Hovgaard, J., Ennow, K.: An Airborne Survey of Natural Radioactivity on Bornholm 1997 and 1999. Department of Automation, Technical University of Denmark, Report IT-NT-47, October 1999.
- 19 Uffe Korsbech, Kim Bargholz, Helle Karina Aage and Jesper Petersen: Simple Calibration of Spectral Components based on Airborne Gamma-Ray Spectrometry Data. In: Sanderson, D. C. W. and McLeod, J. : (eds) (2000). Recent Application and Developments in Mobile and Airborne Gamma Spectrometry. Proceedings Papers of an International Symposium on Recent Applications and Developments in Mobile and Airborne Gamma Spectrometry, University of Glasgow, Glasgow. ISBN 0 85261 685 6.
- 20 Helle Karina Aage and Uffe Korsbech: CGS Measurements in the Copenhagen Area. Standard Environmental Spectra and Special Industrial Spectra. Ørsted-DTU, Measurement & Instrumentation Systems, Technical University of Denmark, Report NT-64, January 2004.

## Appendix A. Theory for Area Specific Stripping

In the standard method for processing a set of gamma spectra from a mobile survey with a NaI(Tl) detector one basically first calculates the net window count rates  $r_{K,K}$ ,  $r_{U,U}$  and  $r_{Th,Th}$  due to  $^{40}\text{K}$  and the decay chains following  $^{238}\text{U}$  and  $^{232}\text{Th}$ . The equations are as follows:

$$r_{Th,B} = 1 \cdot r_{Th,Th} + b \cdot r_{U,U} + g \cdot r_{K,K} \quad (\text{A.1a})$$

$$r_{U,B} = \alpha \cdot r_{Th,Th} + 1 \cdot r_{U,U} + a \cdot r_{K,K} \quad (\text{A.1b})$$

$$r_{K,B} = \beta \cdot r_{Th,Th} + \gamma \cdot r_{U,U} + 1 \cdot r_{K,K} \quad (\text{A.1c})$$

Here for example  $r_{Th,B}$  is the background corrected count rate for an energy window around the typical thorium peak at 2615 keV (from the daughter nuclide  $^{208}\text{Tl}$ ). The meaning of  $r_{U,B}$  and  $r_{K,B}$  is similar with peaks at 1765 keV ( $^{214}\text{Bi}$ ) and 1461 keV ( $^{40}\text{K}$ ).  $r_{Th,Th}$  is the count rate contribution to the Th window from "Th radiation" i.e. from  $^{208}\text{Tl}$ . The meaning of  $r_{U,U}$  and  $r_{K,K}$  is similar.

The parameters  $a$ ,  $b$ ,  $g$ ,  $\alpha$ ,  $\beta$  and  $\gamma$  are the standard stripping parameters that describe the interference between the signals from Th, U, and K. (Ref. 1)

For each measured spectrum the values of  $r_{Th,B}$ ,  $r_{U,B}$ , and  $r_{K,B}$  are determined and then the equations A.1a to A.1c are used for calculation of  $r_{Th,Th}$ ,  $r_{U,U}$ , and  $r_{K,K}$ . Finally, if the sensitivities are known, the net count rates can be converted into concentrations of Th, U, and K.

If the task is to determine the presence (or amount) of some low energy gamma emitter as for example  $^{137}\text{Cs}$  one uses the equation:

$$r_{Cs,B} = 1 \cdot r_{Cs,Cs} + \delta'' \cdot r_{Th,Th} + \epsilon'' \cdot r_{U,U} + \zeta'' \cdot r_{K,K} \quad (\text{A.2})$$

Here  $r_{Cs,B}$  is the measured (and background corrected) count rate in an energy window covering the  $^{137}\text{Cs}$  (662 keV) peak and  $r_{Cs,Cs}$  is the count rate part to this window caused by  $^{137}\text{Cs}$ . The stripping factors  $\delta''$ ,  $\epsilon''$ , and  $\zeta''$  take into account that Th, U, and K also contribute to the count rate of the  $^{137}\text{Cs}$  window. Eq. A.2 may be rewritten as:

$$r_{Cs,Cs} = r_{Cs,B} - \delta'' \cdot r_{Th,Th} - \epsilon'' \cdot r_{U,U} - \zeta'' \cdot r_{K,K} \quad (\text{A.3})$$

The equations A.1a to A.1c tell that there is a linear relation between  $r_{Th}$ ,  $r_U$  and  $r_K$  on one hand and  $r_{Th,Th}$ ,  $r_{U,U}$  and  $r_{K,K}$  on the other hand. Therefore Eq. A.3 may be changed to:

$$r_{Cs,Cs} = r_{Cs,B} - \delta \cdot r_{Th,B} - \epsilon \cdot r_{U,B} - \zeta \cdot r_{K,B} \quad (\text{A.4})$$

Hereby the count rates for caesium becomes related to the measured (and background corrected) count rates of the Th, U, and K windows. When no caesium-137 (or another low energy gamma emitter) is present  $r_{Cs,Cs}$  is equal to zero and for each measured spectrum (number  $i$ ) one may write:

$$r_{Cs,B,i} = \delta \cdot r_{Th,B,i} + \epsilon \cdot r_{U,B,i} + \zeta \cdot r_{K,B,i} + \Delta_i \quad (\text{A.5a})$$

or

$$\Delta_i = r_{Cs,B,i} - (\delta \cdot r_{Th,B,i} + \epsilon \cdot r_{U,B,i} + \zeta \cdot r_{K,B,i}) \quad (\text{A.5b})$$

i.e. the background corrected count rate of the  $^{137}\text{Cs}$  window – or any other low energy window – can be written as a simple linear combination of the background corrected count rate of the windows for Th, U, and K plus an error  $\Delta$  caused by the statistical fluctuations of window count rates.

The task then is to find the best values for  $\delta$ ,  $\epsilon$  and  $\zeta$  for a given set of data for example a set of spectra to be examined for signals from  $^{137}\text{Cs}$ . In principle one should not include spectra with  $^{137}\text{Cs}$  signals in the processing, but experiences tell that a few spectra with a moderate or a low  $^{137}\text{Cs}$  signal have a negligible influence on the results. In case of a widespread contamination with  $^{137}\text{Cs}$  the "contaminated" spectra should at first be eliminated from the set of spectra to be processed. Otherwise a zero shift is obtained for the final result. It is also possible to use stripping parameter values determined for another area with similar "environmental geometry".

The method used for finding the best stripping parameter values is to perform a least squares fitting i.e. the sum  $\sum \Delta_i^2 \cdot w_i$  should be minimised.  $w_i$  is an appropriate weight factor. The mathematics for calculating the values of the stripping parameters  $\delta$ ,  $\epsilon$ , and  $\zeta$  are described in some detail in Ref. 10 and 13.

Basically all calculations should be based on background corrected spectra i.e. measured spectra from which have been subtracted the background signals caused by cosmic radiation and radiation from radioactivity in the carrying vehicle and the detector system itself. However, reliable background spectra may not always be available – especially for carborne measurements – and it has been observed that in practice there is no need for subtraction of the background before the ASS calculations; the method worked anyhow. The equation A.5a hereby becomes:

$$r_{\text{Cs},i} = \delta' \cdot r_{\text{Th},i} + \epsilon' \cdot r_{\text{U},i} + \zeta' \cdot r_{\text{K},i} + \Delta_i \quad (\text{A.6})$$

The reason for the success with this simplification is that the general shape of background spectra resembles that of ordinary environmental spectra. The stripping factors  $\delta'$ ,  $\epsilon'$ , and  $\zeta'$  therefore automatically also strip away the contribution from the background signal to the low energy windows.

For AGS data it has been observed that it is positively beneficial not to subtract background data before processing if spectra with low-level signals are included. Due to statistical fluctuations the background corrected spectra sometimes generate negative window count rates; and the mathematical processing cannot handle negative rates. Window count rates close to zero should also be avoided. The mathematics generate  $\delta$ ,  $\epsilon$ , and  $\zeta$  values that in general cause correct stripping; but the values of especially  $\delta$  and  $\epsilon$  sometimes cannot be related to real world physics. A very low  $\delta$  value may be found together with a very high  $\epsilon$  value - resulting in a combined stripping that is correct.

In the present report it is in general the parameters  $\delta'$ ,  $\epsilon'$ , and  $\zeta'$  that are used.

## Appendix B. Energy calibrations

### SSI: CGS

SSI uses a 3"×3" NaI detector with a 256-channels multichannel analyser for CGS measurements. The energy calibration is unfortunately subject to spectrum drift. - The figures B.2, B.4, and B.6 show that the energy calibration was not constant during the three surveys and it was necessary to make an energy calibration for each file.

All energy calibrations for SSI have been done on the mean spectra only, due to spectrum drift (and peak displacements) in the spectral components of higher numbers, Figure B.1.

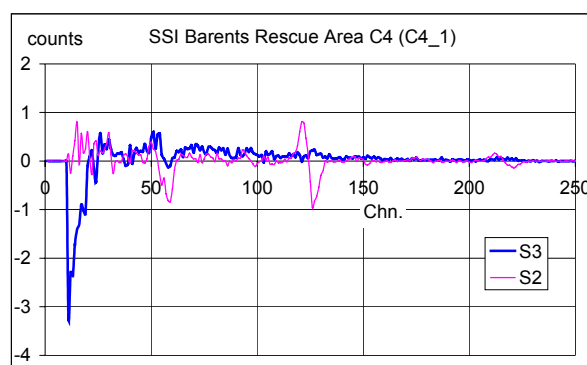


Figure B.1. Example of spectrum drift.

SSI supplied the information in Table B.1 about the windows used in the Barents Rescue exercise, however, all calculations of area specific stripping factors were based on the energy windows recommended by IAEA, Table B2

Table B.1. SSI Barents Rescue windows in channels.

	<sup>137</sup> Cs	<sup>40</sup> K	<sup>214</sup> Bi (U)	<sup>208</sup> Tl (Th)
LL chn.	53	116	135	200
UL chn.	63	138	162	250

Table B.2. Recommended IAEA windows in keV.

	<sup>40</sup> K	<sup>214</sup> Bi (U)	<sup>208</sup> Tl (Th)
LL keV.	1370	1660	2410
UL keV.	1570	1860	2810

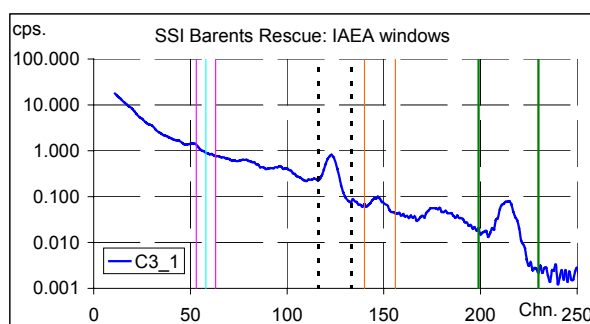


Figure B.2. SSI Barents Rescue, Area C3.

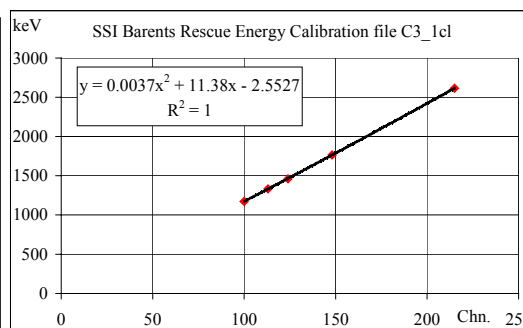


Figure B.3. SSI Barents Rescue, C3, cal. Using channel 0 as the first channel, the offset becomes 8.831 keV.

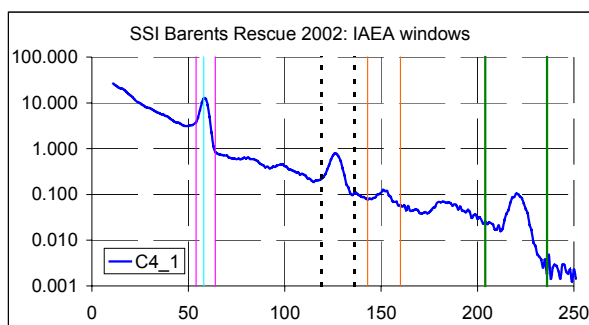


Figure B.4. SSI Barents Rescue, Area C4\_1.

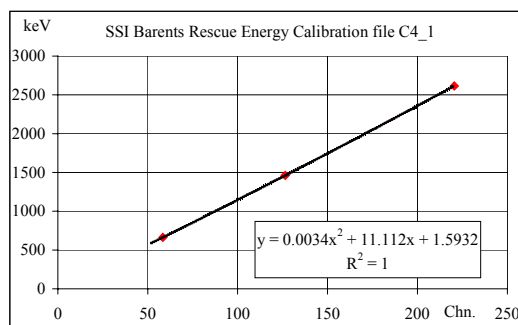


Figure B.5. SSI Barents Rescue, C4\_1cal. Using channel 0 as the first channel, the offset becomes 12.709 keV.

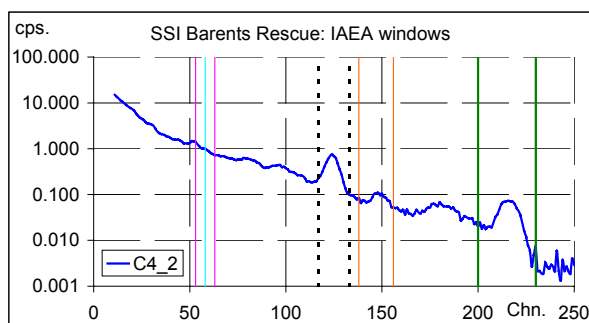


Figure B.6. SSI Barents Rescue, Area C4\_2.

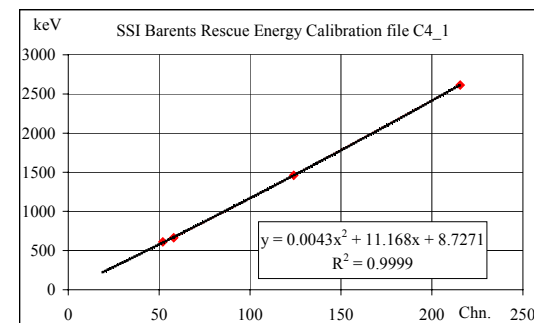


Figure B.7. SSI Barents Rescue, C4\_2, cal. Using channel 0 as the first channel, the offset becomes 19.899 keV.

All figures showing spectrum shapes for SSI measurements have been made using the SSI way of counting, i.e. first channel is channel 1.

## NRPA/NGU: CGS

NRPA (NGU) uses a 16L NaI detector with a 256-channels multichannel analyser.. The energy calibration is very stable. The 662 keV peak from  $^{137}\text{Cs}$  should be in channel 55, with the first channel being number 1, when the system is calibrated according to NRPA (NGU) who has supplied data from the Barents Rescue exercise.

NRPA/NGU uses IAEA standard windows, Table B.3. On basis of those data an energy calibration has been made, assuming that the first channel is channel 1. Additionally an energy calibration has been performed on the spectral components from an NASVD analysis of the file 180901.dat. The latter energy calibration, DTU, counts from channel 0. The two energy calibrations differ in the low energy spectrum region. Figure B.8 presents the two different calibrations. Area specific stripping factors presented here were calculated using the NRPA/NGU energy calibrations.

Table B.3. NGU windows for standard window stripping (IAEA energy windows).

	$^{137}\text{Cs}$	$^{40}\text{K}$	$^{214}\text{Bi}$ (U)	$^{208}\text{Tl}$ (Th)
LL chn.	51	109	132	189
UL chn.	59	125	148	220
LL keV		1370	1660	2410
UL keV		1570	1860	2810



Table B.4. DTU windows for standard window stripping (IAEA energy windows).

	<sup>137</sup> Cs	<sup>40</sup> K	<sup>214</sup> Bi (U)	<sup>208</sup> Tl (Th)
LL chn.	51	108	130	189
UL chn.	60	123	146	221
LL keV	614	1370	1660	2410
UL keV	735	1570	1860	2810

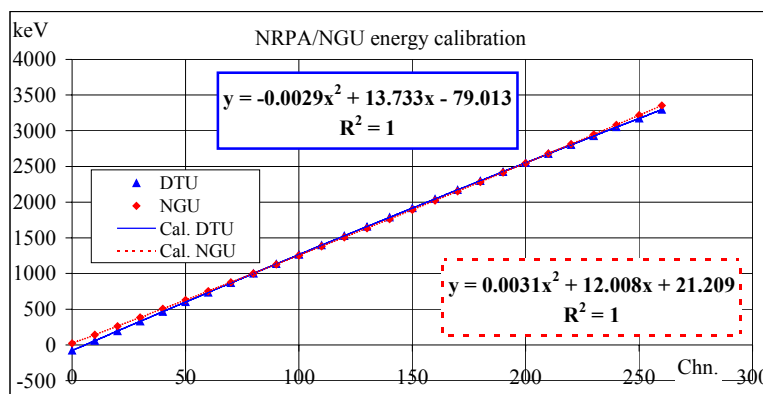


Figure B.8. Energy calibrations for the NRPA (NGU) system.

### SGU: AGS

The spectral components from a NASVD processing of the Area1 AGS file were used for identifying significant peaks for natural radioactivity and <sup>60</sup>Co. No spectrum drift was observed among the first spectral components i.e. the spectrum stabilisation has worked very well. The lowermost peak included here was the <sup>60</sup>Co peak of 1173 keV. Peaks at lower energy had not a well-defined spectrum position. It was assumed that channel 0 corresponds to 0 keV.

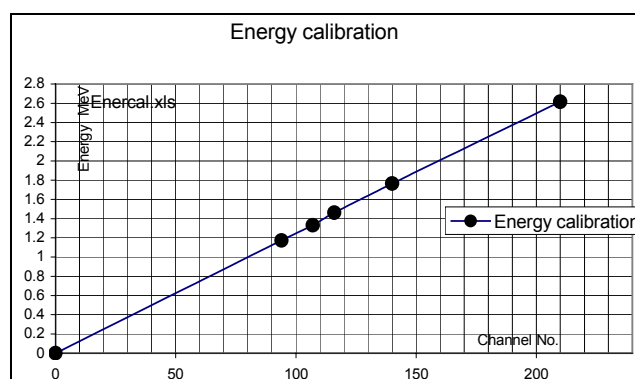


Figure B.9. Energy calibration for the SGU system.

Hereby one gets the energy-channel relation:  $E \text{ (keV)} = 12.5 \times \text{channel No.} + 3.5$  where the calculated energy corresponds to the centre of the channel, which is 12.5 keV width. This width should be taken into account when energy ranges of windows are considered in detail.



## Appendix C. Maps of sources at Barents Rescue LIVEX

Table C1. Sources at the Barents Rescue LIVEX exercise: Area 1.

	Area 1			
No.	1:1	1:2	1:3	1:4
Nuclide	$^{60}\text{Co}$	$^{131}\text{I}$	$^{60}\text{Co}$	$^{60}\text{Co}$
GBq	4.9	10.3-8.5	4.9	4.9
E	1756005	1756005	1755956	1756747
N	7298134	7299224	7299830	7300334

Table C2. Sources at the Barents Rescue LIVEX exercise: Area 2 and Area 3.

	Area 2						Area 3
No.	2:1	2:2	2:3	2:4	2:5	2:6	3:1
Nuclide	$^{60}\text{Co}$	$^{60}\text{Co}$	$^{99}\text{Mo}$	$^{99}\text{Mo}$	$^{137}\text{Cs} / ^{60}\text{Co}$	$^{241}\text{Am}$	$^{60}\text{Co}$
GBq	4.9	4.9	0.9-0.5	5.5-3	$3 \times 0.5 / 3 \times 0.02$	0.0004	$4 \times 4.9$
E	1764029	1764048	1764844	1765350	1763466	1760526	1766304
N	7307246	7307266	7307031	7305451	7306095	7302595	7316848

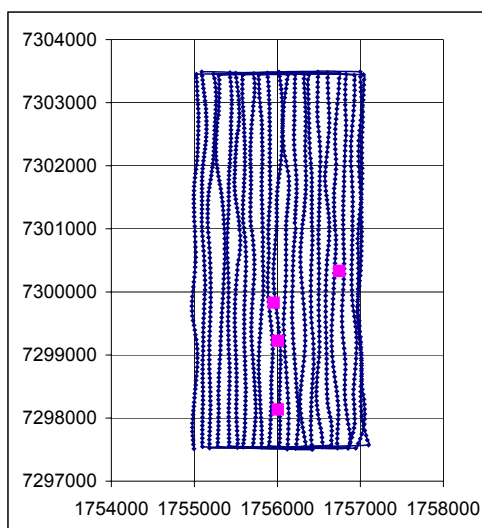


Figure C.1. Flight lines for Swedish team SEA, Area 1. Squares indicate sources

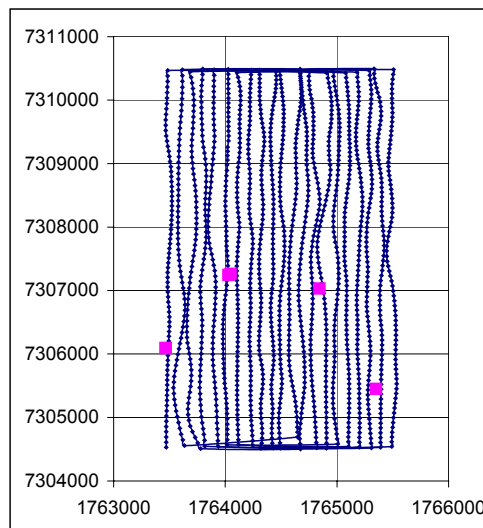


Figure C.2. Flight lines for Swedish team SEA, Area 2. Squares indicate sources.

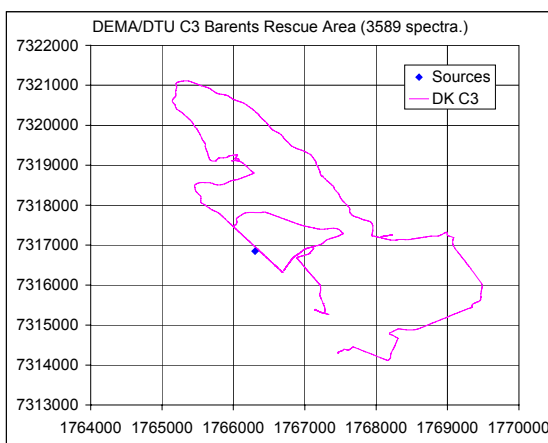


Figure C.3. Track lines for Danish team DKK, Area 3. Diamond indicates source.

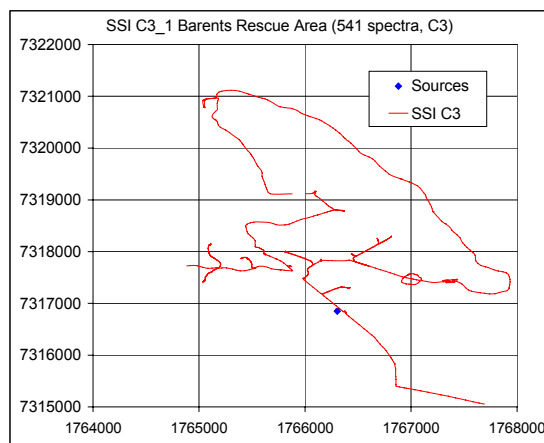


Figure C.4. Track lines for Swedish team SEK, Area 3. Diamond indicates source.

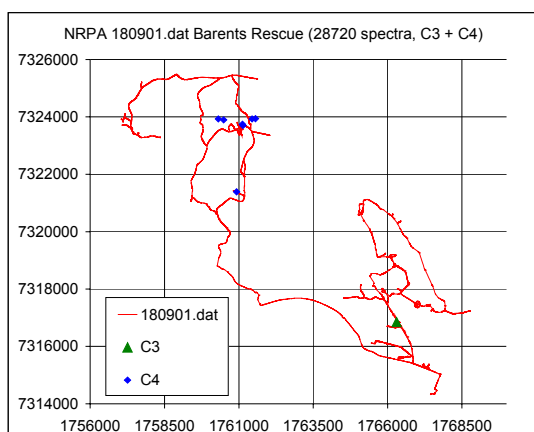


Figure C.5. Track lines for Norwegian NOK, Area 3 and Area 4. Source positions indicated by diamond and triangle.

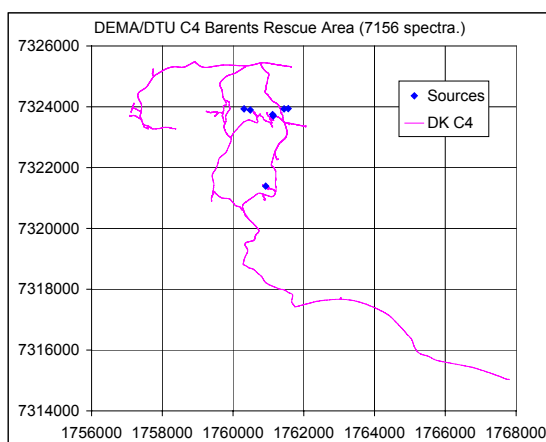


Figure C.6. Track lines for Danish team DKK, Area 4. Diamonds indicate sources.

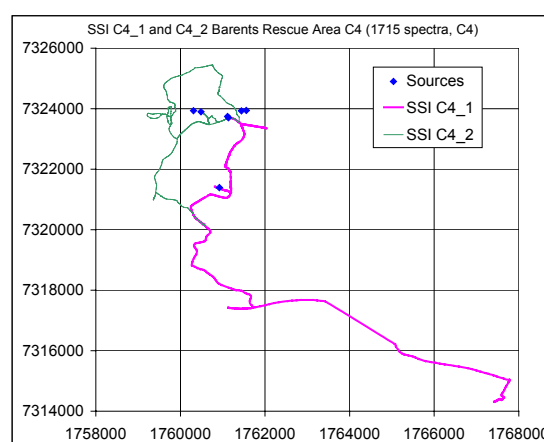


Figure C.7. Track lines for Swedish team SEK, Area 4. Diamonds indicate sources.

Table C.3. Sources at the Barents Rescue LIVEX exercise: Area 7.

	Area 7							
No.	7:1	7:2	7:3	7:4	7:5	7:6	7:7	7:8
Nuclide	$^{60}\text{Co}$	$^{60}\text{Co}$	$^{60}\text{Co}$	$^{60}\text{Co}$	$^{60}\text{Co}$	$^{226}\text{Ra}$	$^{226}\text{Ra}$	$^{226}\text{Ra}$
GBq	4.9	4.9	4.9	4.9	4.9	Nat.	Nat.	Nat.
E	1725376	1721169	1718957	1718983	1711648	1721282	1718765	1712920
N	7340248	7340769	7338223	7338209	7331315	7340593	7337175	7318874

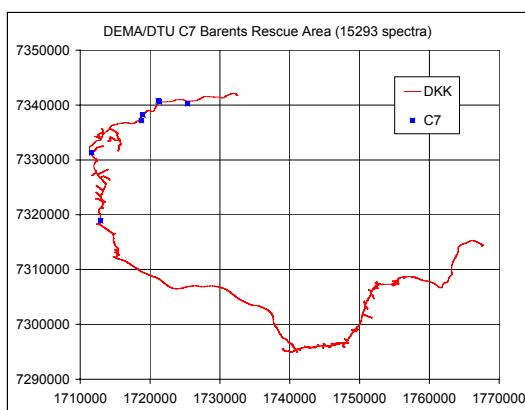


Figure C.8. Track lines for Danish team DKK, Area 7. Squares indicate sources.

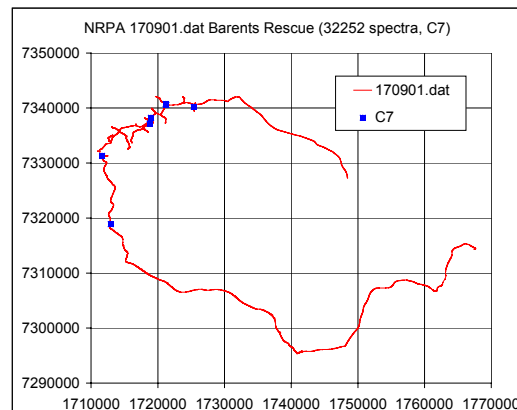


Figure C.9. Track lines for Norwegian team NOK, Area 7. Squares indicate sources.

## Appendix D. Fluence rates and detection limits for Area 2 sources

During the LIVEX exercise the AGS teams only were able to find source 2:4 ( $^{99}\text{Mo}$ ; 5.5-3 GBq). During post processing the source 2:2 ( $^{60}\text{Co}$ ; 4.9 GBq) was also detected in the Danish and the Swedish data sets. Using the ASS technique a signal just exceeding the statistical noise was recognised. In the following is given some theoretical evaluations of the chances for detecting the Area 2 sources.

### Source 2:1 at the co-ordinates E: 1764029, N: 7307246

Source 2:1 was a  $^{60}\text{Co}$  source of activity 4.9 GBq. The source probably was in an open transport container and the beam of photons was directed parallel to the ground and directed towards the nearby road (Ref. 2). The container was placed within a concrete bunker with wall thickness estimated to 25 cm. In addition a 30-40 cm layer of soil covered the bunker. The transport container is assumed to fulfil the specifications for shielding. Therefore with an additional shielding by concrete and soil there is no possibility for detecting the source directly from the air. The only detection possibility, therefore, is from photons that have been Compton scattered upwards somewhere along the beam.

The following calculations refer to source 2:1, but the results also partly cover source 2:2. The mean distance of primary photons (assuming 1.25 MeV as an average of 1.17 MeV and 1.33 MeV) in air before being Compton scattered is about 144 m. Therefore seen from 50-70 m altitude the beam acts as a line source, and within 100 m beam length 50% of the beam photons have been scattered. In order to detect those photons when flying at 60-70 m altitude one should concentrate on photons (from source 2:1) that have been scattered  $45^\circ$ - $90^\circ$ . The probability for  $135^\circ$  or larger scatter is low. Photons scattered a smaller angle than  $45^\circ$  will in average have to pass an additional long path through the air after being scattered in order to reach the aircraft altitude. Some of those photons will experience an additional scatter away from the beam – and with an additional lowering of the photon energy.

There is no information on the beam solid angle, but probably it has been below 10% of  $4\pi$ . The number of primary scattered photons within the first 100 m beam therefore becomes no more than  $N_{\text{scatter}} = 0.1 \cdot 4.9 \cdot 10^9 \cdot 2 \cdot 0.5 = 4.9 \cdot 10^8$  photons per second. (Having two photons per decay causes the factor 2. Having only 50% of the photons interacting within 100 m causes the factor 0.5.) The beam solid angle may have been significantly smaller, and a scatter intensity of only  $1.0 \cdot 10^8$  photons per second is quite realistic.

An investigation of the angular distribution for the Klein-Nishina cross section indicates that about 30% of the primary photons are Compton scattered an angle between  $45^\circ$  and  $90^\circ$ , therefore the beam acts as a 100 m line source of intensity  $1.5 \cdot 10^8$  photon per second ( $0.3 \cdot 4.9 \cdot 10^8 = 1.47 \cdot 10^8$ ). However the intensity may be as low as  $0.3 \cdot 10^8$  photons per second.

Neglecting first additional interactions in the air one will at best at 50 m altitude have a fluence rate of  $45^\circ$ - $90^\circ$  scattered photons of 4680 photons per s and  $\text{m}^2$  ( $1.47 \cdot 10^8 / 2\pi \cdot 50 \cdot 100 = 4679$ ). With attenuation in air and in the aircraft body one gets a realistic optimum count rate of 300 cps. (Detector area  $0.16\text{m}^2$  when seen from below.) The aircraft speed is some 70-80 m per s and therefore the detector will not be in an optimum position relative to the beam for a whole count period (app. 1 s).

Dependent on the angle between beam direction and flight direction the number of counts could be from less than 150 to about 300.

If the beam solid angle is smaller than 10% of  $4\pi$  the optimum number of counts becomes smaller – maybe a factor 5 – and the expected number of counts could be between 30 and 60.

The energy of a 1.25 MeV photon after a  $45^\circ$  Compton scatter is 0.72 MeV and for a  $90^\circ$  scatter the energy is 0.36 MeV. A post-processing search for scattered  $^{60}\text{Co}$  photons therefore should concentrate on the energy range from 0.36 MeV to 0.72 MeV - with appropriate stripping factors for this wide energy window.

### **Source 2:2 at the co-ordinates E: 1764048, N: 7307266**

Source 2:2 also was a  $^{60}\text{Co}$  source of activity 4.9 GBq i.e. similar to the 2:1 source. It was placed in a concrete bunker preventing primary photons from reaching an airborne detector just above the source. A beam of photons, however, was directed  $30^\circ$  upwards reaching 65 m altitude after having passed through 130 m of air.

There is given no information on the beam cone angle. However, it is possible to estimate the count rate for an AGS detector passing through the beam. The best situation is if the aircraft just happens to pass the centre of the beam; this means for an aircraft at 65m-altitude the distance to the source becomes  $L = 130$  m. With 2 photons per decay and an attenuation coefficient of  $6,92 \cdot 10^{-3} \text{ m}^{-1}$  the fluence rate  $\phi$  of primary photons becomes  $1,9 \cdot 10^4$  photons per  $\text{m}^2$  and s.

Using an effective detector area - as seen from the direction of the beam - of  $0,11 \text{ m}^2$  and taking a full energy detection efficiency of 0.5 into account a full energy event count rate of about 1034 cps is obtained.

Now assume a cone angle of  $2 \times 22,5^\circ$ . The "beam diameter" at 130m distance becomes ca. 100 m; and therefore the detector - carried by an aeroplane of speed 70-80 m/s - is exposed to the beam for about 1-2 seconds dependent on the altitude and on the beam direction relative to the flight direction.

If the conditions for this optimistic estimate are fulfilled - i.e. beam width, speed, flight line, angle etc - it should be possible to observe a significant full energy signal; and even less than optimum conditions should generate a detectable signal – at full energy or at a lower energy.

The experiences with detection of full energy events near source 2:2 is described in Chapter 5 where also the signals at lower energies are discussed. The number of surplus counts for a very wide window (Ch. 16 to 105) is 399 counts. This is well below the calculated count rate of 1034 cps mentioned above, which includes only primary photons. Therefore the beam has only been lightly "touched upon" by the detector – or stronger attenuation has to be assumed. (A window for the channels 59-108 has only a surplus count number of 111 counts. This number of counts better represent the detection of primary photons.)

None of the AGS teams participating in the exercise reported the source 2:2. A careful post processing of the Danish AGS data gave a result similar to the results reported here for the Swedish data – a signal just exceeding the statistical noise can be seen near the sources 2:1 and 2:2. But one may wonder why none of the aircrafts had passed directly through the centre of the source 2:2 beam. Is it possible that all teams have followed a flight line that only marginally touches the beam cone?

In the following is examined the possibility for detecting 45-90<sup>0</sup> scattered photons from source 2:1 – but scattered photons from source 2:2 of course could be detected similarly.

Area specific stripping factors for Area 2 were calculated for the low energy windows (channels) 29 to 57 (A), 27-39 (B), and 40-59 (C). The investigations included all Area 2 spectra except three spectra registered with an amplitude higher than 85.0 m (inadvertently not included). Three spectra with signals from source 2:4 (<sup>99</sup>Mo) were not included in the calculation of the stripping factors used for stripping the windows A, B, and C. Additional calculations, however, showed that almost the same stripping factors are obtained if the <sup>99</sup>Mo signals are included; see the Table D.1.

Table D.1. The stripping factors for the windows A, B and C for Area 2. Bold numbers are calculated without inclusion of three spectra with a <sup>99</sup>Mo signal.

ID and keV	$\delta$	$\epsilon$	$\zeta$
A 366-741	<b>4.7716</b>	<b>5.717796</b>	<b>2.589352</b>
	4.775469	5.725232	2.587513
B 341-491	<b>2.82813</b>	<b>3.287193</b>	<b>1.610743</b>
	2.832519	3.288691	1.610008
C 504-741	<b>2.665724</b>	<b>3.211089</b>	<b>1.406761</b>
	2.667812	3.215528	1.405736

### Window A examinations

Figure D.1 shows the stripped window A counts for 1596 spectra, and values above 110 counts are listed in Table D.2. The three highest numbers of stripped counts are found in the spectra Nos. 1343 (<sup>99</sup>Mo source), 916 and 89. Figure D.1 also tells that a "deficit " of 100-150 (stripped) counts is not uncommon and therefore the source signal (counts in window A) may sometimes be undetectable except for the top optimum situation with well above 200 "surplus" counts due to scattered photons.

Table D.2. Spectra with more than 110 stripped counts in Window A (366 keV to 716 keV).

Spectrum No.	Stripped Counts	Spectrum No.	Stripped Counts
89	<b>147.9</b>	1111	114.3
216	111.9	1212	121.4
456	136.8	1216	112.9
478	141.5	1343	<b>740 Source</b>
766	111.0	1421	108.5
796	120.6	1422	110.3
916	<b>163.6</b>	1587	110.8

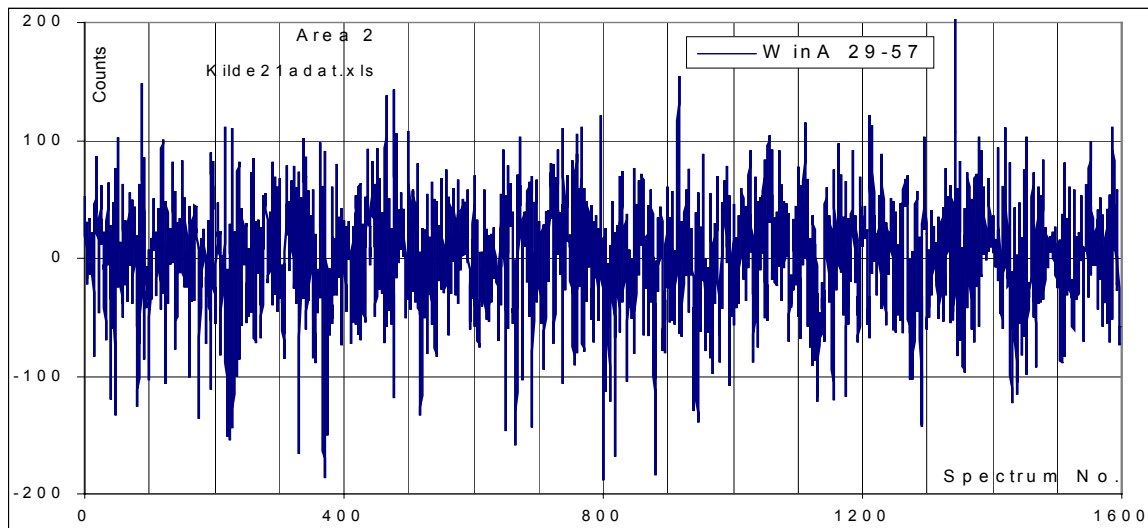


Figure D.1. Stripped counts for window A as a function of spectrum number (measurements above 85.0 m not included).

Figure D.2 shows the results for the examination of the distribution of the stripped window A counts. Out of 1596 spectra 14 spectra have more than 110 (stripped) counts in this window. In the lower right corner is the signal from source 2:4 with 740 (surplus) counts. The next highest number of (surplus) counts (154) is at the large square near source 2:1 indicated by the large circle (position 1764029,7307246). The other source (2:2) is placed nearby – at position 1764048,7307266 i.e. 27 m east of source 2:1 and 20 m towards north; and both sources may contribute to the detector signal.

Photos of the shelters of the sources 2:1 and 2:2 (concrete bunkers) indicate that the photons in both cases are directed towards east or south-east from the sources (Ref. 2). Therefore spectrum No. 916 may contain a signal from both sources.

The number of "surplus" counts for window A in spectrum No. 916 is 164 only surpassed by spectrum 1423 with 740 counts due to source 2:4 ( $^{99}\text{Mo}$ ). Next follows spectrum No. 478 with 142 "surplus" counts. Then follow the other spectra indicated in Figure D.2 (with more than 110 counts).

A higher stripped count rate may be due to a source signal or due to a counting statistical outlier. A source signal may raise the number of counts in two consecutive spectra whereas counting statistics very seldom generate two consecutive outliers. Therefore an averaging of the surplus counts for two consecutive spectra often eliminates the outliers caused by counting statistics. Figure D.3 shows the distribution of window A stripped counts when averaged over two consecutive spectra.

After averaging spectrum No. 916 still stands out with 108 counts. Spectrum No. 87 drops to 90. On the other hand the spectra Nos. 1421 and 1422 give an average of 110 counts slightly surpassing spectrum No. 916.

Finally an examination of the total number of counts in the windows Th, U, K, and A tells that no unusual number of counts are seen in the interesting spectra discussed above. (The numbers are not presented here.)

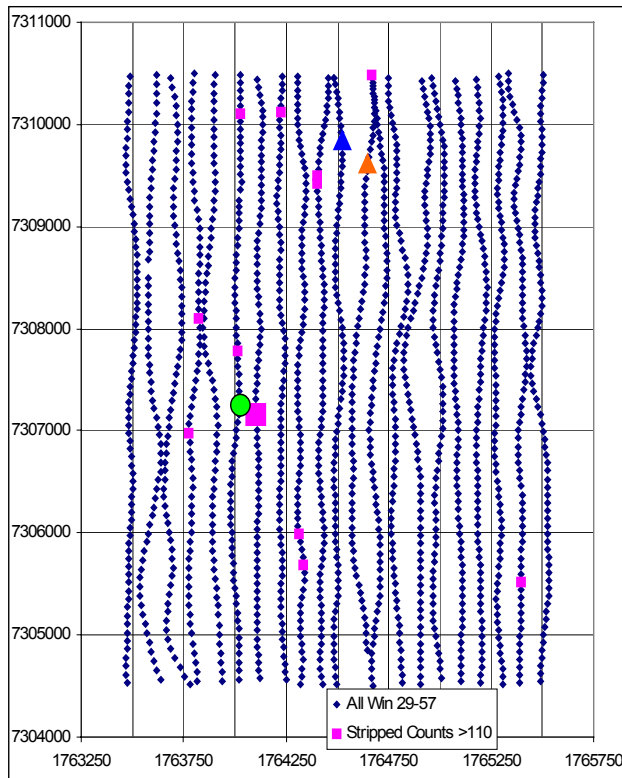


Figure D.2. Positions for AGS spectra recorded within Area 2 by SGU. The twin sources 2:1 and 2:2 are shown as the large green circle near position 1764029, 7307246. Squares and triangles indicate stripped window A counts above 110. The large square indicates spectrum No. 916. The triangles indicate the spectra Nos. 89 (orange) and 1587 (blue). The two neighbouring small squares refer to the spectra Nos. 1421 and 1422.

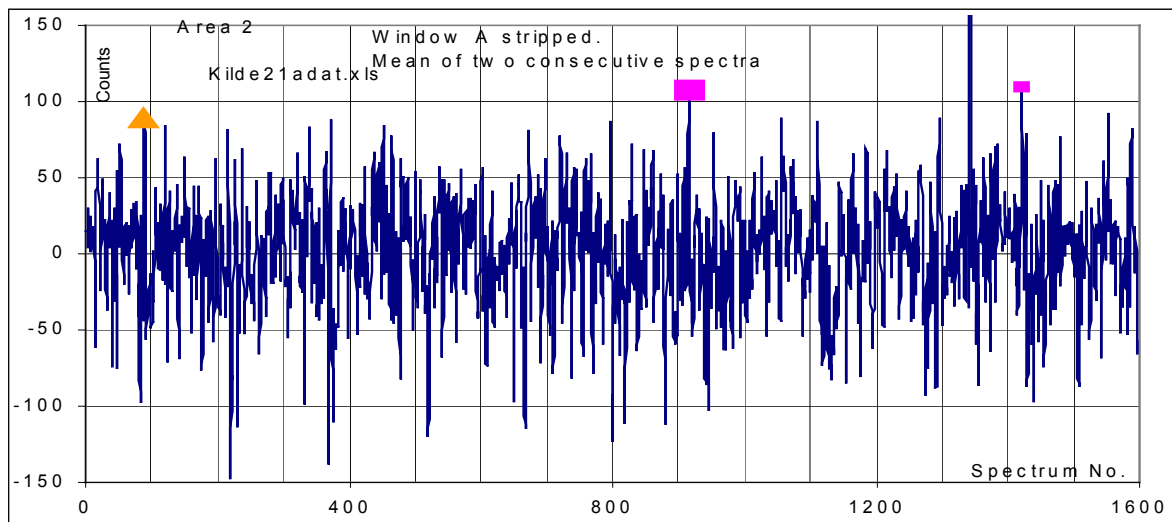


Figure D.3. Average of two consecutive stripped counts for window A with marking of the spectra Nos. 86 (triangle), 916 (large square) and 1422 (small square).

Spectrum 916 is recorded at almost the position where scattered photons from the sources 2:1 and 2:2 are expected. The "surplus" of counts - 148 - is almost what one should expect from source 2:1. The observed surplus counts may, however, also be due to photons from source 2:2. It is concluded that one of the sources – or both – seemingly have been detected. But one also has to conclude that the signal from the

source(s) is at the limit of detection. The signal intensity corresponds almost to what one could expect if scattered photons from the beam of source 2:1 are detected.

In Chapter 5 and above is discussed the possibility for detecting primary photons by having the aircraft passing directly through the beam. During approaching and passing through the centre of the beam surplus signals should also be observed at lower energies. But the count rates actually recorded are well below the level corresponding to the theoretical considerations.

### **Energy distribution of detected photons**

By an investigation of the surplus counts\* in all three special low energy windows one gets the following results:

Spectrum No. 1343 (with the <sup>99</sup>Mo source) has a very significant surplus of stripped counts both for window A, B and C.

Spectrum No. 916 (near the sources 2:1 and 2:2) has a significant surplus of stripped counts both for window A, B and C.

Spectrum No. 89 has a significant surplus of stripped counts both for window A and B but not C i.e. the signal mostly is due to photons of energy below 500 keV – or the result is a "statistical outlier".

Spectrum No. 228 has a significant surplus of stripped counts only for window B i.e. below 500 keV.

Spectrum No. 456 a significant surplus of stripped counts only in window A.

Spectrum No. 465 has a significant surplus of stripped counts only for window C i.e. between app. 500 keV and 745 keV.

Spectrum No. 478 has a significant surplus of stripped counts both for window A and C.

Spectrum No. 1294 has a significant surplus of stripped counts only for window C.

Spectrum No. 1587 has a significant surplus of stripped counts for the windows A and B – and a non-significant surplus for window C.

\*That a spectrum has a significant surplus just means that the number of surplus counts (after stripping) is among the 6 highest surplus counts for the whole area.

One may conclude that spectrum No. 916 clearly shows the presence of unusual radiation in the energy region corresponding to scattered photons from source 2:1 or 2:2. And even without knowing on beforehand the existence of the source one could claim that with a high degree of probability a radiation anomaly is present near the position of spectrum No. 916.

Some of the other spectra listed above could also generate a warning. Spectrum No. 89 for example could be assumed to include signals directly from a low energy source (app. 300 to 500 keV) or signals for higher energy primary photons that have been scattered.

**Source 2:3 at the co-ordinates E: 1764844, N: 7307031**



This source was a  $^{99}\text{Mo}$  source of activity 0.7 GBq (on the day of the survey) i.e. a factor 6 lower than source 2:4 (also  $^{66}\text{Mo}$ ) that was easily detected. The 2:3 source beam was directed upwards with an opening angle of  $45^\circ$  (Ref. 2).

For the 2:4 source a stripped count rate of more than 500 cps was obtained even though not passing directly above the source. For a similar position etc. for source 2:3 a count rate of 80-90 cps should be obtained. The opening angle was about  $45^\circ$  and therefore at the flight height the beam diameter was 55-65 m. It is possible that the flight lines have passed outside the beam. The figures 5.5.2 and 5.5.3 with the "53-66 window" (also appropriate for source 2:3) shows no significant signal at the positions close to the source 2:3.

The spectra Nos. 549, 550, and 551 at the co-ordinates (1764866, 7307116), (1764874, 7307035) and (1764881, 7306955) respectively are close to the source position (1764844, 7307031). They have a moderate surplus of stripped counts, but many spectra recorded far from any source have a larger surplus. The conclusion therefore is that this source cannot be detected from the recorded data although the experiences with source 2:4 indicate that a source with activity as source 2:3 is detectable if the measuring geometry is as for source 2:4. One may wonder why none of the AGS teams detected this source. Although the beam diameter was just 55-65 m at 60 m altitude it seems unlikely that none of the aircrafts have passed through the beam.

#### **The sources 2:5-1 and 2:5-2 at the co-ordinates E: 1763466, N: 7306095.**

At this location were placed three  $^{137}\text{Cs}$  sources each of 0.5 GBq activity together with three 0.02 GBq  $^{60}\text{Co}$  sources. The caesium sources beamed up into the air whereas the cobalt sources beamed in a horizontal direction i.e. they could not be detected from the air. There is no information on the opening angle for the caesium sources. The theoretical count rate for an AGS detector passing at 60 m altitude above one of the sources is calculated as follows:

The attenuation coefficient  $\mu$  for 0.662 MeV photons in air is  $9.3 \cdot 10^{-3} \text{ m}^{-1}$  corresponding to a mean penetration length of 107 m and a "half length" of 75 m. The fluence rate at 60m then becomes:

$\phi_{60\text{m}} = 5 \cdot 10^8 \cdot 0.85 \cdot \exp(-60 \cdot 0.0093) / (4\pi \cdot 60^2) = 5377 \text{ s}^{-1}\text{m}^{-2}$ . (The factor 0.85 refers to the yield/intensity).

Assuming an additional factor 0.5 covering attenuation in source shelter and aircraft body and the peak to total ratio, one gets with a 40cm x 40cm x 10cm detector a count rate of 430 cps. This is the count rate with the detector just above the source. When positioned at an angle of  $45^\circ$  the count rate becomes about 180 cps (longer path in air). If the flight line is 60 m from the source i.e. at 85 m "air distance" – but still within the beam of primary photons the maximum count rate becomes:

$\text{CR}_{\text{max}} = 5 \cdot 10^8 \cdot 0.85 \cdot 0.5 \cdot (0.25 + 0.75 \cdot \cos(45^\circ)) \cdot 0.16 \cdot \exp(-85 \cdot 0.0093) / (4\pi \cdot 85^2) = 132 \text{ cps}$ .

The expression " $(0.25 + 0.75 \cdot \cos(45^\circ))$ " is a crude description of the angular dependency of the relative detection probability.

Near the source position (1763466, 7306095) the spectra Nos. 20 and 21 were recorded at the positions (1763489, 7306053) and (1763492, 7306129) respectively (distance 50m and 60m towards East). A wide caesium window (366 keV to 728

keV) including detection of both of primary photons and forward scattered photons shows no significant surplus count for this window - spectrum #20 has a surplus of 42 counts and spectrum #21 has 12 surplus counts (after stripping). Spectrum #19 (1763487, 7305977) - not as close to the source 2:5 according to the co-ordinates - has a surplus of 90 counts. However, many other spectra recorded within Area 2 have a higher surplus of counts without being near a source.

Therefore the conclusion is that the sources 2:5 cannot be detected. If the sources had a narrow beam cone upwards this can be understood. If the cone angle is larger than  $2 \times 45^\circ$  (and symmetric around vertical) the sources should generate a stronger signal that could be detected.

Also for source 2:5-1 one may wonder why none of the AGS teams were able to detect this.

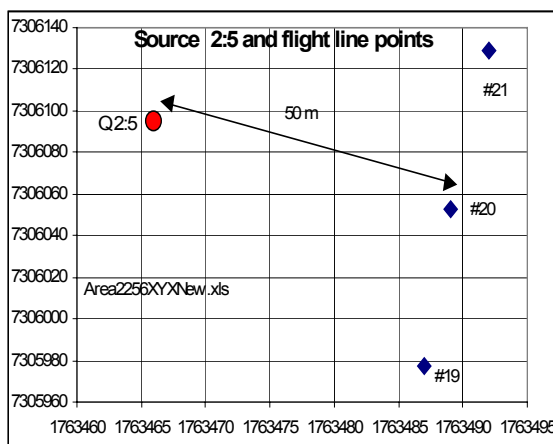


Figure D.4. Positions of source 2:5 and nearby data recordings for SGU AGS data from Area 2. Notice that the x-axis and the y-axis have a different scaling.

## Appendix E. Th and U gamma lines

The variation with energy of the single channel stripping factors can be studied by examining the spectra of thorium and uranium. Figure E.1 shows the thorium spectrum as measured with a high resolution detector (Ge(Li)) in the laboratory. The 2615 keV gamma line (from  $^{208}\text{Tl}$ ) is outside the energy range of the figure – only gamma lines with energy below 1000 keV are included. For thorium this means all the important lines to be stripped away.

A visual examination of the figure tells that the following important gamma lines should be stripped away:

238 keV( $^{212}\text{Pb}$ ; 44%), 338 keV( $^{228}\text{Ac}$ ; 11%), 510 keV( $^{208}\text{Tl}$ ; 7%), 583 keV( $^{208}\text{Tl}$ ; 28%), 727 keV( $^{212}\text{Bi}$ ; 12%), 795 keV( $^{228}\text{Ac}$ ; 5%), 860 keV( $^{208}\text{Tl}$ ; 12%), 911 keV( $^{228}\text{Ac}$ ; 28%), 969 keV( $^{228}\text{Ac}$ ; 17%). The stated percentages are the yields/intensities. For  $^{208}\text{Tl}$  the branching ratio of 33% is included.

A stripping should – besides eliminating the continuous spectrum background of Compton scattered photons – also eliminate the signals from the gamma line shown in the figure. When starting from above (1000 keV) a minor increase could be observed at 910-970 keV, at 583 keV, at 338-350 keV and at 238 keV. The single channel stripping factor for Th (SGU data) shown in Figure 5.7.1 exhibits a "smooth step" starting at channel 60 (753 keV) and ending at channel 46 (578 keV). The lower limit may fit to the 583 keV line whereas the upper "limit" may be a combination of the 727 keV line ( $^{212}\text{Bi}$ ) and the general increase in the amount of Compton scattered photons at lower energies.

At channel 31 another increase starts i.e. at 390 keV. This is somewhat above the gamma-lines between 325 keV and 350 keV. Perhaps there is interference between the Th-stripping and the U-stripping. The uranium decay chain has a very strong gamma line at 352 keV.

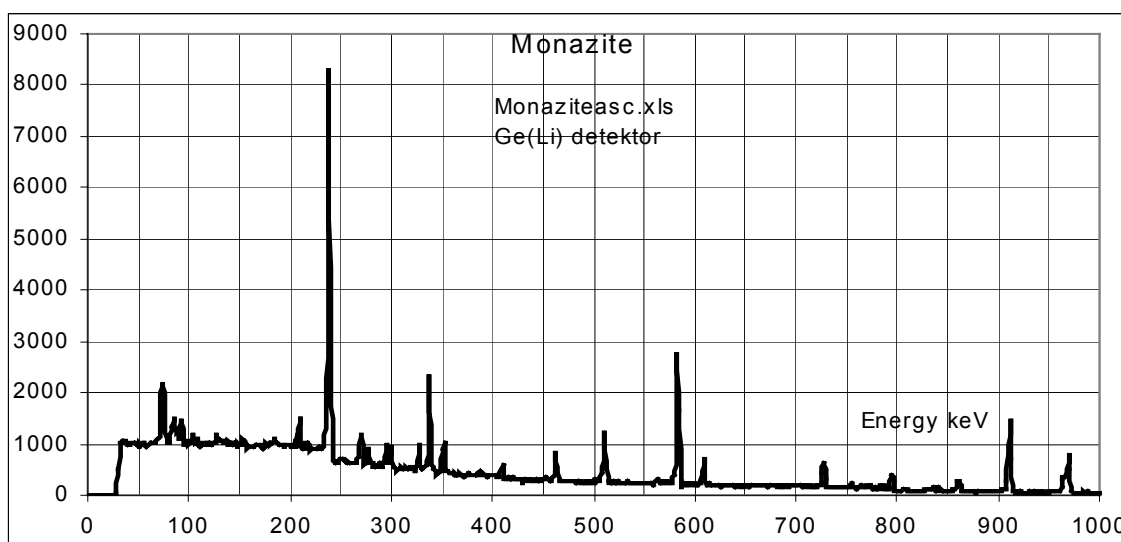


Figure E.1 Gamma lines for the  $^{232}\text{Th}$  decay chain. (Heavy mineral monazite contains a large amount of thorium.)

The most important uranium gamma lines for Figure E.2 are:

242 keV ( $^{214}\text{Pb}$ , 7%), 295 keV ( $^{214}\text{Pb}$ , 19%), 352 keV ( $^{214}\text{Pb}$ , 37%), 609 keV ( $^{214}\text{Bi}$ , 46%), 768 keV ( $^{214}\text{Bi}$ , 5%)

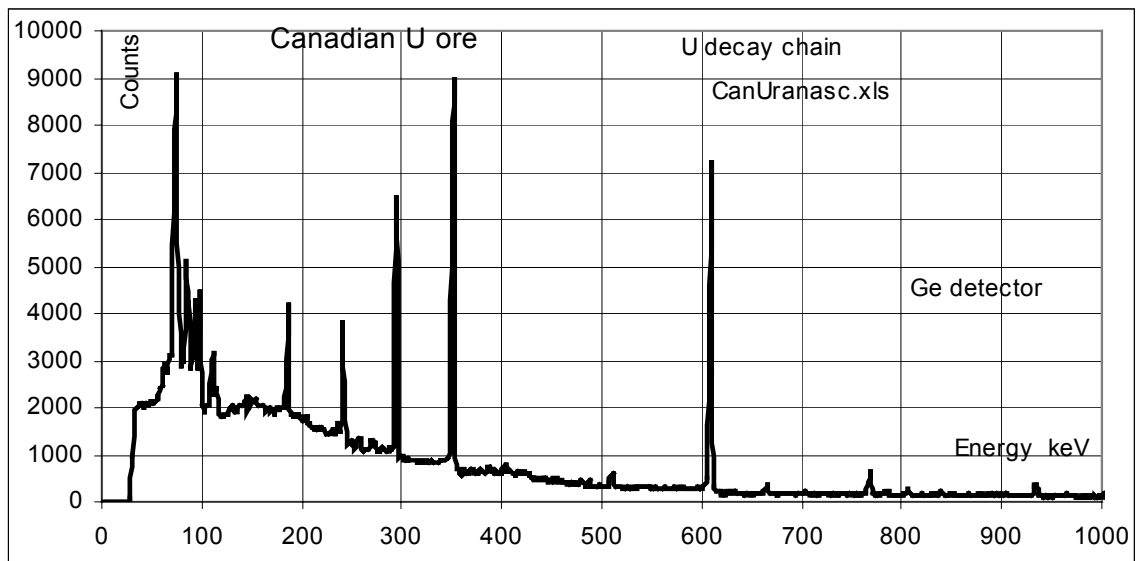


Figure E.2. Gamma lines for the  $^{238}\text{U}$  decay chain measured in the laboratory with a Ge(Li)-detector.

The curve for the single channel stripping factor ( $b''$ ) of Figure 5.7.2 has a "steep step" at channel 54 corresponding to 678 keV. This must be caused the 609 keV gamma line. (Even with a detector FWHM of 10% the step is observed at a rather high energy!)

Another sharp increase in the  $b''$  value is observed at channel 31 corresponding to 390 keV. This must be related to the strong line at 352 keV. Again the increase starts at a rather high energy. The influence of the 295 keV line cannot be separated from the influence from the 352 keV line.

Figure E.3 shows a laboratory (Ge-detector) spectrum of heavy minerals sand that contains high concentrations of Th and U, and very little K.

The most important thorium line ( $^{208}\text{Tl}$ ) at 2615 keV is easily seen. The uranium line ( $^{214}\text{Bi}$ ) at 1765 keV is also easily recognised. Those two lines are the lines used for stripping NaI detector spectra. The potassium line ( $^{40}\text{K}$ ) at 1461 keV is just discernible. In normal environmental spectra this line is the very dominating line.

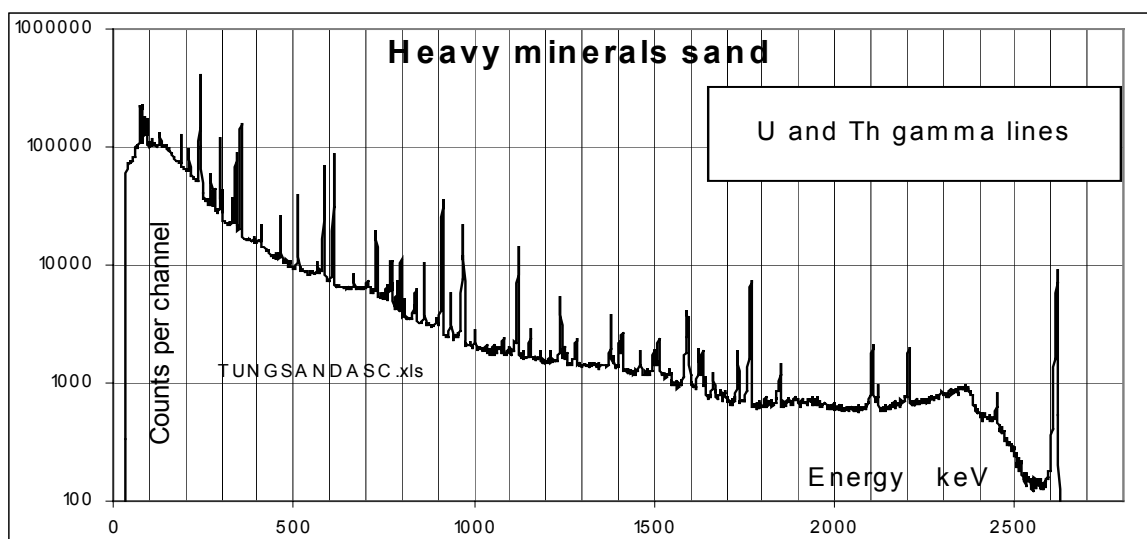


Figure E.3. Ge(Li)-detector spectrum of heavy minerals sand with Th and U.

In the "low energy region" – from 200 keV to 1400 keV – is seen a large number of gamma-lines originating from both Th and U.

When measured with a NaI detector it is only possible to observe the strongest lines. The Th + U lines at 583 keV + 609 keV often are seen as a minor common peak. The same is the case for all lines from 900 keV to 960 keV together. The peaks close to 350 keV may not be as easily observed with AGS NaI detectors as one might expect from their intensity in Figure E.3. All gamma lines in the "low energy region" are attenuated more in the air than the "high energy" lines of Th and U. This influences the height variation of the stripping parameters  $\delta'$  and  $\epsilon'$  as described in Chapter 5. Besides that Compton scattering causes a "build-up" of low energy photons in the air.

It should be pointed out that the ratio between the amount Th and U in the heavy mineral sand sample of the figure is almost the same as is met in most Scandinavian Quaternary deposits. Therefore the relative intensities – Th vs. U – can be estimated from the figure.

At the comparisons above between the "steps" for the single channel stripping factors and the energy of characteristic thorium and uranium gamma photons it was observed that the "steps" seemingly were observed at energies somewhat too high. One therefore may question the energy calibration at the lower energies. The energy calibration – corresponding to Figure B.16 – has no fix-points below 1000 keV except an assumption on having channel 0 almost equivalent to 0 keV (3.5 keV) and a linear relation between energy and channel number all the way through.

However, gamma spectra based on NaI detectors often have a non-linear energy calibration below some 600 keV\*. Therefore 0 keV may for example correspond to channel number 10 (or 5 or 15) resulting in a non-linear relation between energy and channel number at energies from 600 keV and downwards. Hereby the "steps" of the single channel stripping factor curves are better fitted to the characteristic gamma photons emitted by the thorium and the uranium decay chains. Attempt to verify this for the SGU system failed, however.

\* It is a general experience that for NaI detectors  $\Delta E / \Delta_{\text{channel}}$  is lowest at low energies.

## Appendix F. SGU AGS background

The figure F.1 shows the background spectrum used with the SGU AGS data during the first investigations. Later the background was neglected i.e. the data was ASS processed without first subtracting the background spectrum.

It is noticed that the general shape of the background spectrum is very similar to that of ordinary spectra for natural radioactivity. Therefore the influence from not subtracting the background before ASS processing is very little.

(A closer examination of the background spectrum of Figure F.1, however, tells that uranium contributes with a slightly larger fraction of the counts than at a typical environmental spectrum.)

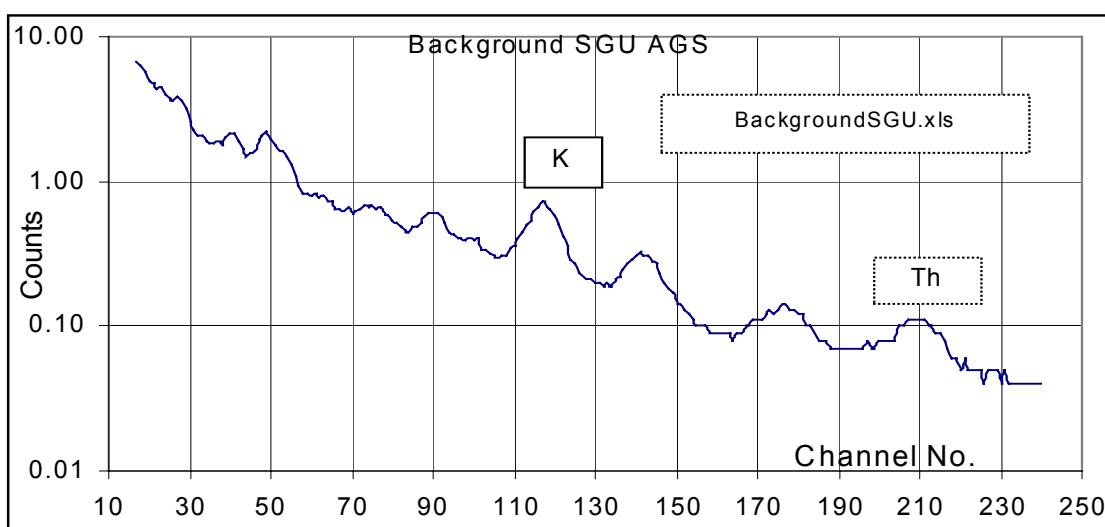


Figure F.1. SGU AGS background spectrum.

## Appendix G. Cross plots for SGU AGS data

In the figures G.1 to G.3 are plotted the stripped counts for three low energy windows "Low", "Medium" and "High" as a function of the altitude. Average (height independent) stripping factors have been used.

The figures tell that there is a tendency for the stripped counts of the energy window to increase with the altitude - i.e. the stripping is (slightly) too weak at "higher" altitudes. This is what one might expect. In Section 5.4 is discussed the altitude dependency of the stripping factors  $\delta'$ ,  $\epsilon'$ , and  $\zeta'$ . For K (i.e.  $\zeta'$ ) the tendency is clear; the stripping increases slightly with increasing altitude. The amount of scattered photons increases smoothly relative to the amount of primary photons when the altitude increases. For Th and U the tendency is not quite as clear.

According to the figures G.1 to G.3 the total stripping should increase with the altitude; by using average stripping factors - not height dependent - a surplus of counts is observed at "higher" altitudes. However, other factors that influence the relative amount of low energy photons in the air may be correlated to the actual altitude for example the mass thickness of the vegetation and/or the moisture content of the soil.

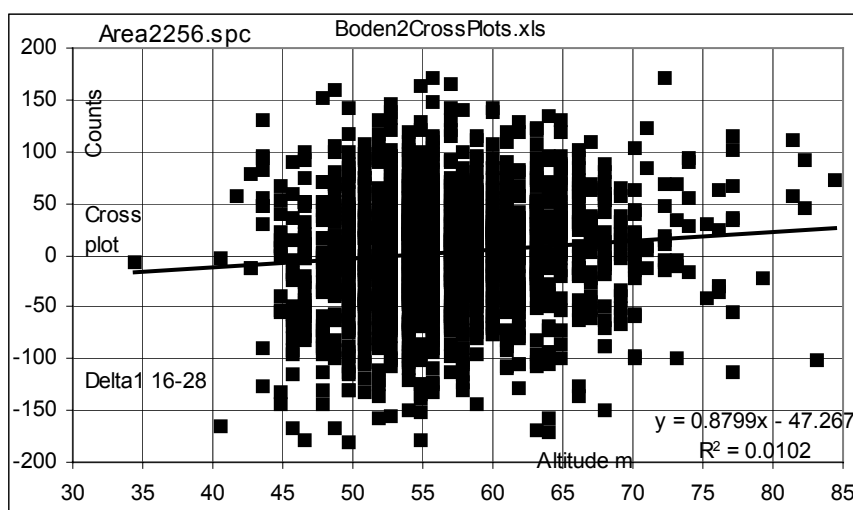


Figure G.1. Stripping of a low energy window counts vs. altitude. SGU, Area 2.

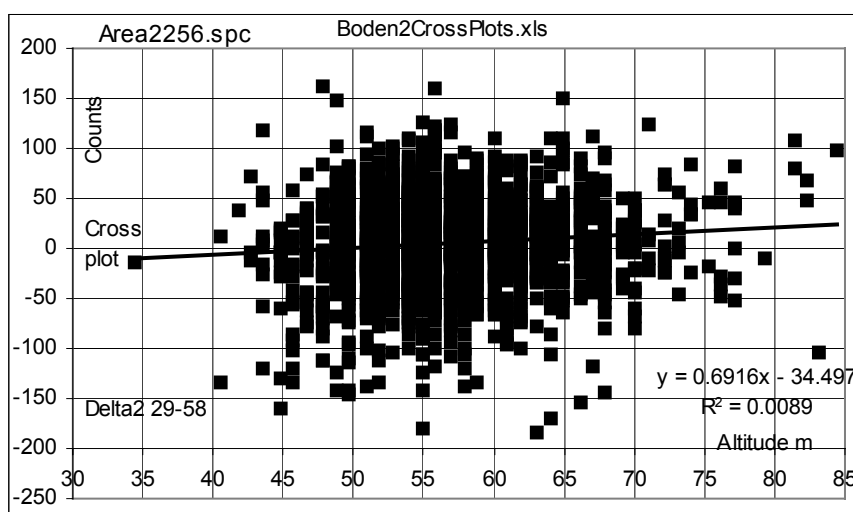


Figure G.2. Stripping of a medium energy window counts vs. altitude. SGU, Area 2.

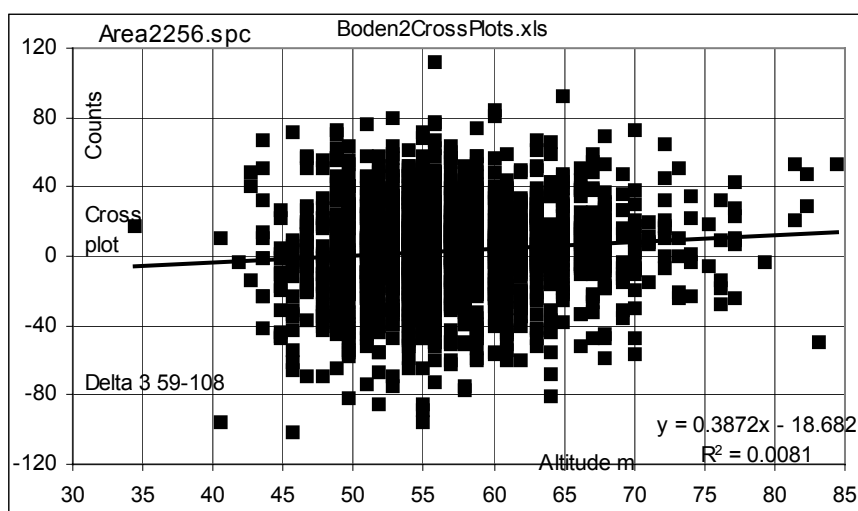


Figure G.3. Stripping of a "high" energy window counts vs. altitude. SGU, Area 2.

The "erroneous" stripping shown in the figures G.1 to G.3 could be compared to the average counts for the windows which are 491, 425 and 252 respectively. Errors (positive or negative "surplus" of stripped counts) may be up to a third of the average number of counts. The scatter is partly caused by the statistics of the window counts partly by the varying geometry. (The signals from the strong source (2:4) are not included in the data processing).

The figure G.4 with the very wide energy window, however, tells that for some energy windows there is no observable height dependency - indeed for window of Figure G.4 there is a very minor decrease with altitude. Other factors than the altitude therefore have the dominating influence on the values of the stripping parameters.

### Counting statistical variations

For Area 2 the average (gross) counts of the windows for Th, U, K, and the windows "Low" (chns.16-28), "Medium" (chns.29-58), and "High" (chns.59-108 and the corresponding stripping factors are:

	Average counts	$\delta'$	$\epsilon'$	$\zeta'$
Th	15.508			
U	16.131			
K	96.644			
Low	490.87	5.608052	7.309054	2.929367
Medium	425.01	4.857516	5.844793	2.635004
High	251.52	2.341648	2.142536	1.834156

Thus the "Low" window is stripped with:

$$5.608052 \cdot 15.50784683 + 7.309054 \cdot 16.13182674 + 2.929367 \cdot 96.6440678 = 487.98$$

(compare with 490.87)

Similarly the "Medium" window is stripped with 424.27 (compare with 425.01), and the "High" window is stripped with 248.14 (compare with 251.52)



The standard deviation  $\sigma_{\text{Low}}$  of the "Low energy " window stripping is determined from:

$$\sigma_{\text{Low}}^2 = \delta^2 \cdot \text{Cts}_{\text{Th}} + \epsilon^2 \cdot \text{Cts}_{\text{U}} + \zeta^2 \cdot \text{Cts}_{\text{K}} \quad (\text{with } \text{Cts}_{\text{Th}} \text{ is the average Th window counts})$$

$$\sigma_{\text{Low}}^2 = 5.608052^2 \cdot 15.50784683 + 7.309054^2 \cdot 16.13182674 + 2.929367^2 \cdot 96.644068$$

$$\sigma_{\text{Low}}^2 = 2178.85 \text{ and } \sigma_{\text{Low}} = 46.7$$

Similarly one gets:

$$\sigma_{\text{Medium}}^2 = 1588.03 \text{ and } \sigma_{\text{Medium}} = 39.9$$

$$\sigma_{\text{High}}^2 = 484.21 \text{ and } \sigma_{\text{High}} = 22.0.$$

Now investigate Figure G.1. It includes 1596 data points and according the calculations above a "typical standard deviation" of 46.7 counts could be assumed. For a normal (Gaussian) distribution of "surplus counts" one might expect that 0.27% measurements - i.e. 4 out of 1596 - deviate more than 3 standard deviations i.e. 140 counts in positive or negative direction. Figure G.1 tells that ten times as many measurements deviate at least 140 counts.

This way of examining the scatter is not the very correct way of doing it. It however, tells that the statistical scatter of window counts cannot alone explain the observed scatter. Thus a varying source and detector geometry also contribute significantly to the observed scatter - as one should expect for a set of spectra recorded in a non-homogeneous area.

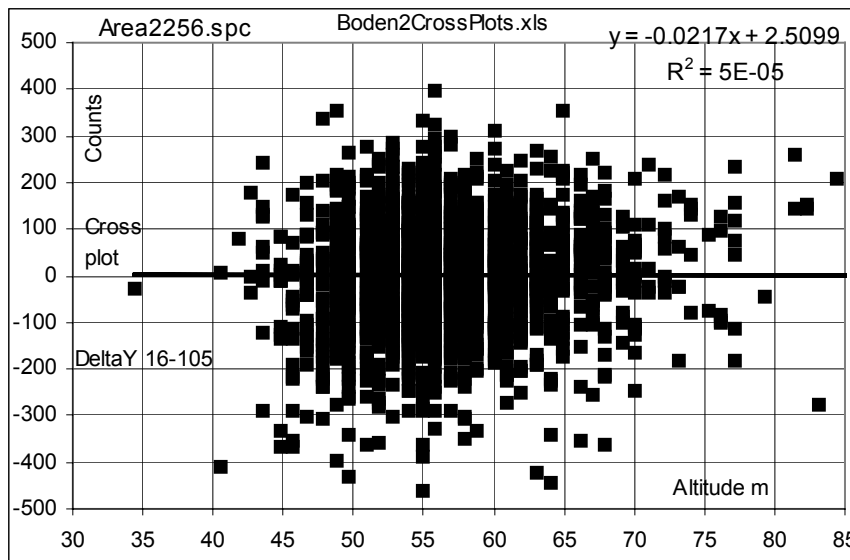


Figure G.4. Stripping of a very wide window vs. altitude. Area 2. SGU data. Average window counts: 1158

## Appendix H. The influence of neglecting background radiation

It has been observed that sometimes oddly looking stripping factors have been calculated when background corrected AGS spectra were used for input. Therefore it was decided to carry out the calculations without subtracting the background spectra first. Basically this is not correct; but the obtained results - the stripped window count rates - seemingly are close to being correct. The primary cause is assumed to be the similarity between the shape of background spectrum and the spectra due to natural radioactivity in and on the ground (see Appendix F.) This question is further examined in some detail below.

Consider a fictive background spectrum with counts only below the K-window. The ASS calculations then generate stripping factors  $\delta'$ ,  $\epsilon'$ , and  $\zeta'$  that fit best for the whole set of spectra, each of which includes this odd background signal. Now assume that the calculated stripping parameters fit very well for some "average spectra" i.e. that after stripping the window counts have an average of zero.

Then consider a low intensity spectrum with very few counts in the Th-, U-, and K-window (for example recorded while flying above water or above a ground with chalk, clean sand or a very thick layer of organic debris). This means that there is only a little stripping - or no stripping at all - of the low energy windows, because there are no - or only few - counts in the Th-, U-, and K-window. But the background signal still is there and causes counts in the low energy windows. This means that after stripping there is still (almost) the full background signal in the low energy windows.

Next consider the opposite situation. A number of spectra - among the whole set of recorded spectra - are recorded when flying above a ground with a higher content of natural radioactivity e.g. a ground with clay or some igneous rocks. Due to the high number of counts in the Th-, U-, and K-window there is a strong stripping of the low energy windows; and there are stripped more counts than actually are recorded in the windows. The stripping factors are fitted for an "average" spectrum. The result is that when flying above a "high intensity" ground, the area specific stripping will generate negative counts in the low energy windows.

One may also consider a fictive background spectrum with a relative large fraction of its counts at energies above the lower limit of the potassium window. Now the opposite tendencies would be observed; i.e. at "low counts spectra" the stripping of the low energy windows would be too strong - and for "high counts spectra" the stripping would be too weak.

The balance occurs when the background spectrum has almost the same shape as a typical/average (net) spectrum for natural radioactivity in the ground. Then the background spectrum in average just strips away its own counts in the low energy windows. Therefore, in order to see if the background signal may introduce problems one just checks whether the calculated stripping parameters  $\delta'$ ,  $\epsilon'$ , and  $\zeta'$  are able to perform a correct stripping of the sole background spectrum (if known).

This is done for the stripping factors listed in Table 5.3.1 (Area 1 and Area 2 stripping factors). They are used with the background window count rates of Table 5.0.1. As an example one may for the background spectrum perform a stripping of window 4 with the stripping factors  $\delta'$ ,  $\epsilon'$ , and  $\zeta'$  calculated for Area 2. The measured window count rate is  $r_{Win4} = 31.91$  cps.

The stripping is:

$$3.05421 \cdot 2.27 + 3.54172 \cdot 4.09 + 1.59726 \cdot 7.44 = 6.933 + 14.379 + 11.883 = 33.196.$$

Therefore a negative result of -1.286 cps is obtained. Due to statistical uncertainties the negative result may be a chance. However, for most other low energy windows negative results in the order of 1-2 counts are also obtained. This indicates that the SGU background spectrum has a relatively large fraction of the counts at energies above the lower limit of the K window. But the "stripping error" for background spectrum can in general be neglected.

Typical environmental low energy window count rates are two orders of magnitude higher than the "errors" of the stripped background rates mentioned here (1-2 counts) and one order of magnitude higher than the background window count rates. Therefore in general most of the stripping is directed towards the elimination of the environmental Th-, U-, and K-signal in the low energy windows. Only for spectra almost being background spectra a zero shift may be detectable.

Therefore it can be concluded that for the SGU AGS system and similar systems one may use the ASS technique without paying attention to the background spectrum. It just is included in the calculations; both when the ASS parameters are calculated and when they are used.

### **Comparisons with cross plots**

The figures H.1 to H.3 show cross plots for stripped window count rates vs. measured count rates calculated for wide (16-105) windows. For all figures one observes a "too strong" stripping at high window counts and a "too low" stripping at low window counts. Could having an imperfect stripping of the background part of the spectra cause this?

The results of stripping the background spectrum using the calculated stripping factors for Area 1 and Area 2 is almost correct; a slightly too strong stripping occurs when all windows are added together. This means that the (environmental) Th + U + K part of the spectra then in "average" has a (slightly) too low stripping i.e. a positive stripped window count (rate).

The result therefore should be that for high intensity environmental spectra a larger (positive) window count surplus should be observed than for low counts environmental spectra (almost equivalent to the background spectrum). The experiences, however, tell that the opposite is the case.

This is for example seen in the figures H.1 to H.3. When the total count rate goes up the stripped count rate goes down - as indicated by the linear regression trend lines. The correlation coefficient is, however, quite low indicating that there is only a very weak connection between the count rate level and the stripped count rate. Other factors that influence result therefore are dominating.

High count rates may be observed especially at locations where the density of vegetation is low - or where igneous rocks are uncovered (protrude the surface). Here one will record a higher fraction of the detections at the higher energies (due to less scattering material between source and detector). Therefore one here gets a too strong stripping - when using stripping factors calculated for the whole set of spectra. This is in agreement with the observed tendency. However, again it should be stressed that the scatter of the results tells that other factors are more important.

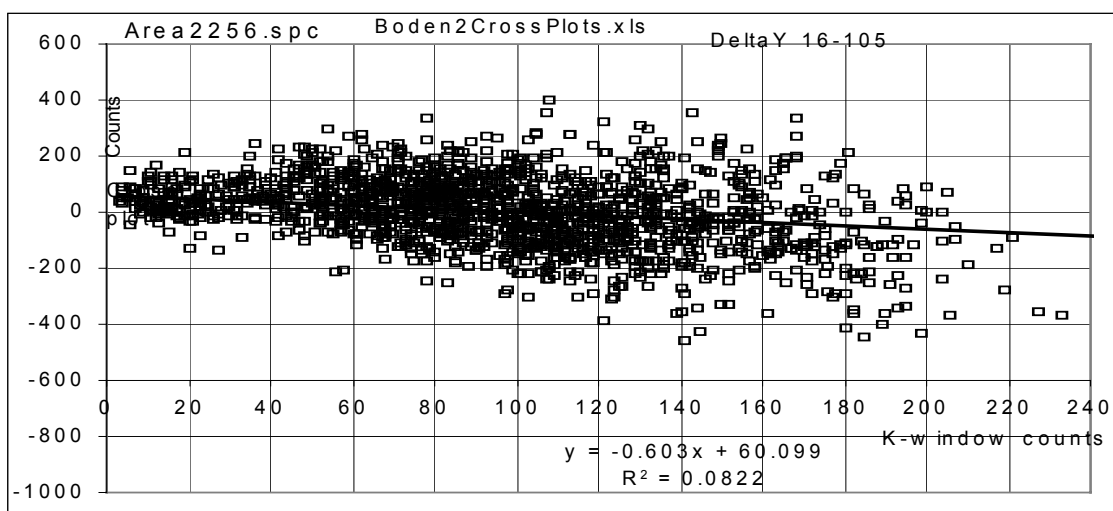


Figure H.1. Stripped counts of the very wide window (channel 16 to 105) versus the gross counts of the K-window.

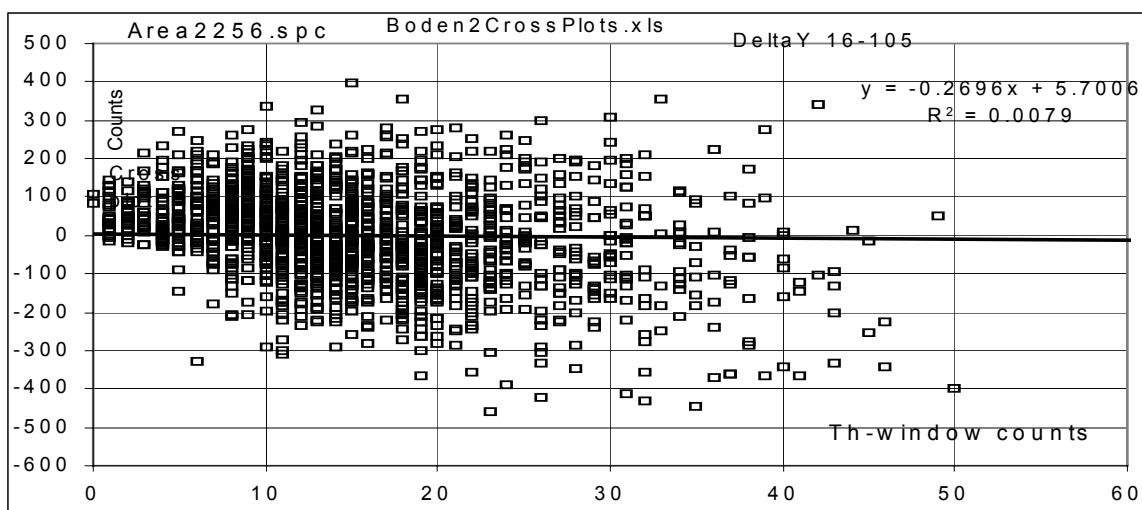


Figure H.2. Stripped counts for the very wide window (channel 16-105) versus Th counts.

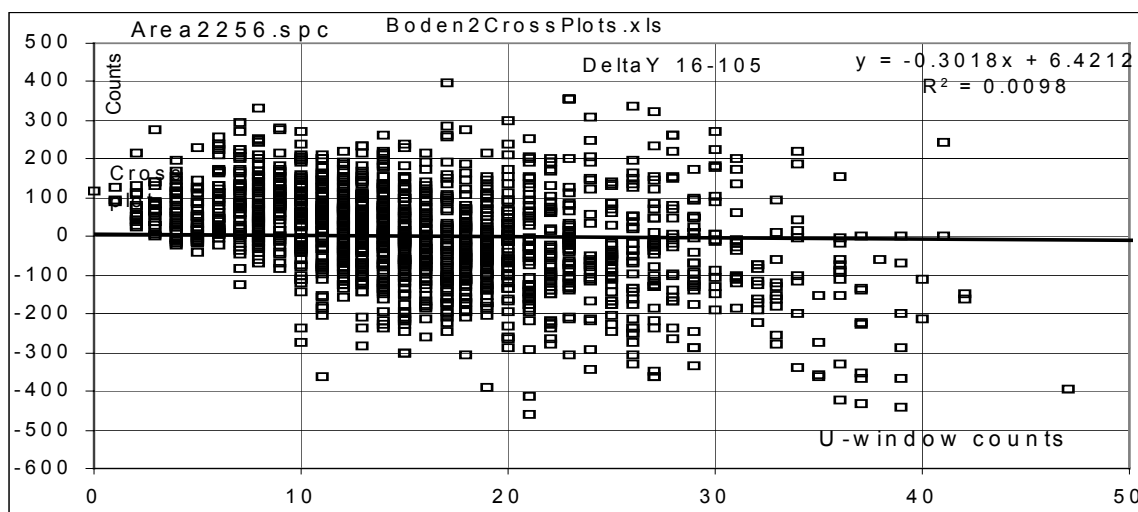


Figure H.3. Stripped counts for the very wide window (channels 16-105) versus U counts.

## Appendix I. Stripped window count rates and altitudes

The altitude of the detector is one of the factors that influence the spectrum shape. At a high altitude one will - if all other influencing parameters are constants - have a relatively higher number of low energy photons than when flying at a lower altitude. Therefore it may be of interest to check whether there is a relation between the (surplus) stripped count rates for some low energy window and the altitude.

Figure I.1 shows the altitude for Area2 when measured with the SGU AGS equipment. The altitude varies from 36 m (blue) to 85 m (violet). The altitude variations along a (south-north) flight line probably are related to the topology of the area (Figure I.3) whereas the east-west variations may have (an) other reason(s).

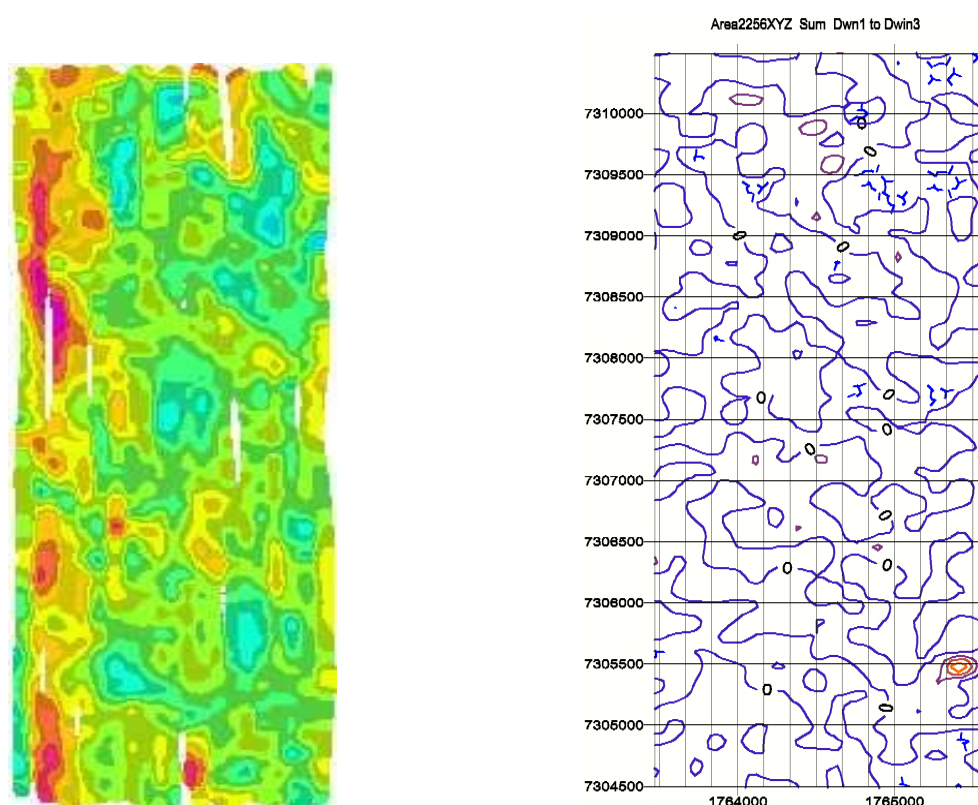


Figure I.1 and I.2. Altitude of SGU AGS equipment during Area 2 measurements (left) and stripped count rate for window 1 to 3 summed (right). The altitude scale is from light blue (below 40 m) to red-violet (above 80 m). The stripped count rate scale goes from -100 to +300 with most curves representing 0 (surplus) counts.

In the western part of the area the altitudes typically are higher than at the other parts of the area. So the question is: Are there some characteristics for the spectra measured in the western part that (in average) deviates from those of the remaining area? Or have other factors a dominating influence that renders the altitude influence negligible?

Near the upper right corner of Figure I.2 there is a significant amount of count rates below -100 cps - i.e. a too strong stripping here. This fits with the relatively low altitudes here - and the topology map shows a hill here. For the remaining part of the area there is no obvious relation between the altitude and (surplus) stripped count rate. Especially there cannot be seen a relation between the high altitudes and count rates in the western part of the area. This is in agreement with Appendix G

(cross plots) where only a weak positive correlation was found between the altitude and the stripped low energy window count rate.

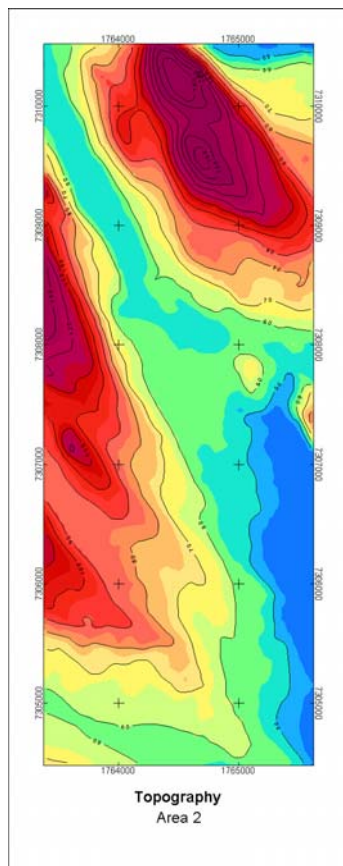


Figure I.3. Topography map for Area 2. Exercise LIVEX at Boden.  
Blue 50 m and violet (max.) 160 m  
Courtesy: SGU and The Swedish Landsurvey.

## Appendix J. Understanding the Area Specific Stripping factors

The Area Specific Stripping factors for a set of AGS or CGS data are determined in a way that ensures the "best" elimination (stripping) of the contribution from natural radioactivity to the count rates of low energy windows. In an area with a dense vegetation the stripping has to ensure stripping of the relatively higher fraction of photons detected in the low energy windows i.e. the stripping factors as a whole will have to increase (a little) when compared to an area with the same type of topology and geology but without a dense vegetation. Therefore the stripping factors are adjusted to fit to the actual situation. The same effect is seen for AGS measurements with different altitudes.

The rocks and sediments of Scandinavia usually contain uranium and thorium in relative amounts corresponding to 0.24-0.28 ppm U per ppm Th. If the ratio is a constant everywhere - for example 0.25 ppm U per ppm Th - the stripping could be done with the Th window alone - or the U window alone. If the ratio is not quite a constant, the stripping is "shared" between the Th window and the U window. The actual stripping factors of course depend on the selected window limits - both for Th, U and K, and for the low energy window in question. However, typical values could be  $\delta' = 3$ ,  $\epsilon' = 3$ , and  $\zeta' = 2$ .

Now assume that an area has been surveyed and the stripping factors actually have been calculated to 3, 3 and 2 respectively. Next assume that the very same area has been surveyed again on a day when the air for a part of the area has included a significant amount of radon. This means that the "uranium signal" has got a variation independently of the Th signal.

By having a stripping from the uranium window already - for example with the stripping factor 3 mentioned above - additional stripping will occur (from the U window) when radon is present in the air. The gamma spectrum due to radon (daughters) in the air, however, differs a little from that caused by uranium (radon daughters) in the ground. (The "radon in air radiation" may include some primary low energy photons that are attenuated significantly in the ground.) Therefore the stripping factors 3, 3, and 2 may not be the very best.

When performing a calculation of the area specific stripping factors for the new data set with a varying radon concentration in the air one may get stripping factors that deviate from 3, 3, and 2. This question has been examined only to a limited extent, but an example tells that the thorium window stripping ( $\delta = 3$  above) may be reduced more than a factor two whereas the stripping from the uranium window goes somewhat up; and the potassium stripping factor only changes a little.

[One should remember that thorium radiation also contributes to the count rates of the uranium window. Therefore some "thorium stripping" occurs through the uranium window.]

However, the (limited) stripping experience with the new stripping factors tells that the stripping only is a little better than the old ones (i.e. 3, 3 and 2). Therefore, the experiences indicate that measurements with a varying radon content in the air could be stripped in an acceptable way with stripping factors that are calculated from data without a varying radon concentration. (Data for extreme "radon episodes" have, however, not been available for investigations.)

This is the same conclusion as that obtained when the same stripping factors are applied for areas with a somewhat different topology, vegetation etc. - and for AGS with some (minor) altitude variations.

## Appendix K. Area Specific Stripping Factors

### SSI

Nine sets of area specific stripping factors were calculated for each of the three Barents Rescue files from SSI. Strong source signals were removed from the data set before the calculation of the stripping factors.

The energy ranges for the low-energy windows correspond to those for SGU. IAEA standard windows were used for the natural radionuclides. (K 1370 keV to 1470 keV, U 1660 keV to 1860 keV, and Th 2410 keV to 2810 keV.)

Plots of stripped counts are shown in Appendix M together with plots of the gross counts in the natural radionuclide windows.

Table K.1. SSI Barents Rescue, C3\_1. IAEA standard windows.

Window	LL (chn.)	UL (chn.)	LL (keV)	UL (keV)
K	116	133	<b>1367.3</b>	<b>1576.4</b>
U	140	156	<b>1663.2</b>	<b>1862.8</b>
Th	199	230	<b>2408.6</b>	<b>2810.6</b>

Table K.2. SSI Barents Rescue, C3\_1. ASS windows.

Window	LL (chn.)	UL (chn.)	LL (keV)	UL (keV)
1	17	21	192.0	238.1
2	22	29	249.6	330.6
3	30	34	342.2	388.6
4	35	44	400.3	505.3
5	53	63	611.0	729.1
6	64	94	740.9	1099.9
7	95	117	1111.9	1379.6
8	35	42	400.3	481.9
9	43	52	493.6	599.2

Table K.3. SSI Barents Rescue, C3\_1. ASS factors.

Window	$\delta'$	$\varepsilon'$	$\zeta'$
1	4.21014	4.10099	3.60304
2	3.44990	4.03128	3.18508
3	1.29028	1.34441	1.21028
4	1.84267	1.77198	1.70392
5	1.01406	1.12703	0.89436
6	1.89339	1.95141	1.66719
7	0.70459	0.51209	0.67653
8	1.49132	1.43938	1.39296
9	1.38857	1.66450	1.31029



Table K.4. SSI Barents Rescue, C4\_1. IAEA standard windows.

Window	LL (chn.)	UL (chn.)	LL (keV)	UL (keV)
K	119	136	<b>1372.1</b>	<b>1575.7</b>
U	143	160	<b>1660.1</b>	<b>1866.6</b>
Th	204	236	<b>2409.9</b>	<b>2813.4</b>

Table K.5. SSI Barents Rescue, Area C4\_1. ASS windows.

Window	LL (chn.)	UL (chn.)	LL (keV)	UL (keV)
1	17	21	191.5	236.4
2	23	29	259.0	326.7
3	30	35	338.0	394.7
4	36	45	406.0	508.5
5	54	64	611.6	726.7
6	65	96	738.2	1099.7
7	97	120	1111.4	1384.0
8	36	42	406.0	474.3
9	43	53	485.7	600.1

Table K.6. SSI Barents Rescue, C4\_1. ASS factors.

Window	$\delta'$	$\varepsilon'$	$\zeta'$
1	4.57778	3.19525	3.71330
2	3.37372	2.50633	2.85551
3	1.81626	1.25900	1.50467
4	2.20108	1.35448	1.64051
5	1.01337	0.75712	0.96437
6	1.88686	1.36008	1.80091
7	0.52523	0.52358	0.72522
8	1.53814	0.97300	1.18620
9	1.82713	1.28190	1.52803

Table K.7. SSI Barents Rescue, C4\_2. IAEA standard windows.

Window	LL (chn.)	UL (chn.)	LL (keV)	UL (keV)
K	117	133	<b>1374.2</b>	<b>1570.1</b>
U	140	156	<b>1656.5</b>	<b>1855.6</b>
Th	200	230	<b>2414.3</b>	<b>2804.8</b>

Table K.8. SSI Barents Rescue, C4\_2. ASS windows.

Window	LL (chn.)	UL (chn.)	LL (keV)	UL (keV)
1	16	21	188.5	245.2
2	22	28	256.5	324.8
3	29	34	336.2	393.4
4	35	44	404.9	508.4
5	53	63	612.7	729.4
6	64	95	741.1	1108.5
7	96	117	1120.5	1374.2
8	35	41	404.9	473.8
9	43	52	496.9	601.1

Table K.9. SSI Barents Rescue, C4\_2. ASS factors.

Window	$\delta'$	$\varepsilon'$	$\zeta'$
1	4.92555	5.30949	4.35757
2	3.37840	3.58213	2.85712
3	1.95664	1.85934	1.50318
4	1.68750	2.10695	1.66868
5	1.15950	0.92255	0.98238
6	1.93950	2.07956	1.71556
7	0.82617	0.67441	0.57073
8	1.28391	1.48563	1.20025
9	1.76269	1.93131	1.24652

## NRPA/NGU

In order to perform the calculations it has been necessary to split the files into shorter files, see Table K10, and to remove from the files strong source signals, Table K11.

For each file, nine sets of stripping factors were calculated according to the windows in Table K12. The calculations were performed using the energy calibration suggested by NRPA/NGU (Appendix B).

Table K.10. NRPA/NGU file information.

Original file	New file	Information		
		Spc. Nos.	Area	ASS Table
170901.dat	170901A.spc	0-8000	"C1,C2,C3"	K13
	170901B.spc	8000-14000	C7	K14
	170901C.spc	14001-25000	C7	K15
	170901D.spc	25001-32251	C7	K16
180901.dat	180901A.spc	0-8000	C3	K17
	180901B.spc	8001-16400	C3	K18
	180901C.spc	16401-28721	C4	K19

Table K.11. NRPA/NGU measurements excluded from ASS calculations.

Original file	New file	Original data file spectrum numbers not included
170901.dat	170901A.spc	None
	170901B.spc	None
	170901C.spc	14446-14959, 23281-24259
	170901D.spc	26157-26826, 27451-27501, 28426-29056, 29551-29601
180901.dat	180901A.spc	1950-2000, 2050-3100, 3450-3900
	180901B.spc	None
	180901C.spc	16982-17560, 17852-17900, 19402-20150, 25722-27150

Table K.12. Energy calibration for NRPA/NGU, Barents Rescue.

Window	LL (chn.)	UL (chn.)	LL (keV)	UL (keV)
1	14	18	189.9	238.4
2	19	25	250.5	323.3
3	26	31	335.5	396.4
4	32	40	408.6	506.5
5	49	58	617.0	728.1
6	59	88	740.5	1101.9
7	89	110	1114.5	1379.6
8	32	38	408.6	482.0
9	39	48	494.2	604.7
<b>K</b>	<b>109</b>	<b>125</b>	<b>1370</b>	<b>1570</b>
<b>U</b>	<b>132</b>	<b>148</b>	<b>1660</b>	<b>1860</b>
<b>Th</b>	<b>189</b>	<b>220</b>	<b>2410</b>	<b>2810</b>

Table K.13. NRPA/NGU Barents Rescue, 170901A. ASS factors.

Window	$\delta'$	$\varepsilon'$	$\zeta'$
1	4.65637	3.81138	1.97537
2	3.75232	3.27126	1.80198
3	1.55503	1.36437	0.75541
4	1.67240	1.49151	0.87128
5	0.93587	0.95274	0.60968
6	1.63387	1.53415	1.08069
7	0.54779	0.56483	0.51761
8	1.36129	1.20625	0.70042
9	1.37096	1.28131	0.77609

Table K.14. NRPA/NGU Barents Rescue, 170901B. ASS factors.

Window	$\delta'$	$\varepsilon'$	$\zeta'$
1	3.00999	3.59605	2.19822
2	2.57801	3.35157	1.92417
3	1.43639	1.91249	0.97549
4	1.16654	1.42750	0.93901
5	0.71624	1.05686	0.63674
6	1.28131	1.55995	1.10714
7	0.48382	0.70146	0.50658
8	0.93954	1.15328	0.75819
9	1.00923	1.26321	0.81223

Table K.15. NRPA/NGU Barents Rescue, 170901C. ASS factors.

Window	$\delta'$	$\varepsilon'$	$\zeta'$
1	3.39008	3.78354	2.10333
2	3.01478	3.33355	1.83368
3	1.55433	1.67605	0.94890
4	1.38779	1.51077	0.88628
5	0.77206	0.91225	0.62777
6	1.55399	1.56568	1.05093
7	0.51918	0.59205	0.49810
8	1.12517	1.20767	0.71542
9	1.18504	1.31807	0.76679

Table K.16. NRPA/NGU Barents Rescue, 170901D. ASS factors.

Window	$\delta'$	$\varepsilon'$	$\zeta'$
1	3.73475	4.74149	1.91612
2	3.72960	4.22682	1.64459
3	2.01274	2.42320	0.81395
4	1.75307	2.18807	0.77078
5	1.11847	1.32346	0.54006
6	1.94917	2.08125	0.95495
7	0.52033	0.80993	0.47673
8	1.41324	1.76932	0.62158
9	1.59603	1.91415	0.65554

Table K.17. NRPA/NGU Barents Rescue, 180901A. ASS factors.

Window	$\delta'$	$\varepsilon'$	$\zeta'$
1	4.22102	3.81506	2.47027
2	3.89206	3.45531	2.05087
3	1.925049	1.90396	1.05039
4	1.67170	1.55987	0.96091
5	0.93721	1.02489	0.67131
6	1.79736	1.72974	1.06510
7	0.49550	0.63655	0.52718
8	1.34706	1.24473	0.77951
9	1.48169	1.42798	0.80847

Table K.18. NRPA/NGU Barents Rescue, 180901B. ASS factors.

Window	$\delta'$	$\varepsilon'$	$\zeta'$
1	4.03972	3.81927	2.41936
2	3.79621	3.79776	1.96110
3	1.70824	1.65606	0.77824
4	1.74113	1.70337	0.91771
5	1.25002	1.23179	0.58653
6	1.89686	1.86737	1.03729
7	0.57407	0.66632	0.51298
8	1.42629	1.34447	0.74378
9	1.54519	1.58896	0.76694

Table K.19. NRPA/NGU Barents Rescue, 180901C. ASS factors.

Window	$\delta'$	$\varepsilon'$	$\zeta'$
1	4.93052	4.54070	1.85827
2	4.63409	4.51850	1.56670
3	2.02835	1.96666	0.63384
4	1.98713	1.93367	0.78666
5	1.42205	1.49211	0.50252
6	2.07253	2.12384	0.95241
7	0.60461	0.63182	0.49617
8	1.62339	1.56831	0.63163
9	1.79634	1.72830	0.66850

## Appendix L. Single channel stripping factors for CGS

- a" ASS factor for Th-window (factor per channel)  
 b" ASS factor for U-window (factor per channel)  
 c" ASS factor for K-window (factor per channel)

The stripping factors are plotted as a function on the center channel in the channel interval for which they were calculated. (Energy calibration, see Appendix B.)

NRPA (NGU) single channel stripping factors for file 170901.

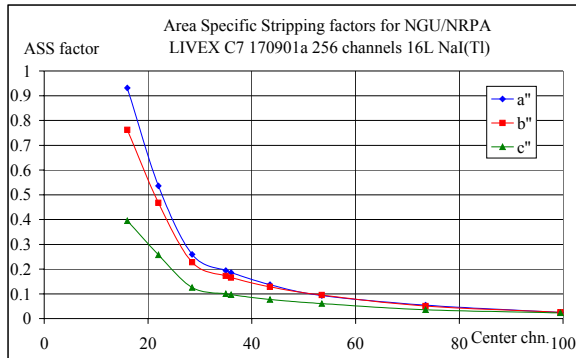


Figure L.1.  
170901 Nos. 0-8000: a", b", and c".

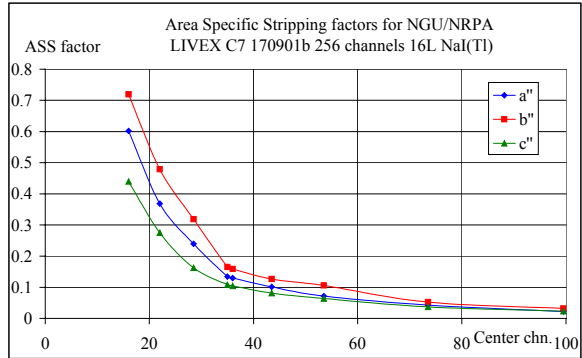


Figure L.2.  
170901 Nos. 8001-14000: a", b", and c".

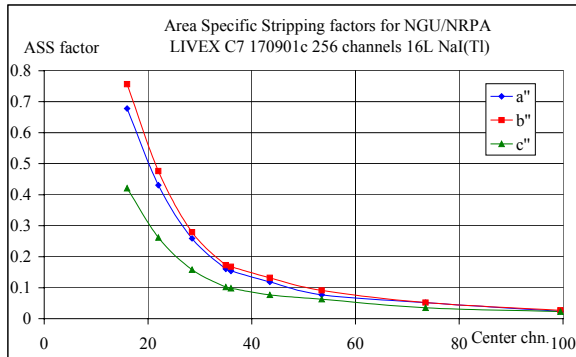


Figure L.3.  
170901 Nos. 14001-25000: a", b", and c".

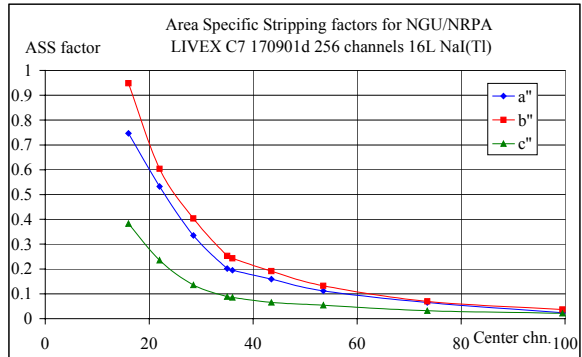


Figure L.4.  
170901 Nos. 25001-32251: a", b", and c".

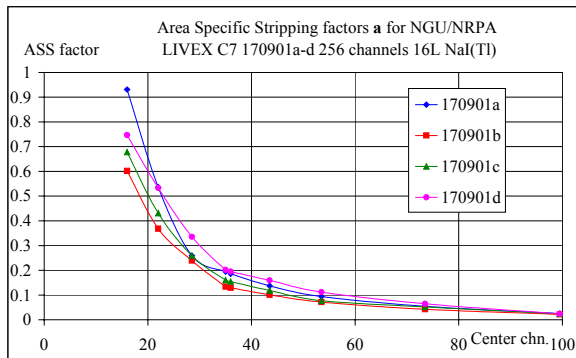


Figure L.5.  
170901 Nos. 0-32251: a".

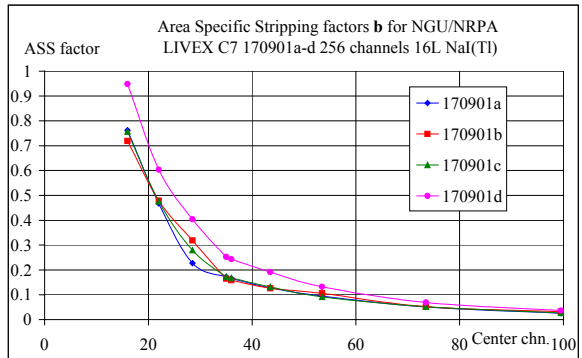


Figure L.6.  
170901 Nos. 0-32251: b".

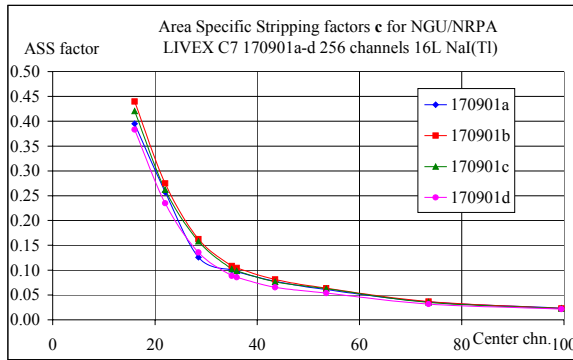


Figure L.7.  
170901 Nos. 0-32251: c".

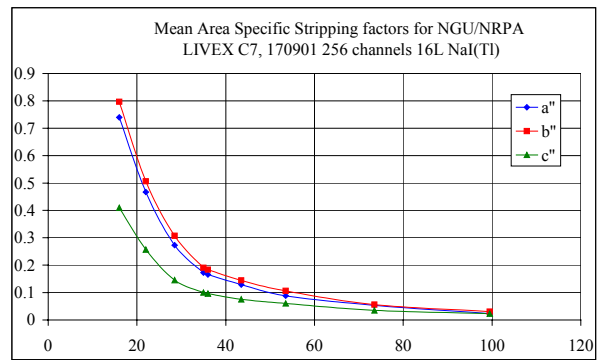


Figure L.8.  
170901: Mean values of a'', b'', and c''.

## NRPA (NGU) single channel stripping factors for file 180901.

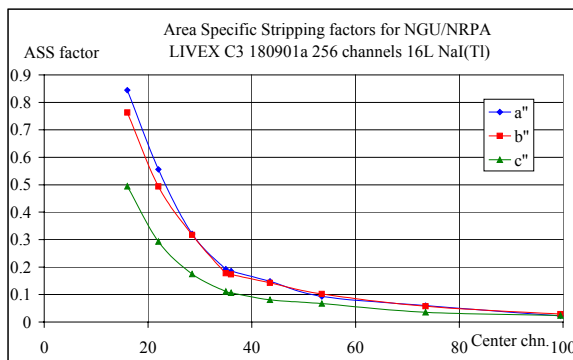


Figure L.9.  
180901 Nos. 0-8000: a'', b'', and c''.

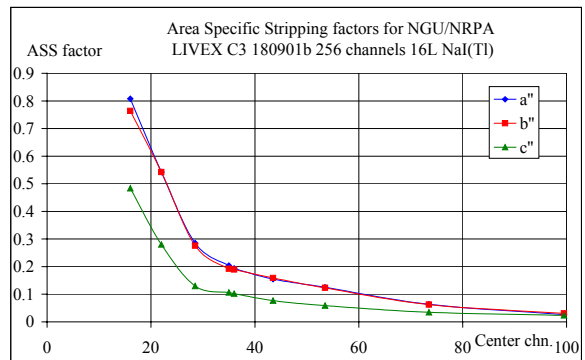


Figure L.10.  
180901 Nos. 8001-16400: a'', b'', and c''.

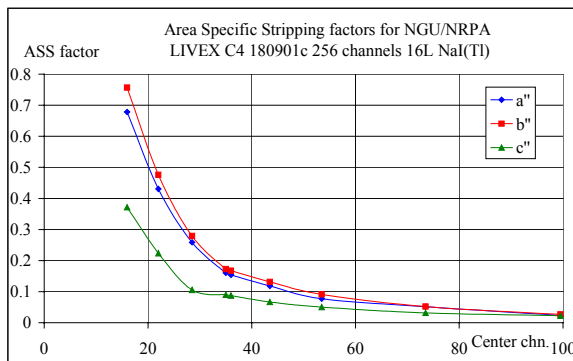


Figure L.11.  
180901 Nos. 16401-28721: a'', b'', and c''.

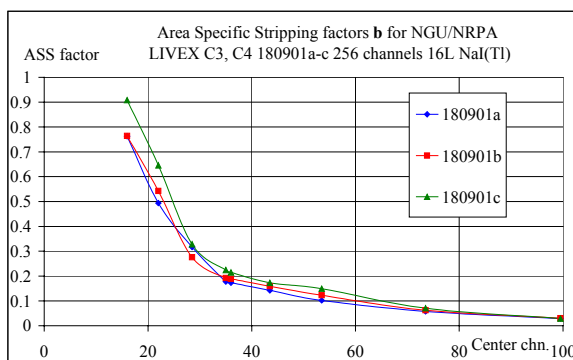


Figure L.12.  
180901 Nos. 0-28721: a''.

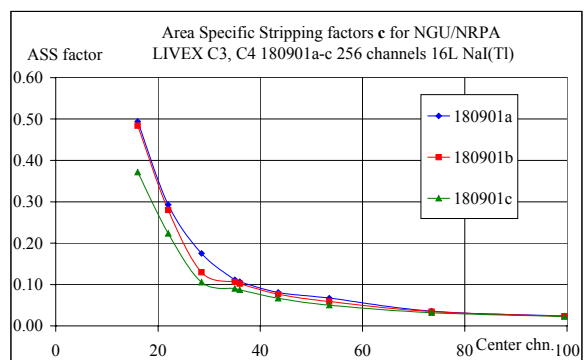


Figure L.13.  
180901 Nos. 0-28721: b''.

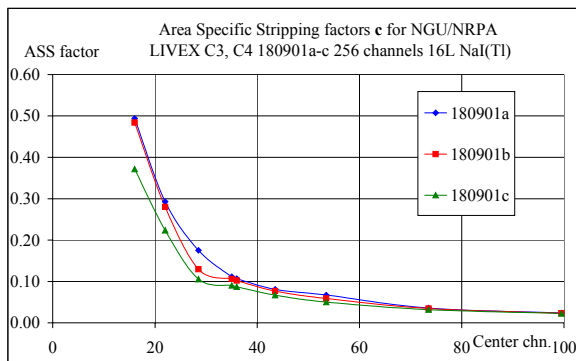


Figure L.14.  
180901 Nos. 0-28721:  $c''$ .

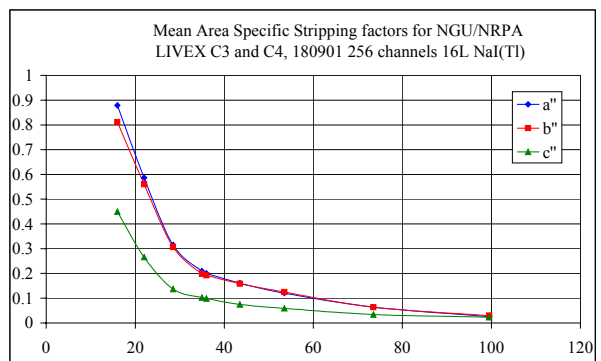


Figure L.15.  
180901: Mean values of  $a''$ ,  $b''$ , and  $c''$ .

Combined mean stripping factors for Norwegian measurements.

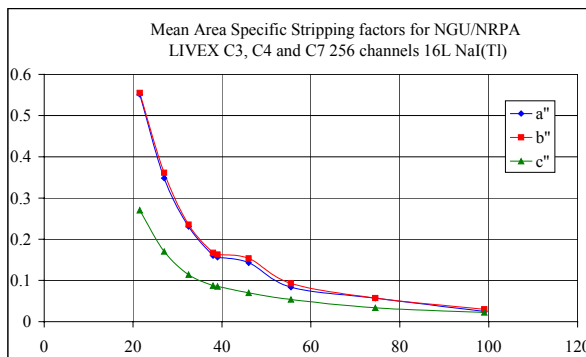


Figure L.16.  
Mean values, DTU energy information.

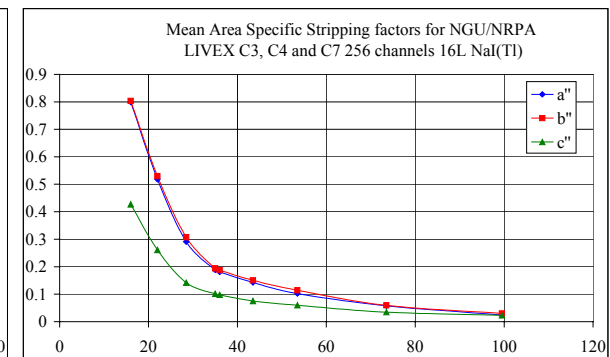


Figure L.17.  
Mean values, NGU energy calibration.

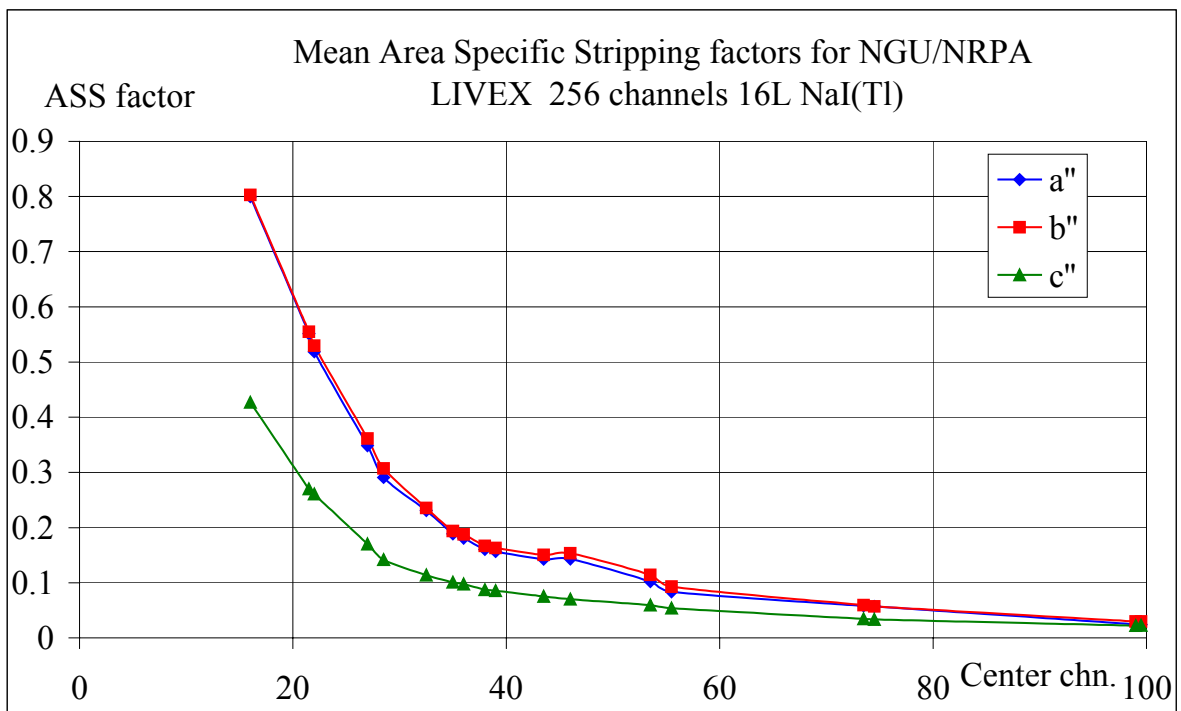


Figure L.18. Common mean values.



Table L.1. Ass factors per window.

Common mean values for Norwegian CGS measurements.

LL (keV)	UL (keV)	LL (chn.)	UL (chn.)	a	b	c
189.9	238.4	14	18	3.99749	4.01536	2.13442
194.5	235.3	20	23	2.20583	2.21960	1.08068
250.5	323.3	19	25	3.62815	3.70782	1.82615
248.9	330.4	24	30	2.43916	2.52914	1.19138
335.5	396.4	26	31	1.74573	1.84325	0.85089
343.9	384.6	31	34	0.92348	0.94190	0.45603
408.6	482	32	38	1.31943	1.35629	0.70722
408.6	506.5	32	40	1.62568	1.68782	0.87609
398.1	479.2	35	41	1.12210	1.16738	0.61031
398.1	506.1	35	43	1.40782	1.46649	0.76836
494.2	604.7	39	48	1.42635	1.50314	0.75065
492.7	600.4	42	50	1.28595	1.38153	0.63060
617	728.1	49	58	1.02170	1.14201	0.59637
613.8	734.5	51	60	0.83534	0.92761	0.53869
740.5	1101.9	59	88	1.74073	1.78028	1.03550
747.9	1107	61	88	1.59596	1.60176	0.93962
1120.3	1383.4	89	109	0.51956	0.62664	0.47295
1114.5	1379.6	89	110	0.53504	0.65756	0.50505

Table L.2. ASS factors per channel.

Common mean values for Norwegian CGS measurements.

LL (keV)	UL (keV)	LL (chn.)	UL (chn.)	a''	b''	c''
189.9	238.4	14	18	0.79950	0.80307	0.42688
194.5	235.3	20	23	0.55146	0.55490	0.27017
250.5	323.3	19	25	0.51831	0.52969	0.26088
248.9	330.4	24	30	0.34845	0.36131	0.17020
335.5	396.4	26	31	0.29096	0.30721	0.14181
343.9	384.6	31	34	0.23087	0.23547	0.11401
408.6	482	32	38	0.18849	0.19376	0.10103
408.6	506.5	32	40	0.18063	0.18754	0.09734
398.1	479.2	35	41	0.16030	0.16677	0.08719
398.1	506.1	35	43	0.15642	0.16294	0.08537
494.2	604.7	39	48	0.14264	0.15031	0.07507
492.7	600.4	42	50	0.14288	0.153503	0.07007
617	728.1	49	58	0.10217	0.114201	0.05964
613.8	734.5	51	60	0.08353	0.09276	0.05387
740.5	1101.9	59	88	0.05802	0.05934	0.03452
747.9	1107	61	88	0.05700	0.05721	0.03356
1120.3	1383.4	89	109	0.02474	0.02984	0.02252
1114.5	1379.6	89	110	0.02432	0.02989	0.02296

## SSI single "channel" stripping factors for Barents Rescue: IAEA-windows

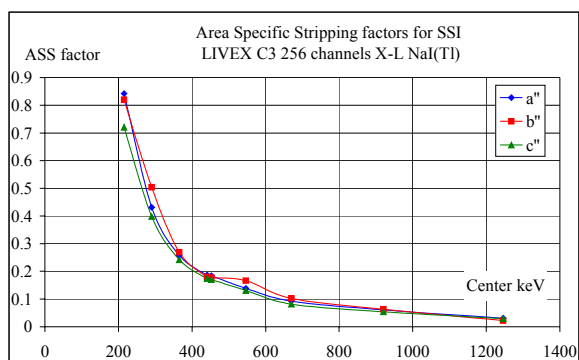


Figure L.19. C3\_1: a'', b'', and c''.

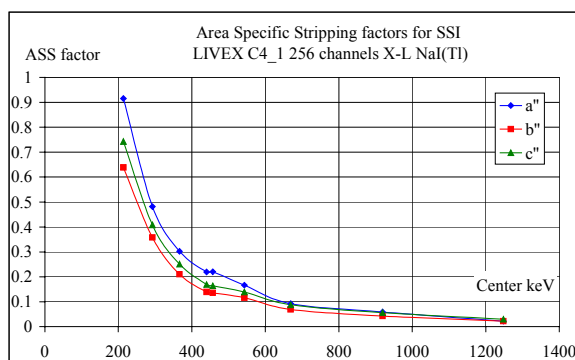


Figure L.20. C4\_1: a'', b'', and c''.

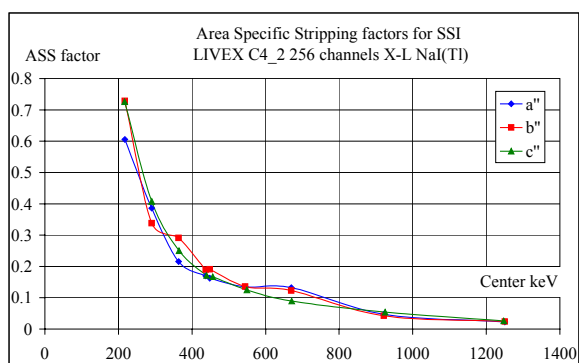


Figure L.21. C4\_2: a'', b'', and c''.

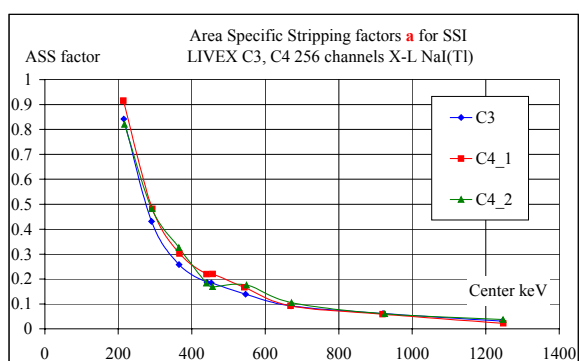


Figure L.22. C3 and C4: a''.

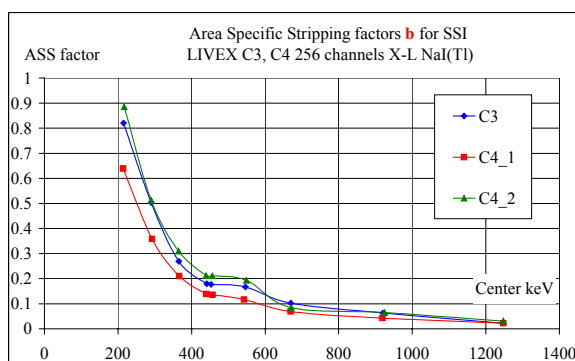


Figure L.23. C3 and C4: b''.

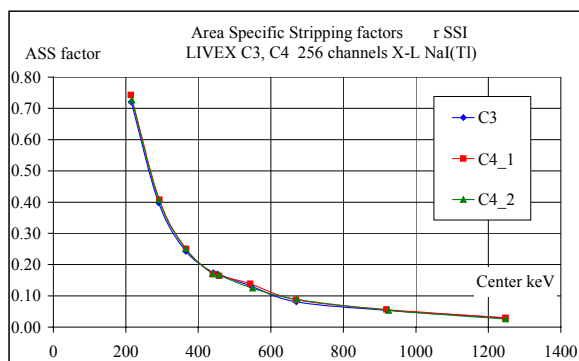


Figure L.24. C3 and C4: c''.

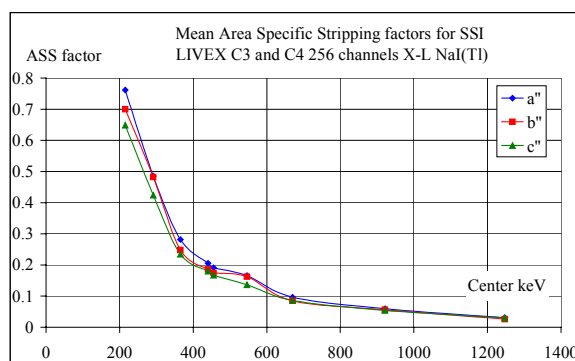


Figure L.25.  
C3 and C4: Mean values of a'', b'', and c''.

## Appendix M: Window count rates

Natural radionuclides: Barents Rescue SSI.

Table M1. Natural radionuclide windows.  
Area C3.

Window	LL (chn.)	UL (chn.)
K	116	133
U	140	156
Th	199	230

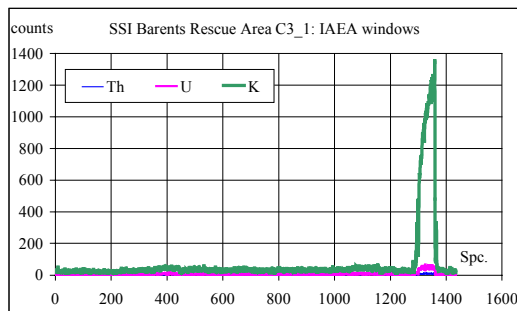


Figure M1. Gross natural counts, C3.

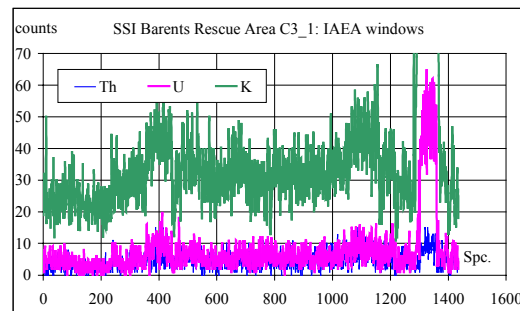


Figure M2. Gross natural counts, C3.

Table M2. Natural radionuclide windows.  
Area C4\_1.

Window	LL (chn.)	UL (chn.)
K	119	136
U	143	160
Th	204	236

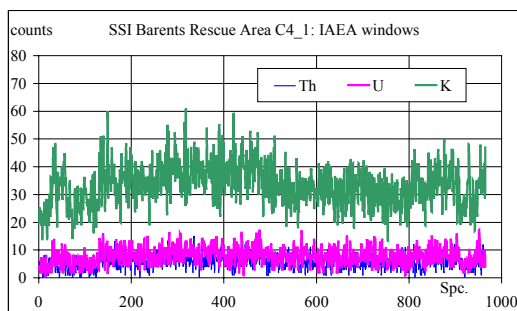


Figure M3. Gross natural counts, C4\_1.

Table M3. Natural radionuclide windows.  
Area C4\_2.

Window	LL (chn.)	UL (chn.)
K	117	133
U	140	156
Th	200	230

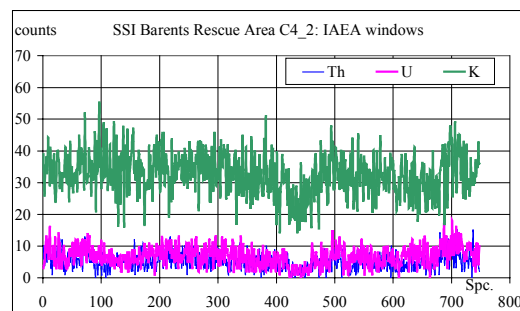


Figure M4. Gross natural counts, C4\_2.

## Barents Rescue C3\_1 SSI.

Table M4. ASS windows, Area C3.

Window	LL (chn.)	UL (chn.)	LL (keV)	UL (keV)
1	17	21	192.0	238.1
2	22	29	249.6	330.6
3	30	34	342.2	388.6
4	35	44	400.3	505.3
5	53	63	611.0	729.1
6	64	94	740.9	1099.9
7	95	117	1111.9	1379.6
8	35	42	400.3	481.9
9	43	52	493.6	599.2

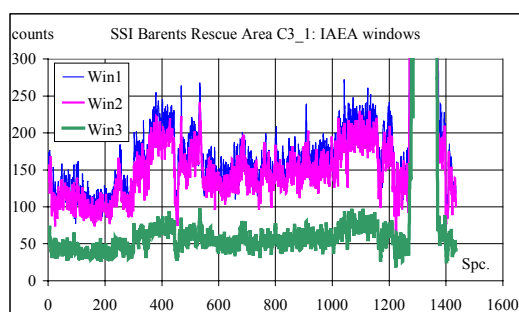


Figure M5. Gross counts Win1-3, C3.

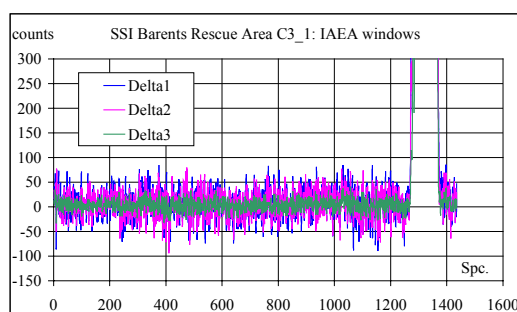


Figure M6. Stripped counts Win1-3, C3.

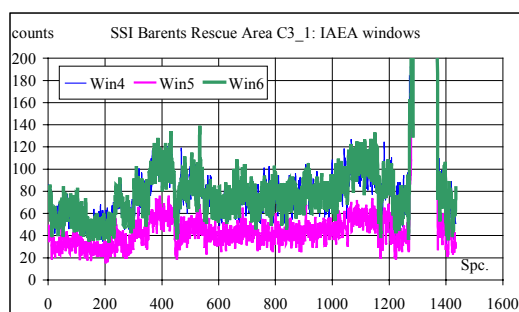


Figure M7. Gross counts Win4-6, C3.

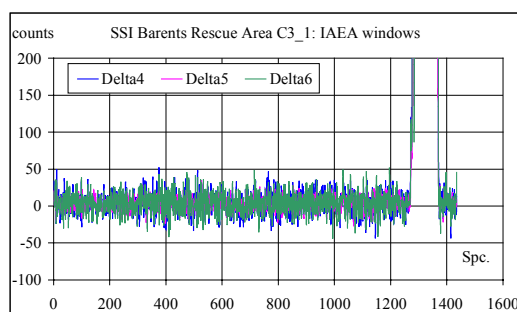


Figure M8. Stripped counts Win4-6, C3.

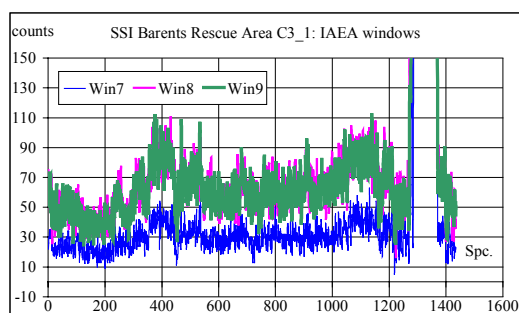


Figure M9. Gross counts Win7-9, C3.

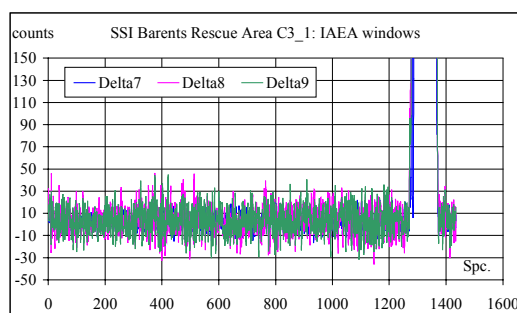


Figure M10. Stripped counts Win7-9, C3.

## Barents Rescue C4\_1 SSI.

Table M5. ASS windows, first half of Area C4.

Window	LL (chn.)	UL (chn.)	LL (keV)	UL (keV)
1	17	21	191.5	236.4
2	23	29	259.0	326.7
3	30	35	338.0	394.7
4	36	45	406.0	508.5
5	54	64	611.6	726.7
6	65	96	738.2	1099.7
7	97	120	1111.4	1384.0
8	36	42	406.0	474.3
9	43	53	485.7	600.1

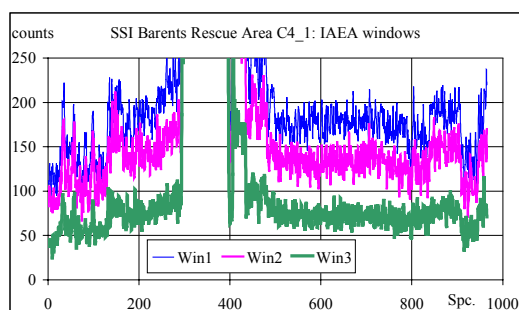


Figure M11. Gross counts Win1-3, C4\_1.

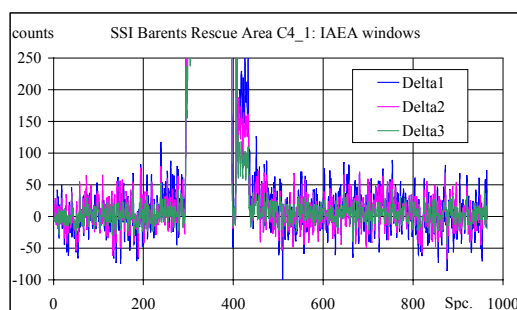


Figure M12. Stripped counts Win1-3, C4\_1.

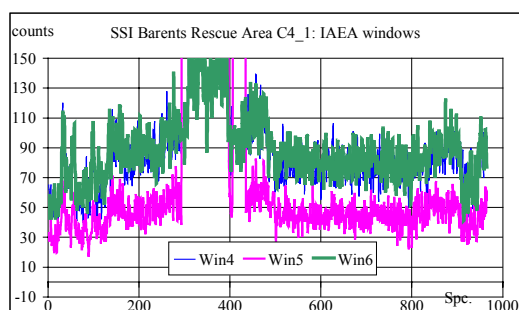


Figure M13. Gross counts Win4-6, C4\_1.

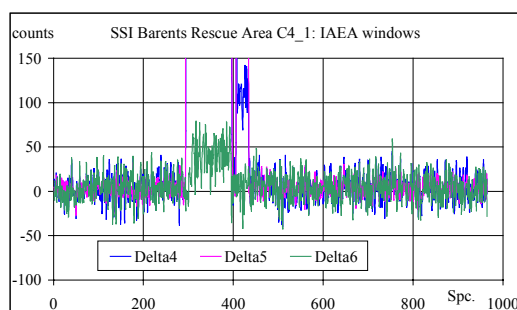


Figure M14. Stripped counts Win4-6, C4\_1.

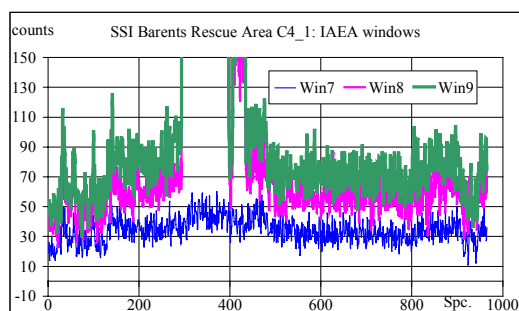


Figure M15. Gross counts Win7-9, C4\_1.

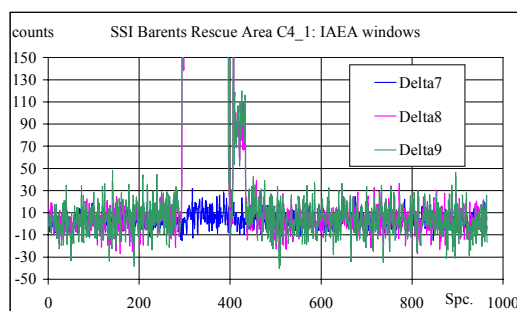


Figure M16. Stripped counts Win7-9, C4\_1.

## Barents Rescue C4\_2 SSI.

Table M6. ASS windows, second half of Area C4.

Window	LL (chn.)	UL (chn.)	LL (keV)	UL (keV)
1	16	21	188.5	245.2
2	22	28	256.5	324.8
3	29	34	336.2	393.4
4	35	44	404.9	508.4
5	53	63	612.7	729.4
6	64	95	741.1	1108.5
7	96	117	1120.5	1374.2
8	35	41	404.9	473.8
9	43	52	496.9	601.1

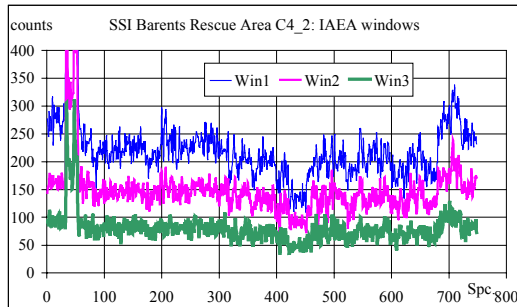


Figure M17. Gross counts Win1-3, C4\_2.

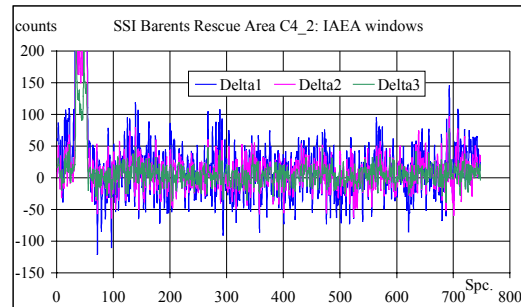


Figure M18. Stripped counts Win1-3, C4\_2.

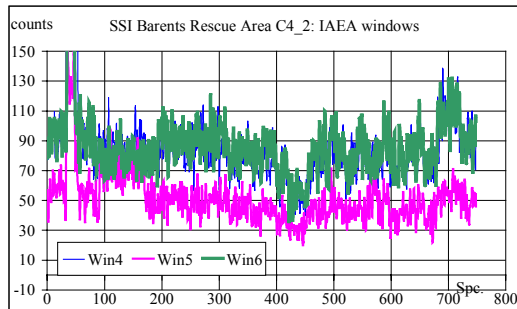


Figure M19. Gross counts Win4-6, C4\_2.

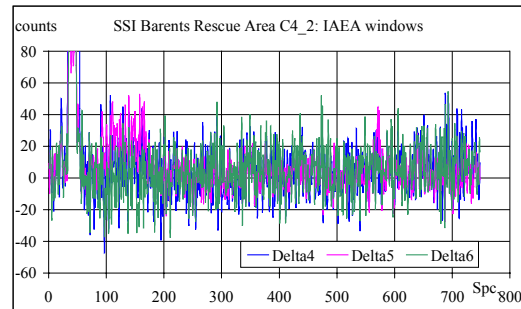


Figure M20. Stripped counts Win4-6, C4\_2.

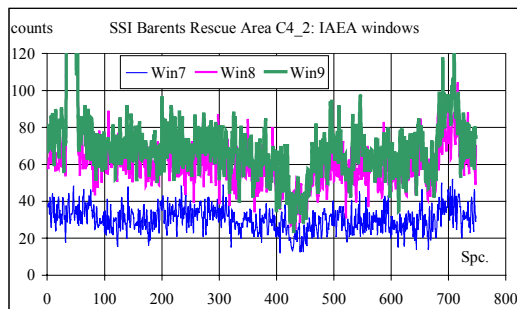


Figure M21. Gross counts Win7-9, C4\_2.

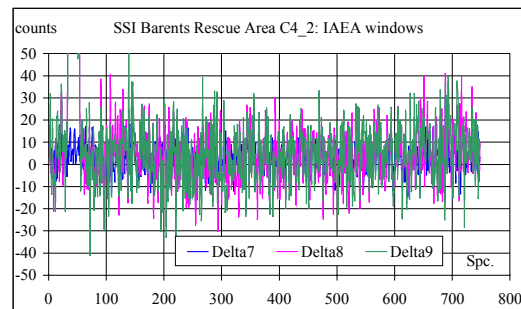


Figure M22. Stripped counts Win7-9, C4\_2.

## Natural radionuclides: Barents Rescue NRPA/NGU.

### File 170901.dat

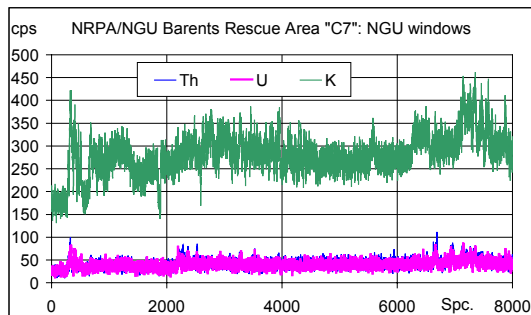


Figure M23. Gross natural cps, C7. 170901A (Nos. 0-8000).

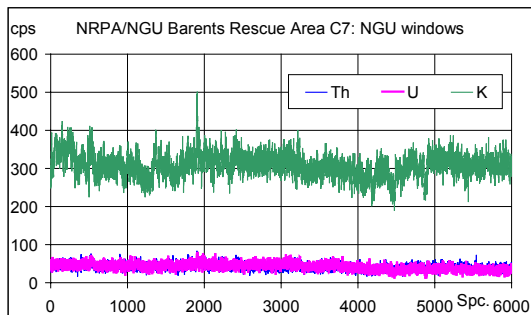


Figure M24. Gross natural cps, C7. 170901B (Nos. 8001-14000).

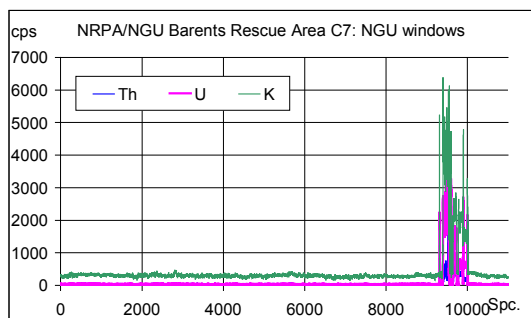


Figure M25. Gross natural cps, C7. 170901C (Nos. 14001-25000).

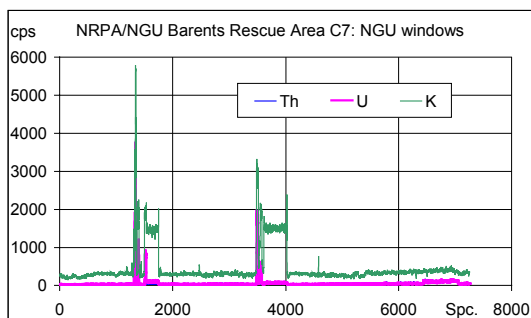


Figure M26. Gross natural cps, C7. 170901D (Nos. 25001-32251).

Table M7. NGU energy calibration.

Win	LL (chn.)	UL (chn.)	LL (keV)	UL (keV)
1	14	18	189.9	238.4
2	19	25	250.5	323.3
3	26	31	335.5	396.4
4	32	40	408.6	506.5
5	49	58	617.0	728.1
6	59	88	740.5	1101.9
7	89	110	1114.5	1379.6
8	32	38	408.6	482.0
9	39	48	494.2	604.7
Th	<b>109</b>	<b>125</b>	1370	1570
U	<b>132</b>	<b>148</b>	1660	1860
K	<b>189</b>	<b>220</b>	2410	2810

# 170901A (170901 Nos. 0-8000)

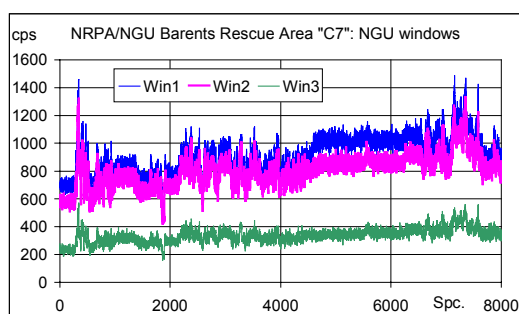


Figure M27.Gross cps Win1-3, C7.

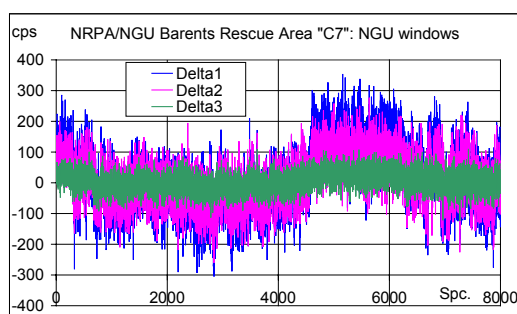


Figure M28.Stripped cps Win1-3, C7.

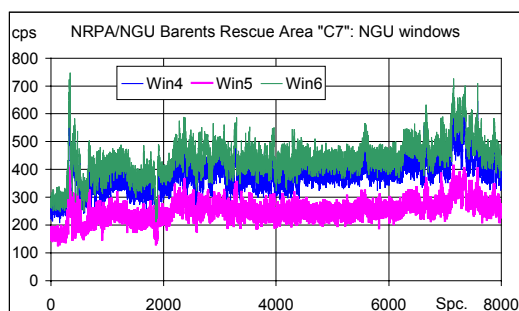


Figure M29.Gross cps Win4-6, C7.

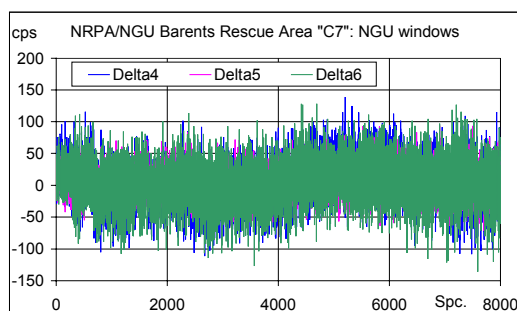


Figure M30.Stripped cps Win4-6, C7.

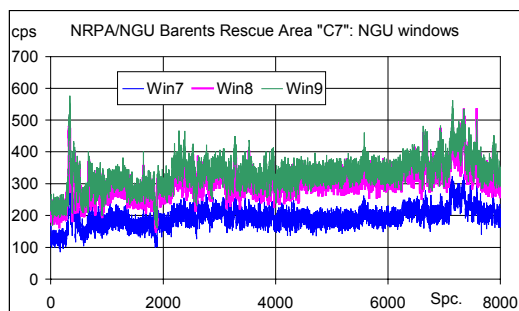


Figure M31.Gross cps Win7-9, C7.

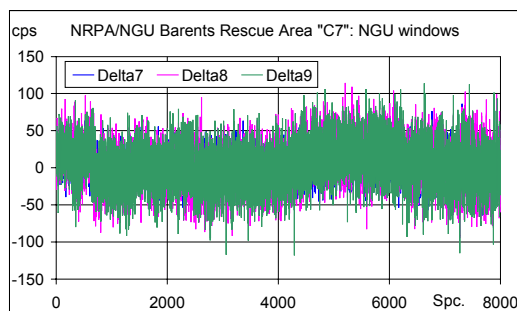


Figure M32.Stripped cps Win7-9, C7.

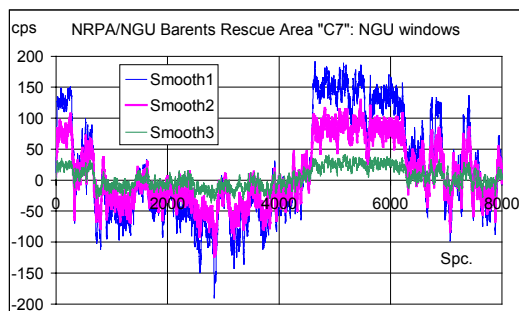


Figure M33.Smoothed, stripped cps. Win1-3.

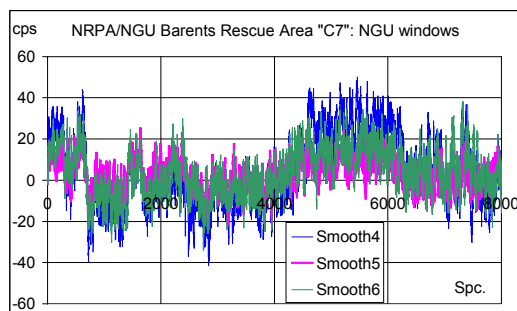


Figure M34.Smoothed, stripped cps. Win4-6.

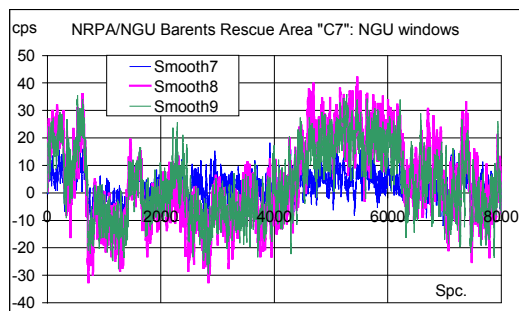


Figure M35.Smoothed, stripped cps. Win7-9.



# 170901B (170901 Nos. 8001-14000)

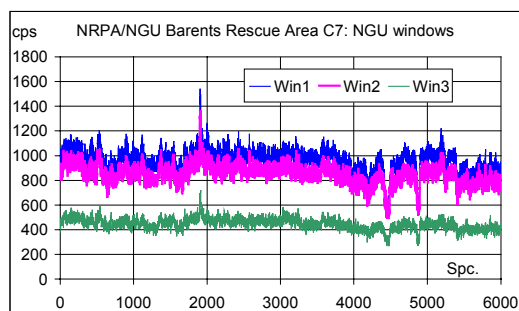


Figure M36.Gross cps Win1-3, C7.

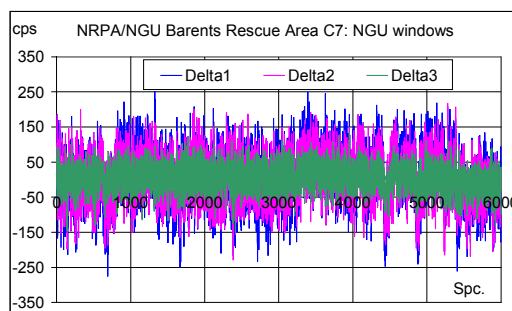


Figure M37.Stripped cps Win1-3, C7.

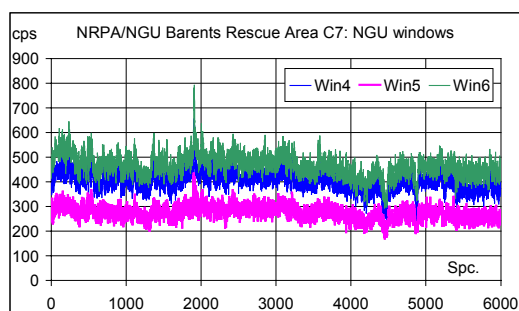


Figure M38.Gross cps Win4-6, C7.

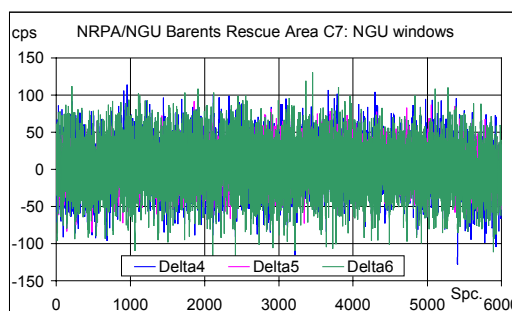


Figure M39. Stripped cps Win4-6, C7.

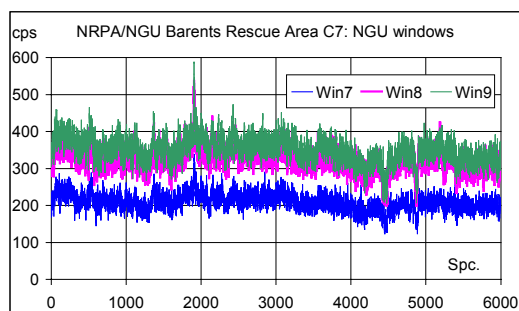


Figure M40.Gross cps Win7-9, C7.

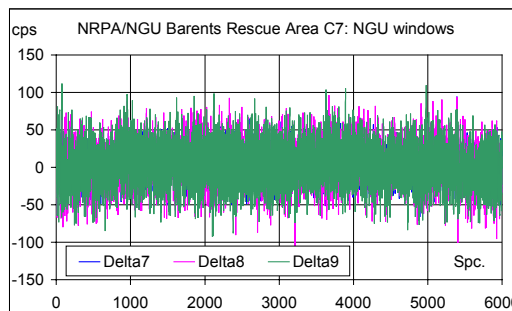


Figure M41.Stripped cps Win7-9, C7.

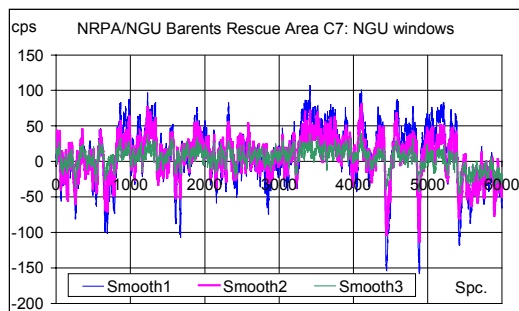


Figure M42.Smoothed, stripped cps. Win1-3.

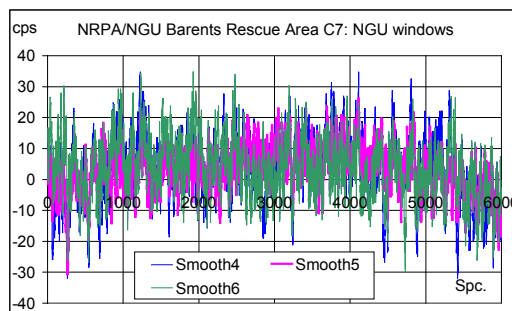


Figure M43.Smoothed, stripped cps. Win4-6.

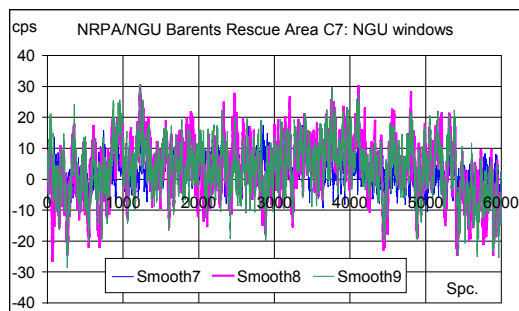


Figure M44.Smoothed, stripped cps. Win7-9, C7.

# 170901C (170901 Nos. 14001-25000)

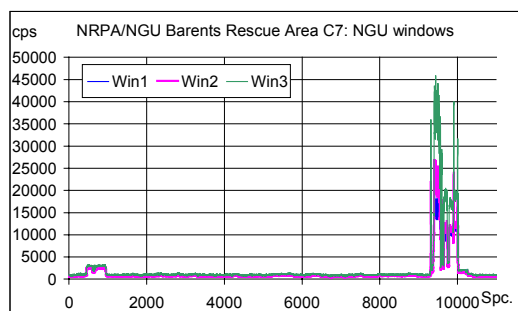


Figure M45.Gross cps Win1-3, C7.

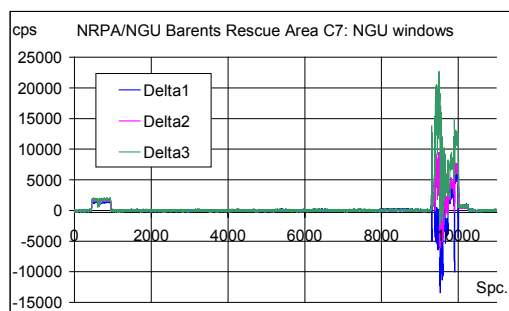


Figure M46.Stripped cps Win1-3, C7.

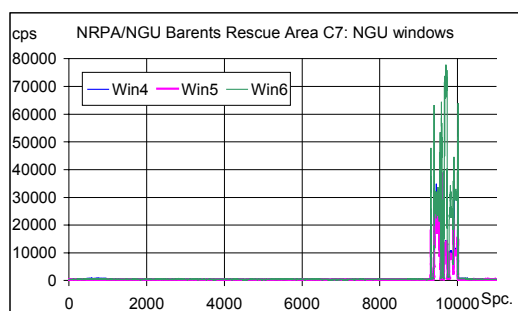


Figure M47.Gross cps Win4-6, C7.

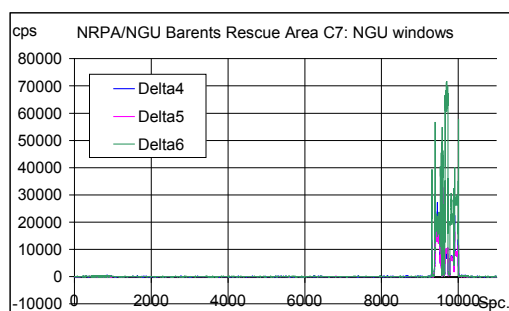


Figure M48.Stripped cps Win4-6, C7.

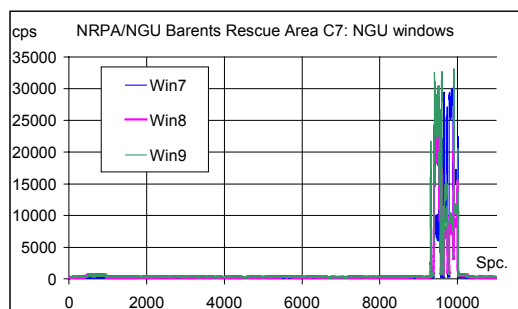


Figure M49.Gross cps Win7-9, C7.

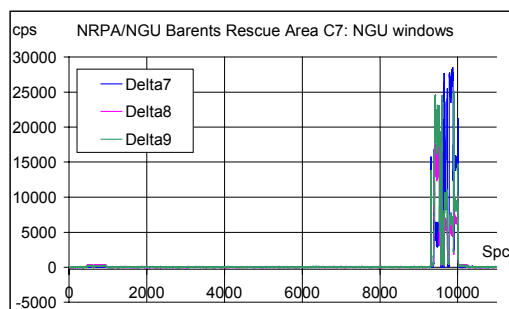


Figure M50.Stripped cps Win7-9, C7.

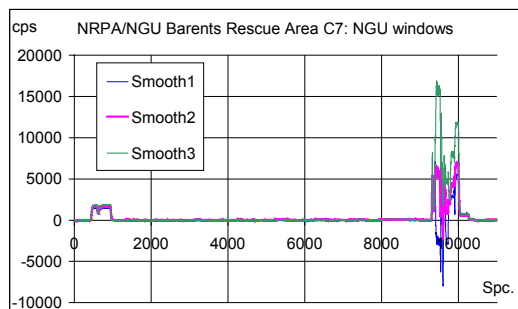


Figure M51.Smoothed, stripped cps. Win 1-3.

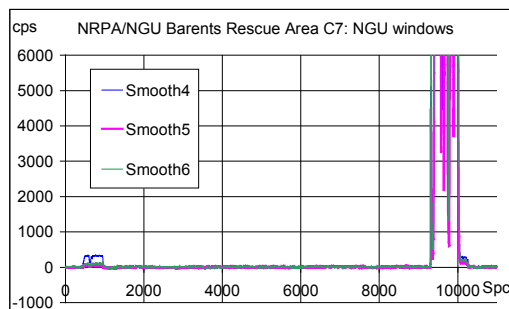


Figure M52.Smoothed, stripped cps. Win4-6.

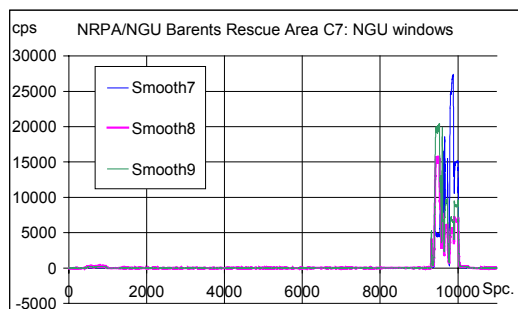


Figure M53.Smoothed, stripped cps. Win7-9, C7.

# 170901D (170901 Nos. 25001-32251)

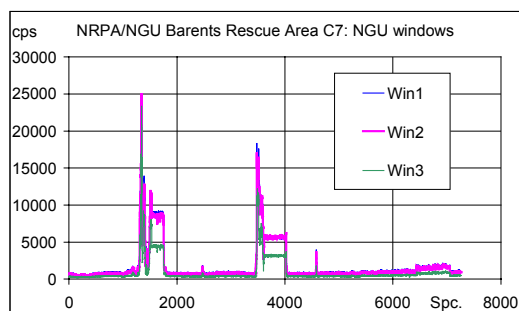


Figure M54.Gross cps Win1-3, C7.

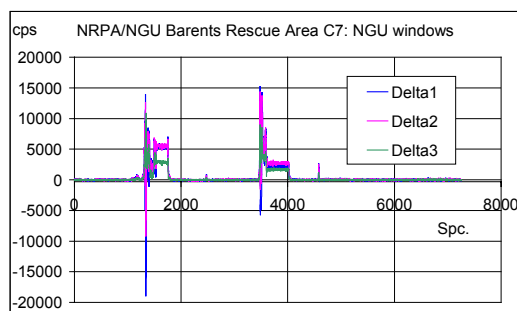


Figure M55.Stripped cps Win1-3, C7.

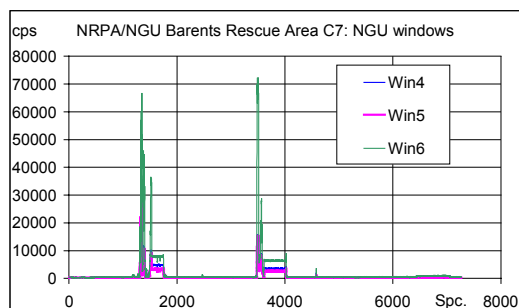


Figure M56.Gross cps Win4-6, C7.

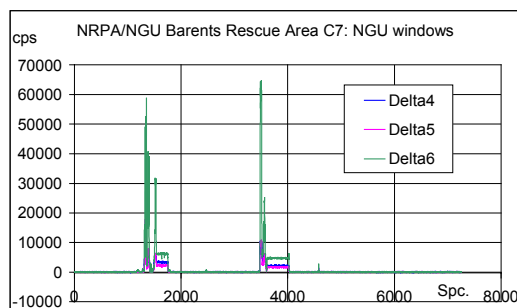


Figure M57.Stripped cps Win4-6, C7.

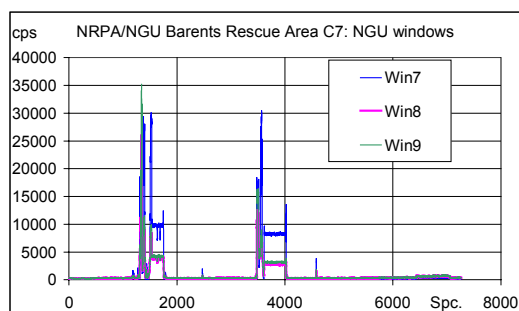


Figure M58.Gross cps Win7-9, C7.

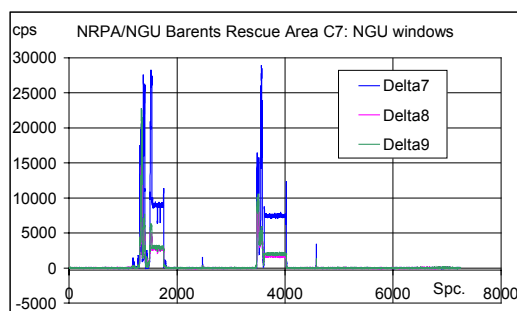


Figure M59.Stripped cps Win7-9, C7.

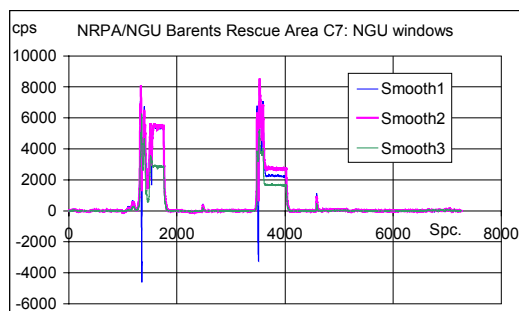


Figure M60.Smoothed, stripped cps. Win1-3-

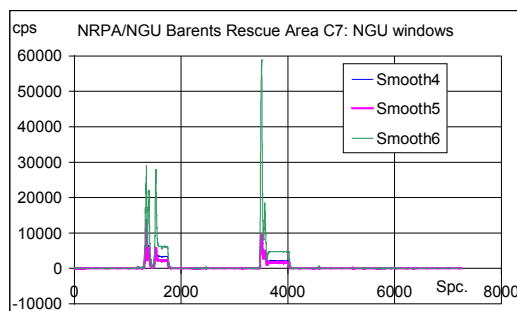


Figure M61.Smoothed, stripped cps. Win4-6.

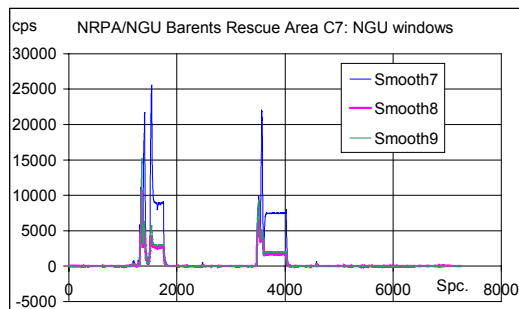


Figure M62.Smoothed, stripped cps. Win7-9, C7.

## 170901D (170901 Nos. 25001-32251)

170901D, Measurements Nos. 950-1150

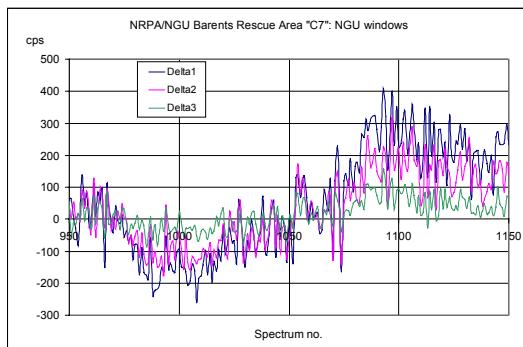


Figure M63. Stripped cps win 1-3, spectrum nos. 950-1150, area C7.

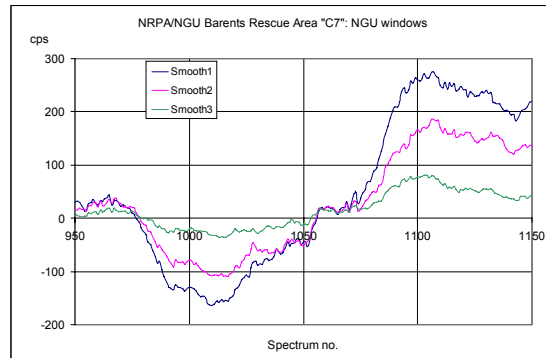


Figure M64. Smoothed stripped cps win 1-3, spectrum nos. 950-1150, area C7.

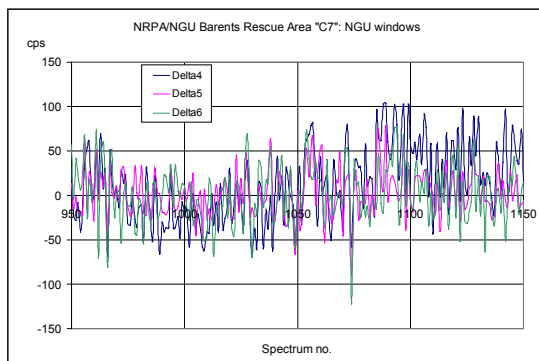


Figure M65. Stripped cps win 4-6, spectrum nos. 950-1150, area C7.

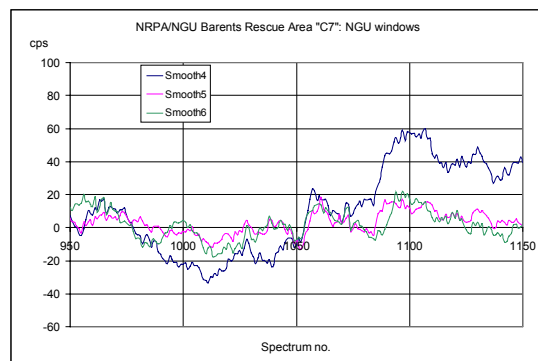


Figure M66. Smoothed stripped cps win 4-6, spectrum nos. 950-1150, area C7.

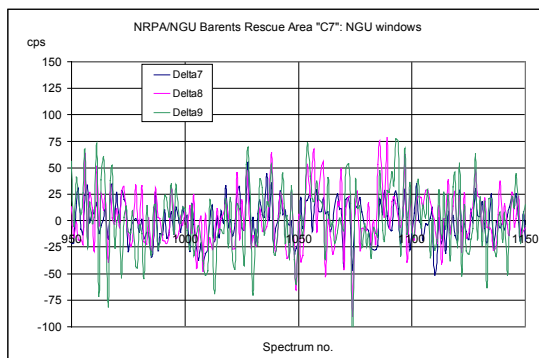


Figure M67. Stripped cps win 7-9, spectrum nos. 950-1150, area C7.

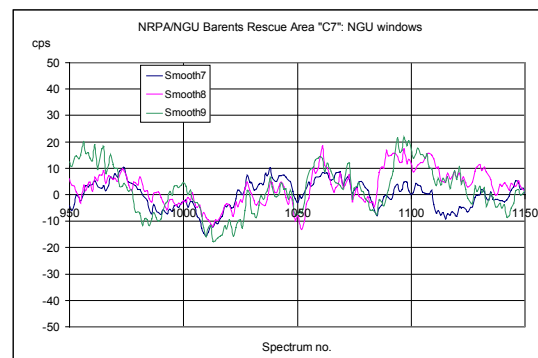


Figure M68. Smoothed stripped cps win 7-9, spectrum nos. 950-1150, area C7.

## Natural radionuclides: Barents Rescue NRPA/NGU.

**File 180901.dat.**

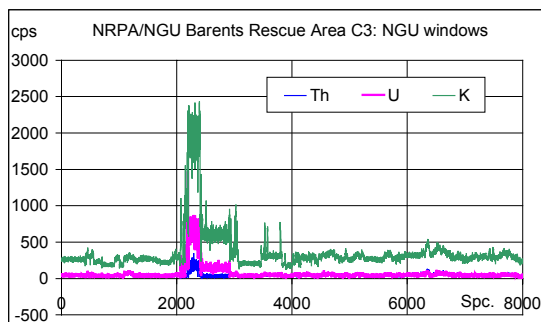


Figure M69. Gross natural cps, C3.  
180901A (Nos. 0-8000).

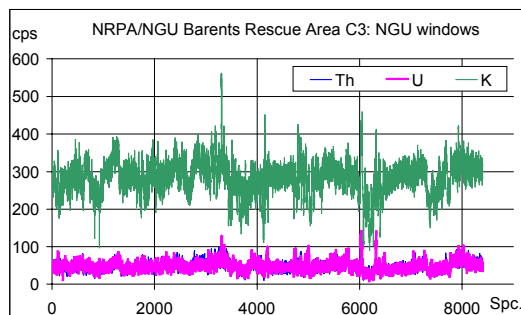


Figure M70. Gross natural cps, C3.  
180901B (Nos. 8001-16400).

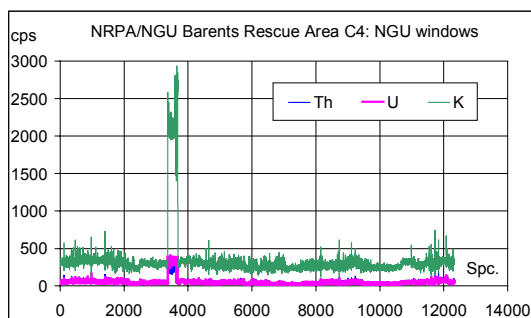


Figure M71. Gross natural cps, C4.  
180901C (Nos. 16401-28721).

Table M8. NGU energy calibration.

Win	LL (chn.)	UL (chn.)	LL (keV)	UL (keV)
1	14	18	189.9	238.4
2	19	25	250.5	323.3
3	26	31	335.5	396.4
4	32	40	408.6	506.5
5	49	58	617.0	728.1
6	59	88	740.5	1101.9
7	89	110	1114.5	1379.6
8	32	38	408.6	482.0
9	39	48	494.2	604.7
Th	<b>109</b>	<b>125</b>	1370	1570
U	<b>132</b>	<b>148</b>	1660	1860
K	<b>189</b>	<b>220</b>	2410	2810

# File 180901A (180901 Nos. 0-8000)

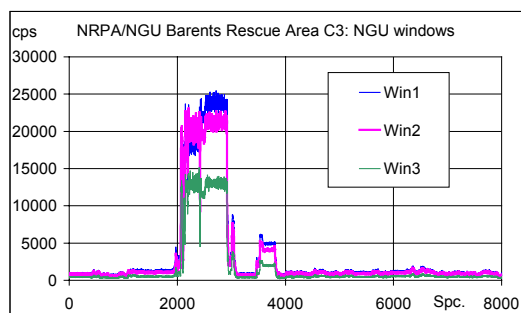


Figure M72.Gross cps Win1-3, C3.

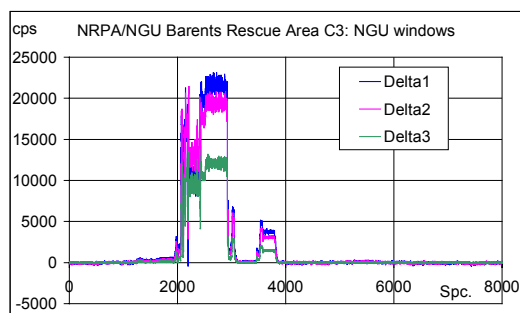


Figure M73.Stripped cps Win1-3, C3.

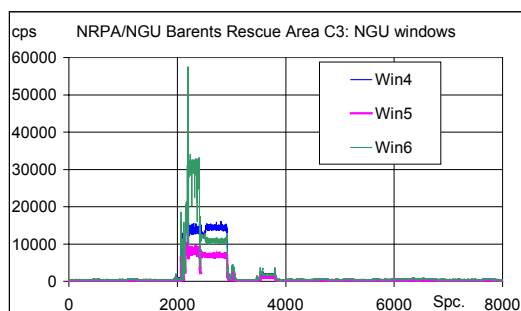


Figure M74.Gross cps Win4-6, C3.

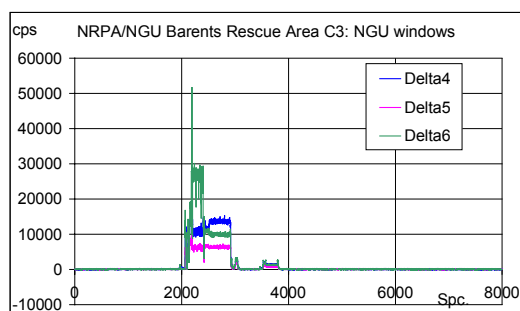


Figure M75.Stripped cps Win4-6, C3.

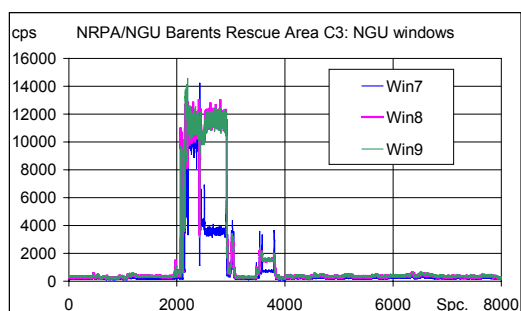


Figure M76.Gross cps Win1-3, C3.

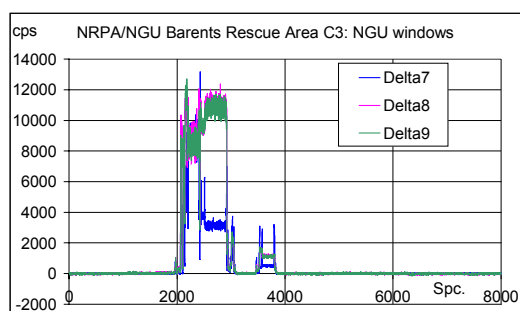


Figure M77.Stripped cps Win7-9, C3.

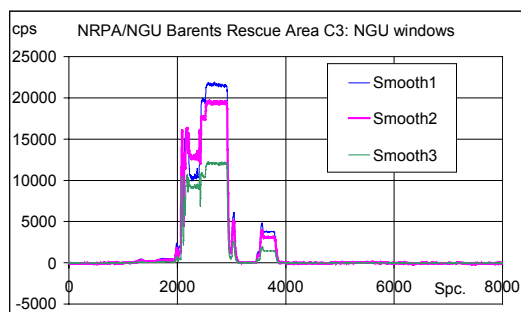


Figure M78.Smoothed, stripped cps. Win1-3.

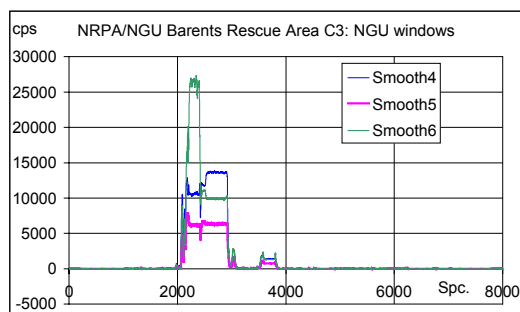


Figure M79.Smoothed, stripped cps. Win4-6.

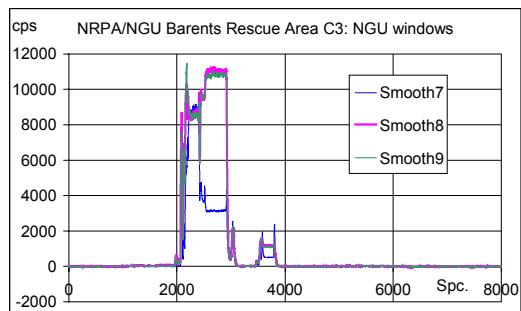


Figure M80.Smoothed, stripped cps. Win7-9.

# File 180901B (180901 Nos. 8001-16400)

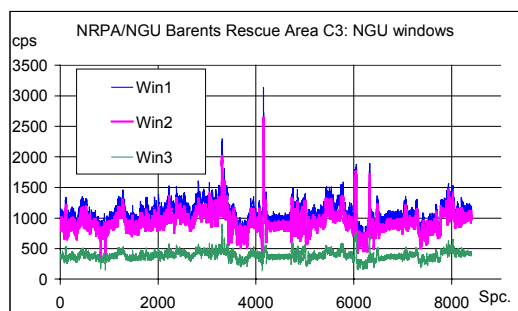


Figure M81.Gross cps Win1-3, C3.

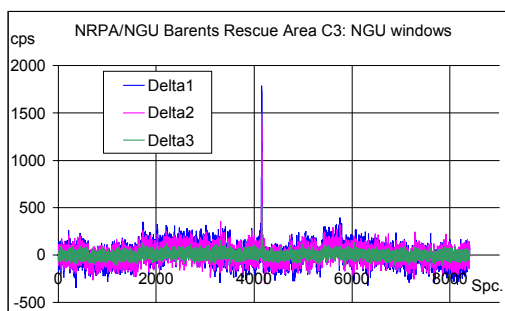


Figure M82.Stripped cps Win1-3, C3.

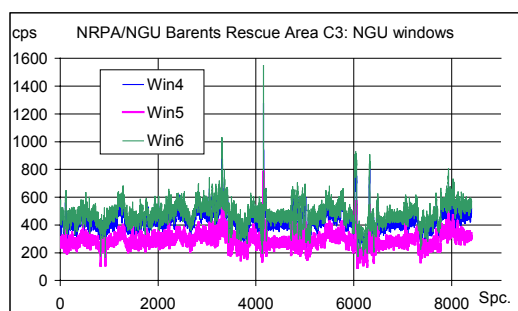


Figure M83.Gross cps Win4-6, C3.

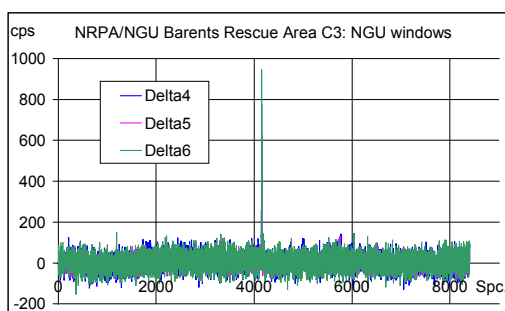


Figure M84.Stripped cps Win4-6, C3.

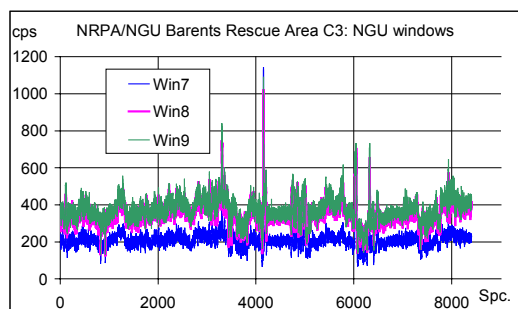


Figure M85.Gross cps Win7-9, C3.

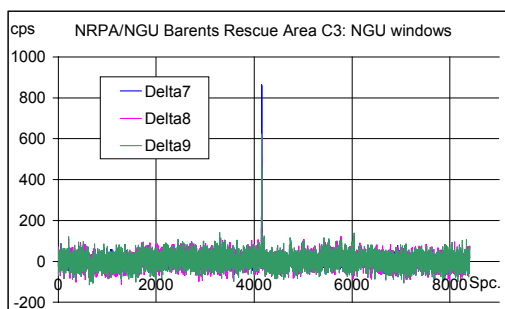


Figure M86.Stripped cps Win7-9, C3.

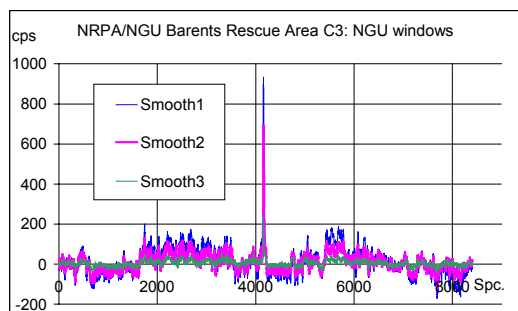


Figure M87.Smoothed, stripped cps. Win1-3.

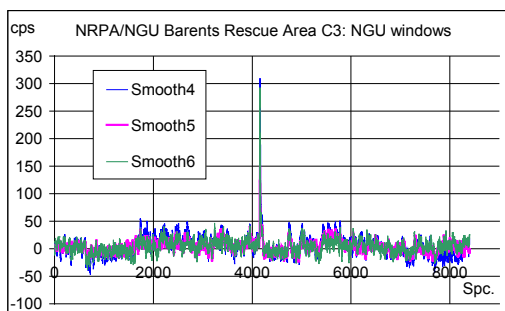


Figure M88.Smoothed, stripped cps. Win4-6

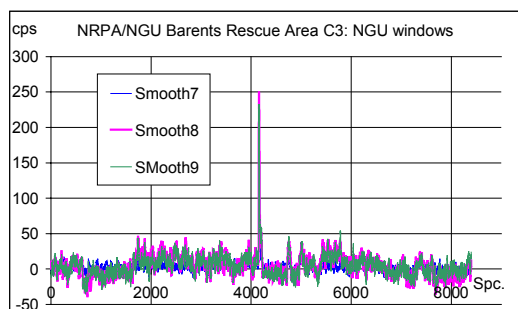


Figure M89.Smoothed, stripped cps. Win7-9.

# **File 180901C (180901 Nos.16401-28721)**

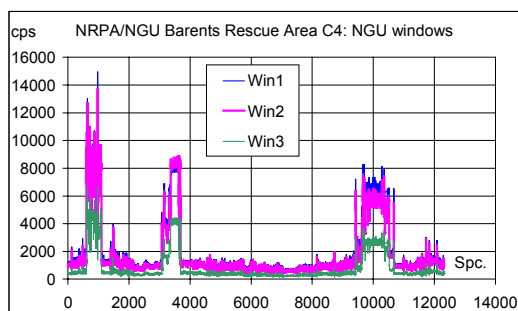


Figure M90.Gross cps Win1-3, C4.

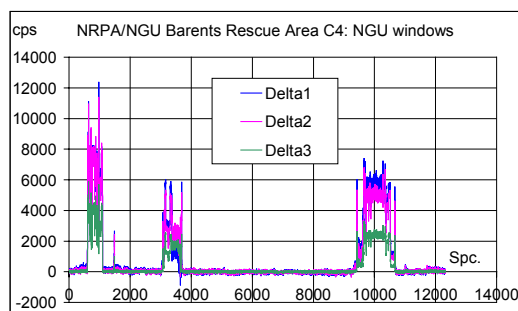


Figure M91.Stripped cps Win1-3, C4

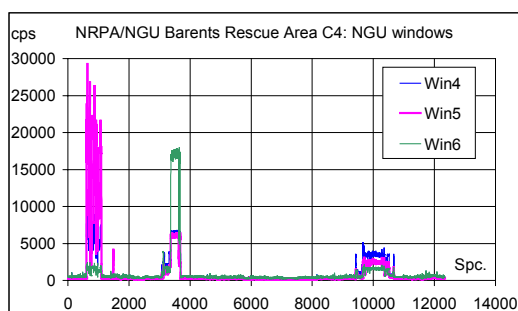


Figure M92.Gross cps Win4-6, C4.

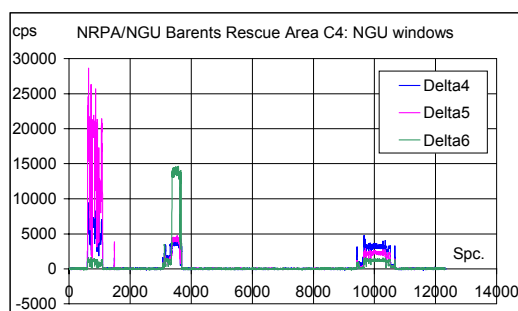


Figure M93.Stripped cps Win4-6, C4. NGU.

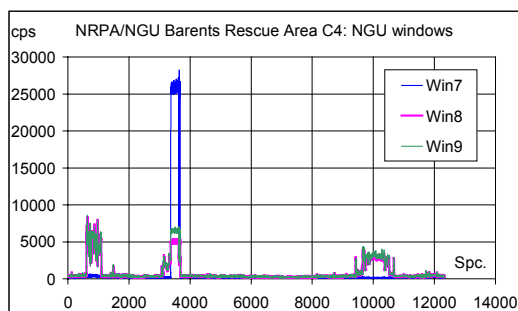


Figure M95.Gross cps Win7-9, C4.

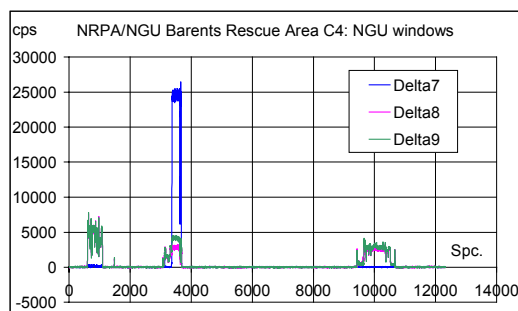


Figure M96.Stripped cps Win7-9, C4.

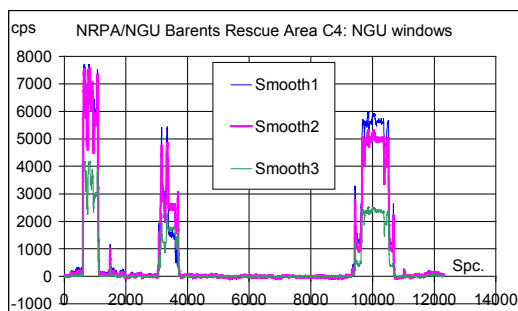


Figure M97.Smoothed, stripped cps. Win1-3.

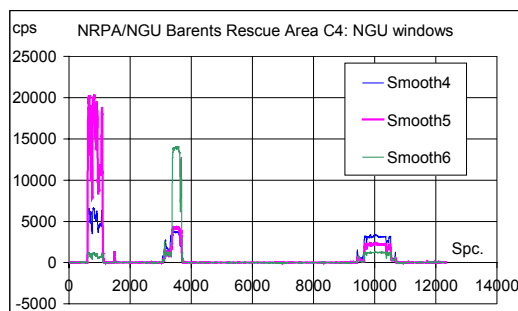


Figure M98.Smoothed, stripped cps. Win4-6.

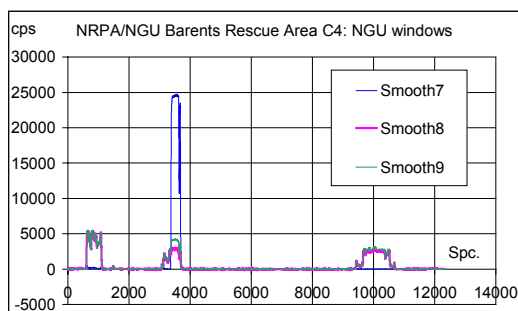


Figure M99.Smoothed, stripped cps. Win7-9.



## Appendix N Data file processing

A program written in BASIC calculated the area specific stripping factors. The program calculates stripping factors for three windows at a time. The output is gross window counts, stripped window counts, and smoothed window counts (plus gross window counts for Th, U, and K).

Data files, originally supplied in Danish AGS format, were first translated to Danish CGS format for be used with the BASIC program. During the translation spectra of special interest (e.g. height intervals) could be extracted.

```
AGS                                // 1052 bytes per struct
float Time
float X
float Y
float Z
byte Error
byte Down
byte Up                             // Wordaligned
unsigned int RTC                    // Not used
unsigned int LTC                    // ms
unsigned int COC                    // ft
unsigned int Nr                     // Spectrum number
unsigned int SPC[512]              // channel 0 contains RTC in ms

CGS                                // 1120 bytes per struct, 380 bytes header
unsigned long Record_number
unsigned long Line_number
float UTC_time
double X
double Y
double Z
int DGPS
int PDOP_error
float PDOP
float Live_time                    // seconds
float ralt                         // AGS altitude placed here
float balt
float roi[10]
unsigned int SPC[512]
```

[int = 2 bytes]

The NucSpec program package from March 2005 or newer versions can perform ASS calculations on files of both AGS and CGS format.

The following data files were received in the Danish AGS layout:

**SGU: 16L NaI detector (Energy stabilisation, very little spectrum drift)**

Area1.256	Barents Rescue	Area 1	AGS	256 chn.	36.6 – 89.3 m
Area2.256	Barents Rescue	Area 2	AGS	256 chn.	34.4 – 88.4 m.
Area3.256	Barents Rescue	Area 3	AGS	256 chn.	25.2 – 107.1 m
07082206.xyz		Gävle	AGS	256 chn	50.0 – 76.0 m

SGUgavl1.dat-spc.

BKG256SGU.txt Background spectrum (cosmic radiation etc. for SGU)

Area1.256 has strong  $^{131}\text{I}$  and  $^{60}\text{Co}$  point source signals.

Area2.256 has a strong  $^{99}\text{Mo}$  point source signal.

Area3.256 has strong  $^{60}\text{Co}$  point source signals.

**SSI: 3" \* 3" NaI detector (No energy stabilisation)**

C3_1.dat	Barents Rescue	Area 3	CGS	256 chn.	No altitude
C4_1.dat	Barents Rescue	Area 4	CGS	256 chn.	No altitude
C4_2.dat	Barents Rescue	Area 4	CGS	256 chn.	No altitude

C3\_1.dat has strong  $^{60}\text{Co}$  point source signals

C4\_1.dat has strong  $^{137}\text{Cs}$  point source signals

C4\_2.dat has strong point source signals

**NRPA: 16L NaI detector (Energy stabilisation)**

170901.dat	Barents Rescue	Area 7 (+)	CGS	256 chn.	No altitude
180901.dat	Barents Rescue	Area 3 + 4	CGS	256 chn	No altitude

The two files were split into smaller data files:

170901A.spc	Barents Rescue	Area "C7"	Meas. Nos.	0-8000
170901B.spc	Barents Rescue	Area C7	Meas. Nos.	8001-14000
170901C.spc	Barents Rescue	Area C7	Meas. Nos.	14001-25000
170901D.spc	Barents Rescue	Area C7	Meas. Nos.	25001-32251
180901A.spc	Barents Rescue	Area C3	Meas. Nos.	0-8000
180901B.spc	Barents Rescue	Area C3	Meas. Nos.	8001-16400
180901C.spc	Barents Rescue	Area C4	Meas. Nos.	16401-28721

All files except 170901A.spc contain strong source signals.

## Appendix O. Definitions and units

**Background count rate:** Count rate for an energy window measured at a location without radioactivity in the environment – except perhaps radon daughters in the air. The contribution to the background count rate originates from cosmic radiation and from radioactivity in the detector system itself (including car or aircraft).

**Detection efficiency** is defined as  $\varepsilon_{\text{int}} \cdot A$  i.e. the count rate (total or full energy peak) per fluence rate.

**Energy calibration:** The relation between the gamma energy deposited in a detector and the number of the channel in which the deposition event is counted. Often the relation is described as a second order polynomial i.e.

$$E = -9.4 + 5.775 \cdot k + 0.00021 \cdot k^2$$

where  $k$  is the channel number and  $E$  is the corresponding energy in keV.

**Environmental background:** Window count rate or spectrum recorded in an environment without artificial (or unusual) radioactivity i.e. it includes cosmic radiation, radioactivity in the detector system itself, radon daughters in the air and Th, U, and K in the environment.

**Fluence rate  $\phi$ :** The number of photons or particles passing 1 m<sup>2</sup> (or 1 cm<sup>2</sup>) per second. See the description below.

**Full energy peak:** A peak in a spectrum corresponding to deposition of all the primary energy of a photon in a detector.

**Net count rate:** Measured (window) count rate minus the background count rate - or minus the environmental background count rate for this window.

**Primary photons:** Photons that still have the same energy as when they were emitted from the radioactive nucleus. They also may be termed original photons or uncollided photons. Older textbooks also use the term unscattered photons.

**Radon daughters (RD)** include <sup>218</sup>Po, <sup>214</sup>Pb, <sup>214</sup>Bi, and <sup>214</sup>Po. They are all part of the decay chain following <sup>222</sup>Rn. <sup>222</sup>Rn itself is one of the decay products of the <sup>238</sup>U decay chain. Normally the gamma photons emitted by <sup>214</sup>Bi are used to identify and quantify the concentration of uranium in the ground and elsewhere.

**Single channel stripping factor:** The stripping factor related to a single channel. One may strip any window consisting of several channels by calculating a total stripping factor for the window as a sum of the single channel stripping factors for the channels that are included in the window.

**Stripped count rate** is the count rate of the X-window from which the contribution to the count rate from other nuclides than the X-nuclide has been subtracted. For energy windows for man-made radioactivity the stripping in general just means that the contribution from natural radioactivity to the window count rate has been subtracted.

**Yield:** “Number” of photons of a specified energy that are emitted per decay. Usually the yield (for a specified energy) is below 1.0. However, in a few cases the yield may be above 1.0. Yield also sometimes is termed intensity - a term that, however, also has other meanings.

**Window count rate:** Total number of counts per second in the channels included in the window in question.

**Window stripping factor:** Stripping factor for a window covering several channels. Window stripping factors are – like single channel stripping factors – subject to changes in system energy calibration.

The scientific definition of **fluence rate**  $\phi$  (Greek letter phi) of photons (or particles) is the number of photons (or particles) that per second enter through the surface of a small sphere divided by the cross section area of the sphere. The unit for fluence rate is photons/(m<sup>2</sup>s) or just 1/(m<sup>2</sup>s) or m<sup>-2</sup>s<sup>-1</sup>. In practice one may just consider the fluence rate as the number of photons passing through an area of 1 m<sup>2</sup> per second.

The **fluence**  $\Phi$  (Capital Greek letter phi) is the accumulated fluence rate over some time i.e.  $\Phi = \phi \times t$  where  $t$  is the time for accumulation of the fluence.

The fluence rate  $\phi(r)$  of primary (original) photons **around a point source** of activity  $Q$  that is placed free in air is  $\phi(r) = Q \times y \times \exp(-\mu R) / (4\pi R^2)$ , where  $R$  is the distance between the source and the point of interest,  $y$  is the “yield” i.e. the fraction of decays that causes an emission of the gamma photons in question.  $\mu$  is the linear attenuation coefficient for the material between the source and the point of interest i.e. here is it air.  $Q$  should be given in Bq (decays per second) and  $R$  in meters.

Title	Area Specific Stripping of lower energy windows for AGS and CGS NaI systems
Authors	Uffe Korsbech*, Helle Karina Aage*, Sören Byström**, Mats Wedmark**, Svein Thorshaug*** and Kim Bargholz****
Affiliations	* Technical University of Denmark ** Geological Survey of Sweden *** Norwegian Radiation Protection Agency **** Danish Emergency Management Agency
ISBN	87-7893-168-1
Date	May 2005
Project	NKS-B ASSb
No. of pages	100
No. of tables	51
No. of illustrations	231
No. of references	21
Abstract	<p>The report describes the results from a NKS (Nordic Nuclear Safety Research) project aiming at examining the possibilities for extracting stripping factors for Airborne Gamma-ray Spectrometry (AGS) data and Carborne Gamma-ray Spectrometry (CGS) data directly from the recorded set of data, i.e. without having to calibrate the detector systems on beforehand.</p> <p>The project – NKS project ASSb - has been carried out between 1 August 2004 and 31 March 2005 by a research group composed of persons from Technical University of Denmark (DTU), Danish Emergency Management Agency (DEMA), Geological Survey of Sweden (SGU), and Norwegian Radiation Protection Authority (NRPA).</p> <p>The AGS and CGS data sets used for the project were recorded by SGU, DEMA, NGU (Geological Survey of Norway), and SSI (Swedish Radiation Protection Institute).</p> <p>Most of the project effort has been directed towards analysing AGS and CGS data with point source signals recorded at the Barents Rescue 2001 LIVEX exercise at Boden in Sweden.</p> <p>Possibilities and limitations for the method have been identified.</p>
Key words	Stripping, Gamma Spectra, AGS, CGS, Area Specific, Source Search, Radiation Anomaly, Barents Rescue, LIVEX